UNCLASSIFIED

DEFENCE RESEARCH ESTABLISHMENT SUFFIELD
RALSTON, ALBERTA

# SUFFIELD SPECIAL PUBLICATION NO. 142


# PROCEEDINGS OF NMR IN DEFENCE SCIENCES 1990 SYMPOSIUM

by

C.A. Boulet

May 1991

UNCLASSIFIED

UNCLASSIFIED

DEFENCE RESEARCH ESTABLISHMENT SUFFIELD
RALSTON ALBERTA

SUFFIELD SPECIAL PUBLICATION NO. 142

# PROCEEDINGS OF NMR IN DEFENCE SCIENCES 1990 SYMPOSIUM

October 10-12, 1990
Defence Research Establishment Suffield

compiled by

C. A. Boulet



UNCLASSIFIED

## ABSTRACT

In these proceedings, 11 papers from the NMR in Defence Sciences 1990 Symposium, held at the Defence Research Establishment Suffield from October 10 – 12, 1990, are presented. The papers cover a number of areas of defence sciences in which nuclear magnetic resonance (NMR) is an important instrumental method. Topics include the use of two dimensional NMR for characterization of defence related compounds, investigation of decontamination chemistry, and solid state NMR for the analysis of materials.



## RÉSUMÉ

Le compte rendu qui suit présente 11 études sur la RNM qui avaient été soumises dans le cadre du Symposium 1990 sur les sciences de la défense qui s'est tenu au Centre de recherches pour la défense Suffield du 10 au 12 octobre dernier. Ces études couvrent toute une gamme de domaines reliés aux sciences de la défense où la résonance nucléaire magnétique (RNM) joue un rôle important Les sujets traités comprennent l'usage de la RNM bidimensionnelle pour la caractérisation des composés à usage militaire, l'étude de la chimie de décontamination et la RNM en phase solide pour l'analyse des matériaux.

# TABLE OF CONTENTS

Abstract i

Table of Contents ii

List of Registrants iii

Social and Scientific Schedule v

2D NMR Studies of the Indicator Dye TBPE. G. W. Buchanan, J. W. Bovenkamp, and D. Thoraval. 1

Use of 2D NMR for the Assignment of Structure of Defence Related Compounds. C. A. Boulet and A. S. Hansen. 13

Search and Retrieval of $^{13}C$ NMR Data. D.A. Ross. 25

Gas Chromatography-Mass Spectrometry: A Technique for the Verification of Chemical Warfare Agents and Related Compounds. P. A. D'Agostino. 37

Kinetics and Mechanisms of the Hydrolysis and Oxidation of HD and VX. L. L. Szafraniec, W. T. Beaudry, D. K. Rohrbaugh, L. J. Szafraniec, J. R. Ward, and Y.-C. Yang. 52

Catalytic $O_2$-Oxidation of Alkyl Sulfides to Sulfoxides using Dioxo-Ruthenium Porphyrins: a $^1H$ NMR Investigation. N. Rajapakse and B. R. James. 65

The Formation of Pyrophophosphates in the Oxidation of Phosphonothiolates. D. R. Leslie, W. T. Beaudry, L. L. Szafraniec, and D. K. Rohrbaugh. 75

NMR of Calixarenes. P. D. Beer, J. P. Martin and A. N. Trethewey. 85

Reactions of CW Agents in DS2. W. T. Beaudry, L. L. Szafraniec, D. K. Rohrbaugh, and D. R. Leslie. 97

$^{27}Al$ and $^{11}B$ NQR of Ceramic Materials. C. Connor, J.-W. Chang, and A. Pines. 108

Solid-State NMR Study of Ambient Temperature Aging of Carbon Black-Filled Rubbers. D. E. Axelson, A. Sharma and J. Collyer. 119

## LIST OF REGISTRANTS

Dr. D. E. Axelson
President
NMR Technologies Inc.
132 Advanced Technology Center
9650-20 Ave.
Edmonton, AB CANADA T6N 1G1

Mr. W. T. Beaudry
US Army Chemical Research,
Development and Engineering Center
Attn: SMCCR-RSC-P/William T. Beaudry
Aberdeen Proving Ground
Maryland, 21010-5423
USA

Dr. C. A. Boulet
CBDS
Defence Research Establishment Suffield
P.O. Box 4000
Medicine Hat, AB CANADA T1A 8K6

Dr. G. W. Buchanan
Department of Chemistry
Carleton University
Colonel By Drive
Ottawa, Ontario CANADA
K1S 5B6

Dr. R. Clewley
CBDS
Defence Research Establishment Suffield
P.O. Box 4000
Medicine Hat, AB CANADA T1A 8K6

Dr. C. Connor
Defence Research Establishment Pacific
FMO
Victoria, BC CANADA V0S 1B0

Dr. P. A. D'Agostino
CBDS
Defence Research Establishment Suffield
P.O. Box 4000
Medicine Hat, AB CANADA T1A 8K6

Mr. A. S. Hansen
CBDS
Defence Research Establishment Suffield
P.O. Box 4000
Medicine Hat, AB CANADA T1A 8K6

Dr. D. Ralph Leslie
Matreials Research Laboratory
Defence Science and Technology Organization
P.O. Box 50
Ascot Vale, VIC 3032
AUSTRALIA

Dr. P. A. Lockwood
CBDS
Defence Research Establishment Suffield
P.O. Box 4000
Medicine Hat, AB CANADA T1A 8K6

Capt. C. H. Pedersen
The Danish Defence Academy
P.O. Box 2715
2100 Koebenhavn OE
DENMARK

Dr. G. Purdon
CBDS
Defence Research Establishment Suffield
P.O. Box 4000
Medicine Hat, AB CANADA T1A 8K6

Dr. Nimal Rajapakse
Department of Chemistry
2036 Main Mall
University of British Columbia
Vancouver, B.C. CANADA
V6T 1Y6

Dr. V. V. Krishnamurthy
Senior Applications Chemist
Manager, Applications Laboratory
25 Hanover Road
Florham Park, New Jersey 07932
USA

Mr. Deryck A. Ross
Directorate Scientific Information Services
Research and Development Branch
101 Colonel By Drive
Ottawa, Ontario, CANADA
K1A 0K2

Mrs. Linda Szafraniec
US Army Chemical Research,
Development and Engineering Center
Attn: SMCCR-RSC-P/Linda L. Szafraniec
Aberdeen Proving Ground
Maryland, 21010-5423
USA

Mr. Mogens Thomsen
Danish Civil Defence
Analytical-Chemical Laboratory
Universitetsparken 2
DK - 2100 Copenhagen
DENMARK

Dr. A. N. Trethewey
CDD
CDE Porton Down
Salisbury, Wiltshire SP4 0JQ
United Kingdom

Mr. Bill Kenney
Varian Canada Inc.
955 Green Valley Crescent
Ottawa, Ontario CANADA
K2C 3V4

## SOCIAL AND SCIENTIFIC SCHEDULE

**October 10, 1990**

| Time | Event | Location |
|---|---|---|
| 0800 | Pick-up at hotels | Medicine Hat Lodge<br>Travelodge |
| 0845 | Registration | DRES Building 1 |
| 0900 | Welcoming Remarks<br>Chief DRES, Symposium Chairman | Large Conference Room<br>Building 1 |
| 0930 | **PLENARY LECTURE**<br>Dr. Krish Krishnamurthy<br>Varian USA | LCR |
| 1015 | Coffee | |
| 1030 | **2D NMR IN DEFENCE SCIENCES**<br><br>G.W. Buchanan, J.W. Bovenkamp, D. Thoraval, and S. Fortier. Solvent Dependent Tautomeric Equilibria in the Indicator Dye TBPE as Elucidated by 2D NMR.<br><br>C.A. Boulet and A.S. Hansen. Use of 2D NMR for the Assignment of Structure of Defence Related Compounds. | |
| 1230 | Lunch | Officer's Mess |
| 1330 | D.A. Ross. Search and Retrieval of $^{13}C$ NMR Data. | |
| 1415 | **RESEARCH DIRECTIONS IN CW VERIFICATION**<br><br>P.A. Lockwood. The Chemical Weapons Convention. Implications for Chemical Defence Research.<br><br>P.A. D'Agostino. Gas Chromatography-Mass Spectrometry: A Technique for the Verification of Chemical Warfare Agents and Related Compounds. | |
| 1630 | Suds and Posters | Officer's Mess |
| 1900 | Return to Hotels | |

**October 11, 1990**

0800 Pick-up at hotels

0900 **NMR STUDIES IN DECONTAMINATION CHEMISTRY**
Session chaired by Dr. G. Purdon

L.L. Szafraniec, W.T. Beaudry, D.K. Rohrbaugh, L.J. Szafraniec, J.R. Ward, and Y.-C. Yang. Kinetics and Mechanisms of the Hydrolysis and Oxidation of HD and VX.

N. Rajapakse and B.R. James. Catalytic $O_2$-Oxidation of Alkyl Sulfides to Sulfoxides using Dioxo-Ruthenium Porphyrins: a $^1H$ NMR Investigation.

1030 Coffee

D.R. Leslie, W.T. Beaudry, L.L. Szafraniec, and D. Rohrbaugh. The Formation of Pyrophophosphates in the Oxidation of Phosphonothiolates.

A.N. Trethewey, P.D. Beer, and J.P. Martin. NMR of Calixarenes.

1230 Lunch

1330 **NMR STUDIES IN DECONTAMINATION CHEMISTRY** (contd).

W.T. Beaudry, L.L. Szafraniec, D.K. Rohrbaugh, and D.R. Leslie. Reactions of CW Agents in DS2.

1430 **SOLID STATE NMR IN DEFENCE RELATED RESEARCH**

C. Connor, J.-W. Chang, and A. Pines. $^{27}Al$ and $^{11}B$ NQR of Ceramic Materials.

D.E. Axelson, A. Sharma, J. Collyer, and M. Scammell-Bullock. Solid-State NMR Study of Ambient Temperature Aging of Carbon Black-Filled Rubbers.

1615 Closing Remarks
1630 Return to Hotels
1900 Banquet

# 2D NMR STUDIES OF THE INDICATOR DYE TBPE

Gerald W. Buchanan
Ottawa-Carleton Chemistry Institute
Department of Chemistry
Carleton University, Ottawa, Canada K1S 5B6

John W. Bovenkamp and Dominic Thoraval
Defence Research Establishment Ottawa
Ottawa, Canada, K1A 0Z2

## Abstract

For 3',3'',5',5''-tetrabromophenolphthalein ethyl ester (TBPE) in 1:1 $CD_2Cl_2$:$CDCl_3$ solution complete $^1H$ and $^{13}C$ NMR signal assignments have been made via $^1H^1H$ COSY and $^1H^{13}C$ HETCOR experiments. The quinoidal and phenolic integrities are retained on the NMR timescale. By contrast for an acetone-$d_6$ solution only 14 $^{13}C$ resonances are found and the colour of the solution changed from green to dark blue. These changes in acetone solution are attributed to the loss of the phenolic proton of TBPE and the existence of resonance forms which render the phenolic and quinoidal rings equivalent.

## Introduction

Indicator dyes have been found useful for the detection of droplets of toxic liquids containing a basic nitrogen. Consequently they have been incorporated into adhesive backed detector papers. In 1981, the commonly used indicator dye ethyl-bis-(2,4-dinitrophenyl)acetate was found to be mutagenic (1). TBPE has been suggested as a replacement (2) and it has been found to be non-mutagenic by the Ontario Research Foundation (3).

TBPE is an acid/base indicator dye which, unlike most phenolphthaleins, exists in an open ester form rather than the usual lactone form. The phenolic proton is removed in the pH range 3.6-4.2 (4). The resulting charge is delocalized between the phenol and quinoid rings producing a change in colour from yellow, at pH below the 3.6-4.2 range, to dark blue above this pH range. TBPE was first synthesized by Davis and Schuhmann (5), using a five step procedure starting with phenolphthalein. Other synthetic studies were reported by Sun et al. (6). The synthetic route which was used to produce the samples for this work is described in reference 2. Patents have been submitted for the use of TBPE for the detection of toxic liquids (7).

## EXPERIMENTAL

NMR Studies: All spectra were recorded at 298K on a Bruker AM-400 spectrometer equipped with an Aspect 3000 computer and process controller using DISNMR version 87. Standard microprograms from the Bruker Software Library were employed.

The $^1H^1H$ COSY experiment used N-type phase cycling with a 45° mixing pulse. Typically, the free induction decays were acquired over 1024 data points for each of the 256 values of the evolution time, with a digital resolution of ca. 5 Hz/point. The raw data were zero filled in F1 prior to Fourier transformation using the sine-bell window function for both F1 and F2. The matrix was symmetrized about the diagonal.

The $^{1}H^{13}C$ COSY spectra were obtained using a low decoupler power in the CW mode (composite phase decoupling) with polarization transfer from $^{1}H$ to $^{13}C$. Typically, the FID's were acquired over 4096 data points for each of the 128 or 256 values of the evolution time, with digital resolution of 7 Hz/point F2 and 5-10 Hz/point in F1. The raw data were zero filled in F1 prior to Fourier transformation using the sine bell window function. Proton relaxation delays of 3-5 s were utilized. For the long range correlations, the delays were chosen normally to emphasize couplings of ca. 7.5 Hz.

**Discussion**

(i) $^{1}H$ NMR Spectrum

The chemical shifts for the fourteen protons of IBPE are presented in Table 1. The numbering scheme is the same as in the X-ray study with the hydrogen atoms labelled according to their parent atom.

The absence of correlations in the $^{1}H^{1}H$ COSY (8) experiment identified the OH proton at 6.40 ppm. The most deshielded proton resonance is the doublet of doublets at 8.05 ppm, which is due to H16. This assignment follows from the observation of a long range ($^{3}J$) correlation to the ester carbonyl carbon at 165.48 ppm and is consistent with the known deshielding influence of an ester function on ortho aromatic protons (9). With this assignment in hand the $^{1}H^{1}H$ COSY experiment leads to ready identification of resonances for H17, H18, and H19. From the spin coupling pattern, chemical shifts and integrated intensities the $CH_2$ and $CH_3$ groups are readily identified.

The remaining resonances in the $^{1}H$ spectrum consist of a three proton singlet at 7.40 ppm and a one proton singlet at 7.90 ppm. Due to rapid rotation about the C1-C2 bond, the protons on C3 and C7 will have identical chemical shifts and thus two of the three protons at 7.40 can be assigned to H3 and H7. The remaining two singlets of one proton intensity must therefore arise from the non equivalent H9 and H13 sites of the quinoid ring. The proton having the chemical shift of 7.90 ppm must lie in the deshielding "outer" region of one of the adjacent aromatic moieties.

From the X-ray data one can obtain information regarding the preferred conformation of TBPE in the solid. Assuming similar solution geometry, a distinction between H9 and H13 resonances can be made. 

The X-ray data show that the interplanar angle between ring A and B is 45.2(3) while that between rings A and C is 102.2(3) and between B and C is 92.4(3)°. From molecular models it is clear that H9 lies in the "outer" i.e. deshielding region of ring B while H13 is situated almost directly above the C14 site of ring C. On the basis of the known anisotropic effect of aromatic rings on $^{1}H$ resonances (*10*), one can assign H9 as giving rise to the deshielded resonance at 7.90 ppm.

(ii) $^{13}C$ NMR Spectrum

The $^{1}H$ decoupled $^{13}C$ NMR spectrum of TBPE in 1:1 $CD_2Cl_2$:$CDCl_3$ solution at 298K shows 20 resonances, whose chemical shifts are presented in Table 2.

Initially, the APT (*11*) experiment was used to distinguish between protonated and nonprotonated aromatic carbons. Secondly, the relative intensities of the resonances as determined from a suppressed nuclear Overhauser experiment furnished information regarding sites which are averaged by bond rotation, since only 20 lines are observed for TBPE which possesses 22 carbons.

Since the $^{1}H$ spectrum has been completely assigned, the $^{13}C$ chemical shifts for the ten carbons bearing hydrogen follow directly from the 1-bond $^{1}H$-$^{13}C$ correlation experiment (*8*). A typical spectrum illustrating these correlations is shown in figure 1. The double intensity $^{13}C$ resonance at 134.94 ppm for the C3,C7 pair, which are rendered equivalent by rapid rotation about the C1-C2 bond, is readily apparent.

For assignment of the non-protonated (quaternary) aromatic carbon resonances, the long range (i.e. $^{2}J$ or $^{3}J$) correlation experiments are valuable along with consideration of chemical shifts for related molecules. The brominated quinoid carbons C10 and C12 are distinguished by the fact that C12 exhibits a $^{2}J$ correlation to the proton at 7.40 ppm (H13) while C10

correlates to the proton resonance at 7.90 ppm (H9). The quinoid carbonyl (C11) at 172.69 ppm correlates to both H9 and H13 as expected, and its chemical shift is in close accord with data for related 1,3-dibromo-2 quinoid molecules (12).

In the phenolic ring, the well documented effects of substituents on aromatic $^{13}C$ shifts (13) lead to the prediction that the brominated carbons C4,C6 should resonate near 110 ppm. The intensity 2 quaternary resonance at 109.83 ppm shows the expected single long range ($^2J$) correlation to the H3,H7 protons. For C5 the expected chemical shift is near 160 ppm based on model phenolic compounds (13). Accordingly, the resonance at 158.98 can be assigned to C5 and it shows the expected correlation ($^3J$) to the H3,H7 protons. The remaining quaternary carbon which correlates to H3,H7 only, appears at 151.26 ppm and must, by elimination, be attributed to C2.

At this point, four resonances remain to be assigned which arise from the quaternary carbons C1, C8, C14 and C15. The resonance at 139.49 ppm shows "long range" correlation to H16 and H18, while the 131.53 resonance correlates with H17 and H19. Initially, the delays in the long range C-H correlation experiment were set to emphasize C-H couplings of 7.5 Hz so that the strongest correlations will be observed for couplings of this magnitude. It is known from early work (14) that $^3J_{CCCH}$ in benzene is 7.4 Hz, while the $^2J_{CCH}$ value is 1.0 Hz. Hence the correlations which are observed under these conditions will arise via $^3J$ networks. Accordingly we assign the 139.49 resonance to C14 and the 131.53 line to C15. Finally, the $^{13}C$ resonance at 129.62 ppm shows a correlation with a proton resonance at 7.40 ppm while the carbon at 129.71 shows no correlations under these conditions. The remaining unassigned carbons are C1 and C8. In the case of C8, there are no vicinal hydrogens and hence the lack of observed correlations would not be surprising in view of the lower magnitudes for $^2J$ couplings mentioned above. For C1, however, there are five vicinal hydrogens. Failure to observe correlations to more than one site here must be due to dihedral angle effects arising from the non-planarity of the three aromatic rings with respect to the plane occupied by C1,C2,C8 and

C14. From the X-ray data, the dihedral angle between C1 and H19 is 110.1°. Assuming a similar geometry in solution, the $^3J_{CCCH}$ value is expected to be less than 2 Hz (15). Again on the basis of the X-ray data, the expected dihedral angles between C1 and the H3, H7 pair will be ca. 40° different from the planar situations which lead to maximal coupling. In the solid state, however, the H9 and H13 sites are within 12.6° of being coplanar with C1. Thus it is reasonable to expect a correlation with one or both of these sites. Experimentally, the correlation to the 7.40 proton resonance indicates that this arises from the vicinal C1-H13 interaction.

With the delays set to emphasize 3.75 Hz $^{13}C$-$^1H$ coupling, the $^{13}C$ resonance at 129.71 correlates to the $^1H$ line at 7.90 ppm. This confirms the identity of C8 and the correlation arises from a $^2J$ pathway to H9.

**(iii) 13C NMR Spectrum in Acetone-$d_6$**

The initial point to note here is that the colour of the acetone-d6 solution of TBPE is dark blue in contrast to the green solution in the 1:1 $CD_2Cl_2$-$CDCl_3$ solvent mixture. A further difference is that the $^{13}C$ NMR spectrum in acetone-$d_6$ shows a total of 14 resonances in contrast to the 20 observed in the $CD_2Cl_2$-$CDCl_3$ medium. Methods of resonance assignment were similar for the two solvent media and results are presented in Table 6 for the acetone-$d_6$ case. Clearly, there is, in acetone-$d_6$, a situation in which the environments of C4,6,10,12 are averaged to one as are the environments of C3,7,9,13 as well as the C2,8 and C5,11 pairs respectively.

We believe that the explanation for the colour change between media and the differing number of $^{13}C$ resonances lies with the normal

trace of acid present in $CDCl_3$. This gives the solution in $CD_2Cl_2$-$CDCl_3$ a lower pH , consistent with its green colour. In this medium there is a keto-enol type tautomerism as shown below. These equilibria are usually slow on the NMR timescale and hence separate $^{13}C$ resonances are seen for the phenolic vs. the quinoidal ring carbons of TBPE.

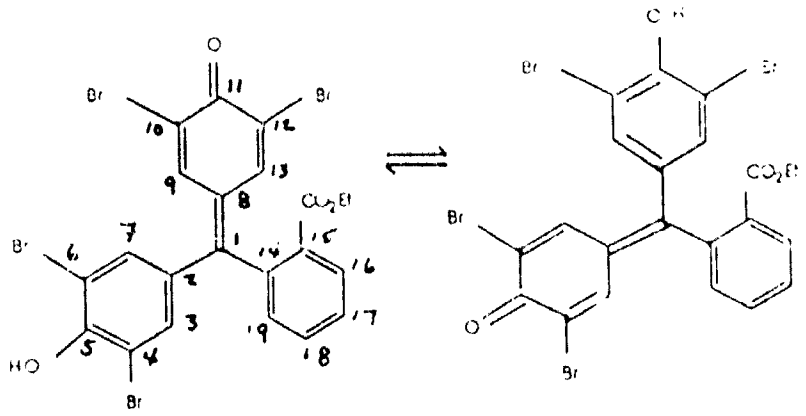

As stated in the Introduction, TBPE loses its phenolic proton above pH 4.2 and changes colour to dark blue. The $^{13}C$ NMR behaviour of TBPE in acetone-$d_6$ is consistent with such an occurence, since the groups of carbons C4,6,10,12; C3,7,9,13; C5,11 and C2,8 are rendered degenerate due to the existence of resonance between rings A and B as depicted below.

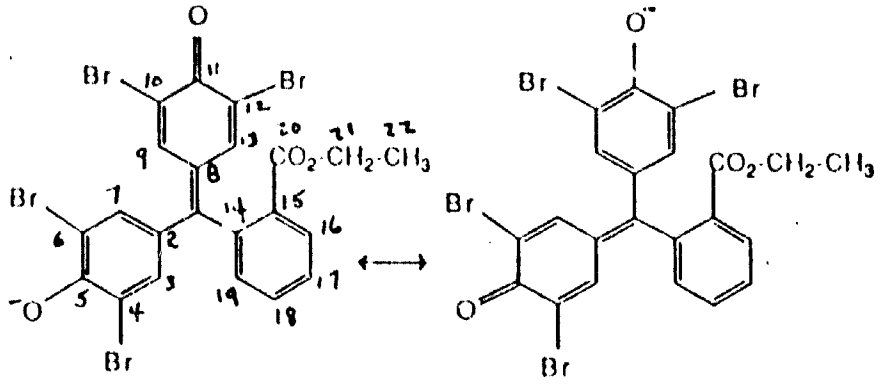

Assuming minimal influence of solvent on $^{13}C$ chemical shifts, one can check for the existence of averaging of the assigned $^{13}C$ shifts in the two media using additivity and weighted chemical shift averaging. Such data are presented in Table 7. It is evident that the agreement between predicted and observed shifts on the basis of averaging is excellent for the C4,6,10,12 positions as well as for the C3,7,9,13 and C2,8 sites.

There is poor agreement between predicted and observed $^{13}C$ data for the C5,11 pair, with the observed shift in acetone-$d_6$ being ca. 5 ppm more shielded than predicted. This is, however entirely consistent with the suggested protonation will lead to an increase in electron density at the C5,11 site and thus a more shielded $^{13}C$ resonance.

**REFERENCES**


1. E.R. Nestmann, D.J. Kowbel and J.A. Wheat. Carcinogenisis, **2**, 879 (1981).
2. D. Thoraval, J.W. Bovenkamp, R.W. Bets and B.V. Lacroix. Defence Research Establishment Ottawa, Report No. 963, June 1988.(UNCLASSIFIED)
3. A.J. Horton. Ontario Research Foundation, Report No. 48-30082, 1984.
4. E.A. Fehnel and E.D. Amsturz. Ind. Eng. Chem. Anal. **16**, 53 (1944).
5. M.M. Davis and P.J. Schuhmann. J. Research Natl. Bur. Standards. **39**, 221 (1947).
6. Chia-Lin Sun, Yo-T'ein Shen and I. Ch'ing Shen. Hua Hsueh Shih Chieh, **13**, 570 (1958); C.A. **54**, 22486c (1960).
7. D. Thoraval and J.W. Bovenkamp. Canadian Patent Application, 562, 507 (25 March 1988); US Patent Application 263, 186 (27 October 1988) and European Patent Application 89302952 0 (23 March 1988).

8. A. Bax. Two Dimensional Magnetic Resonance in Liquids. Reidel, Boston (1982).

9 L M. Jackman. Applications of Nuclear Magnetic Resonance in Organic Chemistry. Pergamon Press New York, N.Y. (1959).

10. N. Jonathan, S. Gordon and B.P. Dailey. J.Chem.Phys. 36, 2443 (1962).

11. S.L. Patt and J.N. Shoolery. J.Mag.Res. 46, 535 (1982).

12. S. Berger and A.Rieker. Tetrahedron 28, 3123 (1972).

13. J.B. Stothers. Carbon-13 NMR Spectroscopy. Academic Press New York N.Y. (1972).

14. F.J.Weigert and J.D. Roberts. J.Am.Chem.Soc. 89, 2967 (1967).

15. F.W. Wehrli and T. Wirthlin. Interpretation of C-13 NMR Spectra. Heyden New York (1976).

Table 1. $^1$H NMR Chemical Shifts ($\delta_H$ from TMS ± 0.01) for TBPE*

| Position | $\delta_H$ |
|---|---|
| OH | 6.40 |
| H-3,7 | 7.40 |
| H-9 | 7.90 |
| H-13 | 7.40 |
| H-16 | 8.05 |
| H-17 | 7.63 |
| H-18 | 7.68 |
| H-19 | 7.27 |
| H-21 | 4.15 |
| H-22 | 1.20 |

*For 0.1 M solution in 1:1 $CD_2Cl_2$:$CDCl_3$

Table 2. $^{13}C$ chemical shifts for TBPE ($\delta_C$ from TMS ± 0.01)*



| $\delta_C$ | relative intensity | type | assignment |
|---|---|---|---|
| 13.75 | 1 | $CH_3$ | C-22 |
| 61.63 | 1 | $CH_2$ | C-21 |
| 109.83 | 2 | quaternary | C-4,6 |
| 124.02 | 1 | quaternary | C-12 |
| 124 69 | 1 | quaternary | C-10 |
| 129.71 | 1 | quaternary | C-8 |
| 130.26 | 1 | CH | C-17 |
| 130.90 | 1 | CH | C-16 |
| 131.56 | 1 | CH | C-19 |
| 131.53 | 1 | quaternary | C-15 |
| 131.92 | 1 | CH | C-18 |
| 132.62 | 1 | quaternary | C-1 |
| 134.94 | 2 | CH | C-3,7 |
| 139.36 | 1 | CH | C-9 |
| 139.49 | 1 | quaternary | C-14 |
| 139.59 | 1 | CH | C-13 |
| 151.53 | 1 | quaternary | C-2 |
| 158.98 | 1 | quaternary | C-5 |
| 165.47 | 1 | quaternary | C-20 |
| 172.96 | 1 | quaternary | C-11 |

*0.1 M solution in 1:1 $CD_2Cl_2CDCl_3$

Table 3. $^{13}C$ Chemical Shifts for TBPE in acetone-$d_6$ ($\delta_C$ from TMS ± 0.01)*

| $\delta_C$ | relative intensity | assignment |
|---|---|---|
| 14.28 | 1 | $CH_3$(C-22) |
| 62.75 | 1 | $CH_2$(C-21) |
| 117.96 | 4 | C-4,6,10,12 |
| 131.35 | 1 | C-17 |
| 131.55 | 1 | C-16 |
| 132.04 | 1 | C-15 |
| 132.87 | 1 | C-19 |
| 133.02 | 1 | C-18 |
| 133.16 | 1 | C-1 |
| 138.60 | 4 | C-3,7,9,13 |
| 138.89 | 1 | C-14 |
| 140.28 | 2 | C-2,8 |
| 160.72 | 2 | C-5,11 |
| 166.62 | 1 | C-20 |

*0.05 M solution

Table 4 Comparison of Observed $^{13}C$ Shifts for TBPE in Acetone-$d_6$ and Values Predicted On the Basis of Averaging of Shifts in $CD_2Cl_2$-$CDCl_3$.

| site | $\partial_c$ in $CD_2Cl_2$-$CDCl_3$ | average | $\partial_c$ in acetone-$d_6$ |
|---|---|---|---|
| C4,6;C10;12 | 109.83;124.69;124.02 | 117.09 | 117.96 |
| C3,7;C9;13 | 134.94;139.36;139.59 | 137.21 | 138.60 |
| C2;C8 | 151.53;129.71 | 140.62 | 140.28 |
| C5;C11 | 158.98; 172.96 | 165.97 | 160.72 |

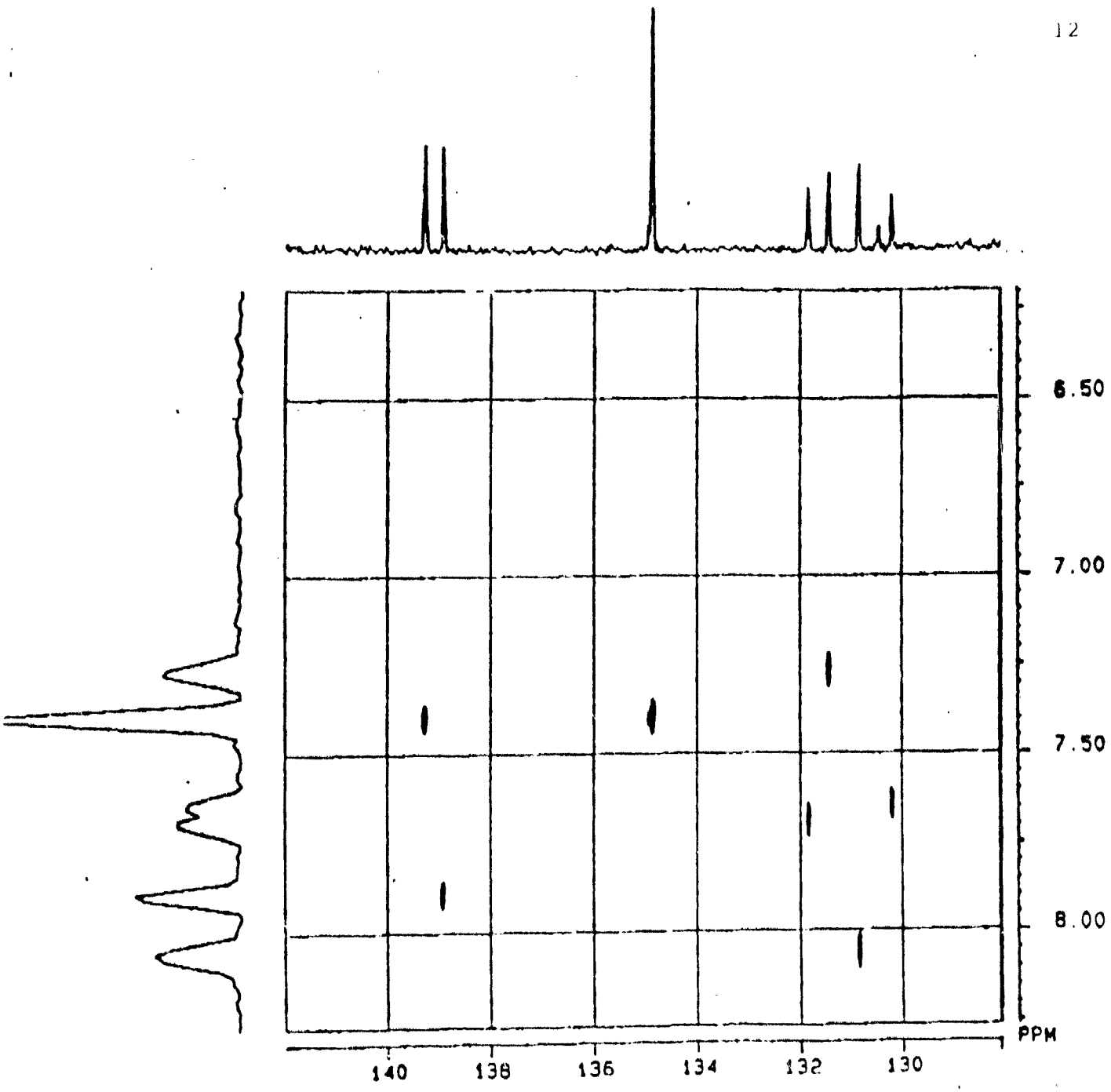


Fig. 1

# USE OF 2D NMR FOR THE ASSIGNMENT OF STRUCTURE OF SOME DEFENCE RELATED COMPOUNDS

C. A. Boulet, S. J. Tregear and A. S. Hansen
Defence Research Establishment Suffield
Medicine Hat, Alberta

ABSTRACT

Organophosphorus nerve agents such as GA, GB, and GD, exist as mixtures of enantiomers. Studies by Benschop and co-workers (TNO) have shown substantial differences in activity between each enantiomer (and sets of diastereomers) of GD. However the synthesis, separation, and purification of the enantiomers of the G agents is laborious and impractical. Since we are interested in investigating the molecular mechanism of the reactivation of inhibited acetylcholinesterase by chiral Hagedorn oximes, a source of chiral phosphorus of known configuration was required.

Reaction of a chiral amino alcohol with an alkyl phosphorodichloridate gives a mixture of diastereomers, epimeric at phosphorus, which can be separated by conventional chromatographic means. A series of diastereotopic 1,3,2-oxazaphospholidine-2-ones were prepared from (+) and (-)-ephedrine. Analysis by 1D and 2D NMR has shown that it may be possible to establish the absolute configaration by NMR techniques. In particular, Nuclear Overhauser Effect SpectroscopY (NOESY) provides information about through-space relationships of protons.

Stereospecific differences in chemical shifts and NOESY spectra for each isomer are used to establish the absolute stereochemistry at phosphorus for (4*R*,5*S*)-2-alkoxy-3,4-dimethyl-5-phenyl-1,3,2-oxazaphospholidine-2-one diastereomers. With the stereochemistry of these compounds established, these cyclic phosphoramidates will provide a source of chiral phosphorus for inhibited acetylcholinesterase reactivation studies.[a]

## INTRODUCTION

Organophosphorus nerve agents, by virtue of a tetrahedral phosphorus, exist as mixtures of enantiomers. Soman contains an additional chiral centre in the pinacolyl moiety giving rise to four stereoisomers. These isomers show stereospecific differences in the rates of AChE inhibition, detoxification, reactivation and toxicological properties. The isomers of soman are usually designated as C(±)P(±) depending on the optical rotatory sign of 3,3-

[a] The relative activity of the 2-phenoxy diastereomers has been investigated in a primary tissue culture assay for measuring anti-Ache activity in chick embryo neurons. Isomer A was found to be the more active isomer; Isomer A: $3.29 \pm 0.90 \times 10^8$ pM, Isomer B: $9.04 \pm 2.7 \times 10^8$ pM. The anti-AChE activity of GA is ~ $3 \times 10^4$ pM. T. S. Sawyer, unpublished data.

dimethyl-2-butanol, "C", (pinacolyl alcohol) or the phosphorus centre, "P".[1] The C(±)P(-) isomers are 1 x $10^5$ times more active AChE inhibitors and 100 fold more toxic (Table 1).[2]

**Table 1.** Bimolecular Reaction Rates for Electric Eel AChE Inhibition and $LD_{50}$ Values for Female (BCBA) $F_1$ Mice for the Four Stereoisomers of Soman.

| | Bimolecular Reaction Rates ($M^{-1}$ $min^{-1}$) | $LD_{50}$ (μg/kg) |
|---|---|---|
| C(+)P(-) | $2.8 \times 10^8$ | 98 |
| C(-)P(-) | $1.8 \times 10^8$ | 38 |
| C(+)P(+) | $< 5 \times 10^3$ | $> 5 \times 10^3$; $< 10^4$ |
| C(-)P(+) | $< 5 \times 10^3$ | $> 2 \times 10^3$; $< 2.5 \times 10^3$ |

The methods employed by Benschop *et al* for the isolation of the stereoisomers of soman, although an elegant demonstration of stereochemistry, are complicated and laborious. The pinacolyl alcohol is resolved into the dextro- and laevorotatory enantiomers using systematic chiral recrystallizations and diastereomeric resolution. From these resolved alcohols, the C(-)P(±) and C(+)P(±) soman isomers were prepared. The pairs of diastereomers are then further resolved using either the stereospecific inhibition of α-chymotrypsin [P(+) isomers] or stereospecific "somanase" hydrolysis [P(-) isomers].

The differences in AChE inhibitory activity and toxicological properties in soman are mainly due to differences in the absolute configuration at phosphorus. Because of the reported differences in reactivation rates of soman inhibited human brain and erythrocyte AChE by therapeutic oximes[3], and this laboratory's ongoing investigation into the medicinal chemistry of HI-6[4], a stereospecific synthesis of chiral AChE inhibitors of known configuration, would be valuable for further inhibition and reactivation studies.

Cyclic phosphoramidates, such as the 1,3,2-oxazaphospholidine-2-ones were chosen as analogues for GA. In the reaction of ephedrine and an alkyl phosphorodichloridate, the stereochemistry at the C-4 and C-5 centres is retained giving a pair of diastereomers differing only in their absolute configuration at phosphorus. These diastereomers should be separable by conventional chromatographic methods. Should substantial differences in the rates of AChE inhibition be observed between diastereomers, these compounds may be suitable models for nerve agent inhibition of AChE.

## EXPERIMENTAL SECTION

### General

All reactions, unless otherwise indicated, were performed under a positive pressure of dry $N_2$. All solvents employed were reagent grade or better. N-methyl morpholine was distilled from NaH and stored over 3 Å molecular sieves. The term *in vacuo* refers to removal of solvent by Buchi Rotavapor at water aspirator vacuum followed by 0.1 Torr vacuum. Thin-layer chromatography was done on E. Merck 0.2 mm precoated silica plastic sheets (60 $F_{254}$); spot detection was done with 254 nm UV light without staining. Preparative layer chromatography was done on E. Merck 1 mm precoated silica gel plates (60 $F_{254}$). Gravity column chromatography was performed on Mallinckrodt 7087 silica gel (SilicAR CC-7 Special). Melting points were taken on a Thomas Hoover capillary melting point apparatus in open capillary tubes and are uncorrected. Angular rotatory powers at the sodium D line were measured with an Optical Activity AA-10 automatic polarimeter and a 0.5 dm sample tube or as otherwise noted.

$^1H$, $^{13}C$, $^{31}P$ NMR spectra were recorded on a Varian VXR 300S spectrometer using standard Varian pulse sequences except where noted. Sample temperature was regulated at 25 C and 2D NMR experiments were run on non-spinning samples in deuterochloroform ($CDCl_3$, 99.8 atom % D, 0.03 % v/v TMS) unless otherwise indicated. $^1H$ and $^{13}C$ NMR spectra were referenced to an internal tetramethylsilane standard at 0.000 ppm. Chemical shifts are reported in $\delta$ ppm units and coupling constants in Hz units. $^{31}P$ NMR spectra were referenced relative to an external triethylphosphate standard at -1.00 ppm. NOESY experimental parameters: spectral width (sw) = 2039 Hz, pulse width (pw) = 14.5 μs, d1 = 4 s, mix = 2.5 s, 512 increments in the second frequency domain (fn = 512) and 16 repetitions at each increment (nt = 16) , NOESY data was zero filled (fn1 = fn) before processing and symmetrization.

The following abbreviations are used herein: h (hours), min (minutes), sec (seconds), rt (room temperature), tlc (thin-layer chromatography), plc (preparative layer chromatography), *c* (concentration, g per 100 ml), *b* (path length, dm), s (singlet), d (doublet), t (triplet), q (quartet), quint (quintet), sep (septet), m (multiplet). Full gas chromatography-mass spectrometric data was obtained for all compounds and will be appear in future publications.

**(4*R*,5*S*)-2-Phenoxy-3,4-dimethyl-5-phenyl-1,3,2-oxazaphospholidine-2-one(1).** Phenylphosphoredichloridate(0.02 mol, 4.22 g) was dissolved in dichloromethane (35 ml) and cooled to 0°C. Separately mixed anhydrous (1*S*,2*R*)-(+) ephedrine (0.022 mol, 3.64 g obtained from (1*S*,2*R*)-(+)-ephedrine hemihydrate dried with $P_2O_5$ *in vacuo* at rt) and N-methyl morpholine (0.044 mol, 4.84 ml) were added dropwise to the phosphorodichloridate solution. The reaction mixture was stirred at 0°C for 135 min. The suspension was filtered, the filtrate concentrated *in vacuo*, dissolved in ethanol: petroleum ether and filtered. The filtrate was again concentrated *in vacuo* and redissolved in dichloromethane, filtered through glass wool, the filtrate concentrated *in vacuo* and vacuum pumped to give a viscous orange oil (6.00 g, diastereomeric ratio 2.02: 1). The major and minor diastereomers were assigned by the $^1H$ NMR methine signals at $\delta$ 5.752 and 5.362 respectively. The oil was gravity column chromatographed on silica (40 % ethyl acetate/petroleum ether) to give pale yellow crystals. Recrystallization from ethyl acetate/petroleum ether gave white platelets (1a, 1.66 g, 27 %): $[\alpha]_D^{24.6}$ + 16° (*c* 2.012, $CH_2Cl_2$; *b*

0.75); mp 129-131°C; $R_f$(EtOAc) 0.53; and white needles (**1b**, 2.41 g, 40 %):$[\alpha]_D^{25.1}$ +104° (c 2.007, $CH_2Cl_2$); mp 97-98°C; $R_f$(EtOAc) 0.35. $^1$H NMR (300 MHz, $CDCl_3$): **1b**, $\delta$ 7.40-7.17 (m, 10 H, Ar), 5.752 (d, $J$ = 6.2 Hz, 1 H, H-5), 3.701 (dquint, $J$ = 17.9, 6.7 Hz, 1 H, H-4), 2.853 (d, $J$ = 10.1 Hz, 3 H, $NCH_3$), 0.634 (d, $J$ = 6.7 Hz, 3 H, Me-4); **1a**, $\delta$ 7.40-7.15 (m, 10 H, Ar), 5.362 (dd, $J$ = 6.4, 3.8 Hz, 1 H, H-5), 3.605 (dquint, $J$ = 12.0, 6.5 Hz, 1 H, H-4), 2.793 (d, $J$ = 10.3 Hz, 3 H, $NCH_3$), 0.804 (d, $J$ = 6.7 Hz, 3 H, Me-4). $^{13}$C NMR (75 MHz, $CDCl_3$): **1b**, $\delta$ 151.29 (d, $J$ = 8.5 Hz, Ar), 135.58 (d, $J$ = 7.[illegible] Hz, Ar), 129.62 (d, $J$ = 0.9 Hz, Ar), 128.42 (s, Ar), 128.25 (s, Ar), 125.65 (s, Ar), 124.94 (d, $J$ = 1.8 Hz, Ar), 120.78 (d, $J$ = 4.5 Hz, Ar), 80.98 (d, $J$ = 3.1 Hz, C-5), 60.06 (d, $J$ = 13.2 Hz, C-4), 29.54 (d, $J$ = 5.5 Hz, $NCH_3$), 13.30 (s, Me-4); **1a**, $\delta$ 151.19 (d, $J$ = 8.9 Hz, Ar), 135.49 (d, $J$ = 7.6 Hz, Ar), 129.68 (d, $J$ = 1.3 Hz, Ar), 128.41 (s, Ar), 126.04 (s, Ar), 124.93 (d, $J$ = 1.3 Hz, Ar), 120.61 (d, $J$ = 4.5 Hz, Ar), 81.09 (d, $J$ = 1.3 Hz, C-5), 58.95 (d, $J$ = 13.2 Hz, C-4), 28.79 (d, $J$ = 4.4 Hz, $NCH_3$), 14.26 (d, $J$ = 3.3 Hz, Me-4). $^{31}$P NMR (121 MHz, $CDCl_3$): **1b**, $\delta$ 14.33 (s); **1a**, $\delta$ 14.24 (s).

**(4*R*,5*S*)-2-Ethoxy-3,4-dimethyl-5-phenyl-1,3,2-oxazaphospholidine-2-one (2).** Ethyl phosphorodichloridate (0.02 mol, 3.26 g) was dissolved in dichloromethane (35 ml) and cooled to 0°C. Separately mixed (1*S*,2*R*)-(+)-ephedrine (0.022 mol, 3.83 g) and N-methyl morpholine (0.044 mol, 4.84 ml) were added dropwise to the phosphorodichloridate solution. The reaction mixture was stirred at 0°C for 2 h. The suspension was filtered, the filtrate concentrated *in vacuo*, redissolved in petroleum ether, filtered and again concentrated *in vacuo* to give a clear colourless oil (1.00 g, 19.6%, diastereomeric ratio 1.38). The major and minor diastereomers were assigned by the $^1$H NMR methine signals at $\delta$ 5.641 and 5.500 respectively. The oil was chromatographed on plc plates (100 % ethyl acetate) to give a pale yellow liquid: $R_f$(EtOAc) 0.25; $R_f$(EtOAc) 0.39. $^1$H NMR (300 MHz, $CDCl_3$): **2a** (minor isomer), $\delta$ 7.41-7.25 (m, 5 H, ArH), 5.501 (dd, $J$ = 6.3, 3.3 Hz, 1 H, H-5), 4.180 (m, 2 H, 2-$OCH_2CH_3$), 3.648 (sep, $J$ = 6.3 Hz, 1 H, H-4), 2.674 (d, $J$ = 10.2, 3 H, $NCH_3$), 1.362 (dt, $J$ = 7.1, 0.6 Hz, 3 H, 2-$OCH_2CH_3$), 0.797 (d, $J$ = 6.6 Hz, 3 H, 4-$CH_3$); **2b** (major isomer), 7.41-7.21 (m, 5 H, 5-Ph), 5.638 (dd, $J$ = 6.3, 2.2 Hz, 1 H, H-5), 4.223 (m, 2 H, $OCH_2CH_3$), 3.672 (dq, $J$ = 16.5, 6.6 Hz, 1 H, H-4), 2.714 (d, $J$ = 10.2 Hz, 3 H, $NCH_3$), 1.400 (dt, $J$ = 7.2, 0.6 Hz, 3 H, 2-$OCH_2CH_3$), 0.759 (d, $J$ = 6.6 Hz, 3 H, 4-$CH_3$).

## RESULTS AND DISCUSSION

(4*R*,5*S*)-2-Phenoxy-3,4-dimethyl-5-phenyl-1,3,2-oxazaphospholidine-2-one (**1**) and (4*R*,5*S*)-2-ethoxy-3,4-dimethyl-5-phenyl-1,3,2-oxazaphospholidine-2-one (**2**) were prepared from (1*S*,2*R*)-(+)-ephedrine in moderate yield (Scheme 1). The synthesis and conformational analyses of **1** have been previously described.[5] The diastereomers were readily separable by preparative layer and column chromatography. Recrystallization of the solid 2-phenoxy diastereomers afforded high purity products whereas the 2-ethoxy derivative necessitated repeated plc to obtain pure samples.

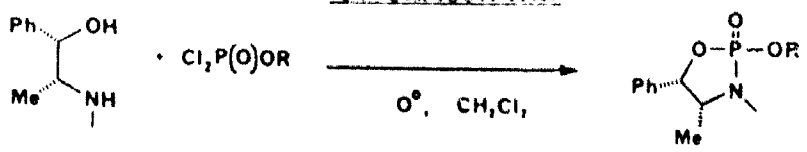


Scheme 1

R = Ph(1); Et(2)

Assignments of the $^1H$ chemical shifts were straightforward and are given in the experimental section.[b] The 1,3,2-oxazaphospholidine-2-ones possess several structural and stereochemical features which make the use of the NOESY experiment attractive for establishing the absolute configuration at phosphorus. Although x-ray analysis has been used to unambiguously assign the solid-state configuration of one diastereomer of 1[6], not all 1,3,2-oxazaphospholidines are solids, making the NOESY experiment particularly attractive for studying solution-state configurations.

The synthesis affords a mixture of diastereomers, epimeric at P, where the 2-alkyl substituent (R = ethyl, phenyl) is either *cis* or *trans* with respect to H-4 and H-5. The NOE effects between the P-OR group and either the H-4,5 or 4-$CH_3$ and 5-phenyl substituents should be identifiable. In the NOE experiment, the longitudinal magnetization of one nucleus can result in changes in the equilibrium magnetization of other nuclei through mutual, non-J-coupled, relaxation. In the conventional NOE experiment, one nucleus is saturated through the use of a selective 180° pulse and the transfer of magnetization to another nucleus is observed as a function of time.

The NOESY experiment[7] allows for all NOE effects to be observed at once in a 2D manner without operator prejudice. However, in the literature, there are few examples NOESY experiments for small molecules due to practical limitations, chiefly due to the long relaxation delay and mixing times required for such experiments. The initial rate of intensity change for a nucleus A upon perturbation of the z magnetization of X, as described by Bax[8] is dependent on the angular proton frequency ($\omega$), the correlation time ($\tau$, time to tumble through one radian), and interproton distance (r). Thus the rate of NOE buildup (the intensity of the off-diagonal peak) is proportional to $r^{-6}$ and on the correlation time ($\tau$). Small molecules have relatively small $\tau$ values requiring long mixing times in the order of $T_1$, the longitudinal relation time, which can be long for small molecules. Careful

[b] Integration of the H-5 proton signals was used to determine the relative ratio of diastereomers in the crude reaction products. In this paper no attempt is made to describe the conformation of the 1,3,2-oxazaphospholidine-2-one ring system. Although the conformation of five-membered rings is usually discussed in terms of envelope or half-chair conformations, it is apparent from the NMR data (reference 5) that the these heterocycles do not have simple half-chair or envelopes conformations. X-ray analysis of 1b (S. J. Tregear and G. W. Bushnell, unpublished data) that the conformation of the ring is nearly planar except at C-1 which dips slightly out of the pseudoplane of the ring.

optimization of parameters is required to obtain meaningful data. Usually, the preaquisition delay (d1) is set at 1-3$T_1$ and the mixing time is in the order of $T_1$.

The NOESY experimental parameters were optimized based on the measured $T_1$ values for the 1,3,2-oxazaphospholidines. Values ranged from 2.5 sec for H-4/5 to 0.5 sec for the 4-$CH_3$. Pulse widths were also optimized. Experiments showed that variations in the preaquisition delay and the mix times had dramatic changes on the spectrum. With d1 = 1 sec and a mix time of 0.1 sec, there was little cross-peak information and the diagonal showed a number of artifacts as well as a greatly enhanced water signal at 1.58 ppm which was imperceptible in the high resolution 1D NMR. Increasing the mix time gave enhanced cross peaks and parameters of d1 = 4 and mix = 2.5 were used for the NOESY experiments.

Analysis of the NOESY spectra for the diastereomers of **1** is complicated by the overlapping aromatic signals. For five and six membered phosphorus heterocycles, it is well established that protons in a 1,3-cis relationship to the P=O group are deshielded.[9] For example, five member bicyclic phosphoramides show a $\Delta\delta$ deshielding effect of 0.2-0.6 ppm for protons *cis* to the P=O.[10] Analysis of the anisotropic effects of the P=O on the chemical shifts of the various substituents is important for the assignment of the overlapping aromatic signals. Table 2 shows the $\Delta\delta$ ($\delta$ **1b** major isomer - $\delta$ **1a** minor isomer) for each substituent. Where a positive $\Delta\delta$ is observed, the substituent in **1b** is *cis* to the P=O; where a negative $\Delta\delta$ is observed, the substituent is *trans* to P=O. Figure 1 shows the distinct H-5 doublet and doublet of doublets at $\delta$ 5.752 and 5.362 respectively for the major (**1b**) and minor (**1a**) isomers of 2-phenoxy-1,3,2-oxazaphospholidine-2-one. Thus, in **1b**, the P=O is *cis* to H-5; in **1a**, the P=O is *trans* to H-5.

The NOESY data is consistent with the 1D NMR data; however, careful analysis is required due to the overlapping phenyl signals. Figure 2 shows a comparison of the aromatic regions of the NOESY spectra for the diastereomers of **1**. In addition, it is expected that there will be approximately the same NOEs observed between the 5-phenyl and H-4, H-5, and 4$CH_3$ in both diastereomers.In the NOESY spectum of **1a**, two sets (lines) of crosspeaks are observed. In the spectrum of **1b**, these crosspeaks now appear on a single line further indicating that it is 5-phenyl group that is deshielded by the *cis* P=O.

**Table 2.** Anisotropic Chemical Shifts Differences ($\Delta\delta$) for the Various Substituents of 2-Phenoxy-1,3,2-oxazaphospholidine-2-one (**1**).

| Substituent | Isomer **1b** $\delta$ (ppm) | Isomer **1a** $\delta$ (ppm) | $\Delta\delta$ (ppm) |
|---|---|---|---|
| 4-$CH_3$ | 0.634 | 0.804 | -0.170 |
| $NCH_3$ | 2.853 | 2.793 | 0.060 |
| H-4 | 3.701 | 3.605 | 0.960 |
| H-5 | 5.752 | 5.362 | 0.390 |
| 5-Ph | 7.25 | 7.30 | -0.05 |
| 2-OPh | 7.34 | 7.19 | 0.15 |

In the NOESY spectrum of **1a**, there is a clear NOE crosspeak between the 2-OPh and H-5. From this analysis, **1a** is thus assigned the *R* absolute configuration and **1b** the *S* configuration at phosphorus.

The 1D $^1$H NMR and NOESY spectra of the 2-ethoxy-1,3,2-oxazaphospholidine-2-one diastereomers were also examined. A distinct downfield shift is observed for the H-5 protons: $\delta$ 5.638 (**2b**) and 5.501 (**2a**) (Figure 3). By analogy to the previous 2-phenoxy assignments, in **2b**, where H-5 is deshielded relative to the other diastereomer, the P=O is *cis* to H-5 and the 2-OEt group is *trans*; in **2a**, the P=O is *trans* to H-5.

The 2-ethoxy-1,3,2-oxazaphospholidine NOESY spectra are more easily interpreted because the NOEs of interest are well separated. Figure 4 shows the NOESY spectra of both diastereomers. For **2a**, where the 2-ethoxy group is *trans* to the 4-$CH_3$ and 5-phenyl groups, the only cross peak of relevance is that between the 2-O$CH_2$$CH_3$ methylene protons and H-5. In contrast, the NOESY spectrum of the major diastereomer, **2b**, where the 2-ethoxy group is *cis* to the 4-$CH_3$ and 5-phenyl groups, clearly shows a number of cross-peaks as expected. Cross-peaks are observed between the 2-O$CH_2$$CH_3$ methylene protons and the 5-phenyl, 4-$NCH_3$, and the 4-$CH_3$, clearly establishing the configuration at phosphorus. From this analysis, **2a** is thus assigned the *S* absolute configuration and **2b** the *R* configuration at phosphorus.[c]

[c] Although the relative configuration is the same in the 2-ethoxy and 2-phenoxy diastereomers, the absolute configuration is reversed due to a change in the priority rules.

## CONCLUSIONS

NMR is a powerful method for the analysis of stereochemistry and 1- and 2-dimensional experiments provide complementary data for the unambiguous assignment of absolute stereochemistry. From the 1D and 2D NMR data absolute configuration of the diastereomers of (4*R*,5*S*)-2-phenoxy-3,4-dimethyl-5-phenyl-1,3,2-oxazaphospholidine-2-one are as follows; **1a** (minor isomer) 2*R*; **1b** (major isomer) 2*S*. The absolute configuration of the diastereomers of (4*R*,5*S*)-2-ethoxy-3,4-dimethyl-5-phenyl-1,3,2-oxazaphospholidine-2-one are: **2a** (minor isomer) 2*S*; **2b** (major isomer) 2*R*. NOESY allows for the analysis of all potential NOE interactions. Careful selection of experimental parameters is required in order to obtain good NOESY data. These NOESY experiments provide an independent corroboration of other methods established in the literature. The establishment, by NMR, of the stereochemistry of these cyclic phosphoramidates now affords a series of potential acetylcholinesterase inhibitors for which the absolute stereochemistry at phosphorus is established.

## REFERENCES

1. Benschop, H. P.; Konings, C. A. G.; de Jong, L. P. A. *J. Am. Chem. Soc.*, **1981**, 103, 4260.

2. Benschop, H. P.; Konings, C. A. G.; Van Genderen, J.; de Jong, L. P. A. *Toxicol. Appl. Pharmacol.* **1984**, 72, 61.

3. (a) de Jong, L. P. A.; Wolring, G. Z. *Biochem. Pharmacol.* **1984**, 33, 119. (b) de Jong, L. P. A.; Kossen, S. P. *Biochimica et Biophysica Acta*, **1985**, 830, 345.

4. Clement, J. G.; Lockwood, P. A., *Toxicol. Appl. Pharmacol.*, **1982**, 64, pp 140-146.

5. Setzer, W. N.; Black, B. G.; Hovanes, B. A. *J. Org. Chem.*, **1989**, 54, 1709 and references therein.

6. Setzer, W. N.; Black, B. G.; Hubbard, J. L. *Phosphorus, Sulfur, Silicon Relat. Elem.*, **1990**, 47, 207

7. Jeener, J., Meier, B. H., Bachmann, P., Ernst, R. R. *J. Am. Chem. Soc.* **1979**, 101, 6441.

8. Bax, A.D., Lerner, L. *Science*, **1986**, 232, 960.

9. Quin, L. D. *The Heterocyclic Chemistry of Phosphorus*, Wiley-Interscience, New York, 1981.

10. Peyronel, J.-F.; Samuel, O.; Fiaud, J.-C., *J. Org. Chem.*, **1987**, 52, 5320.

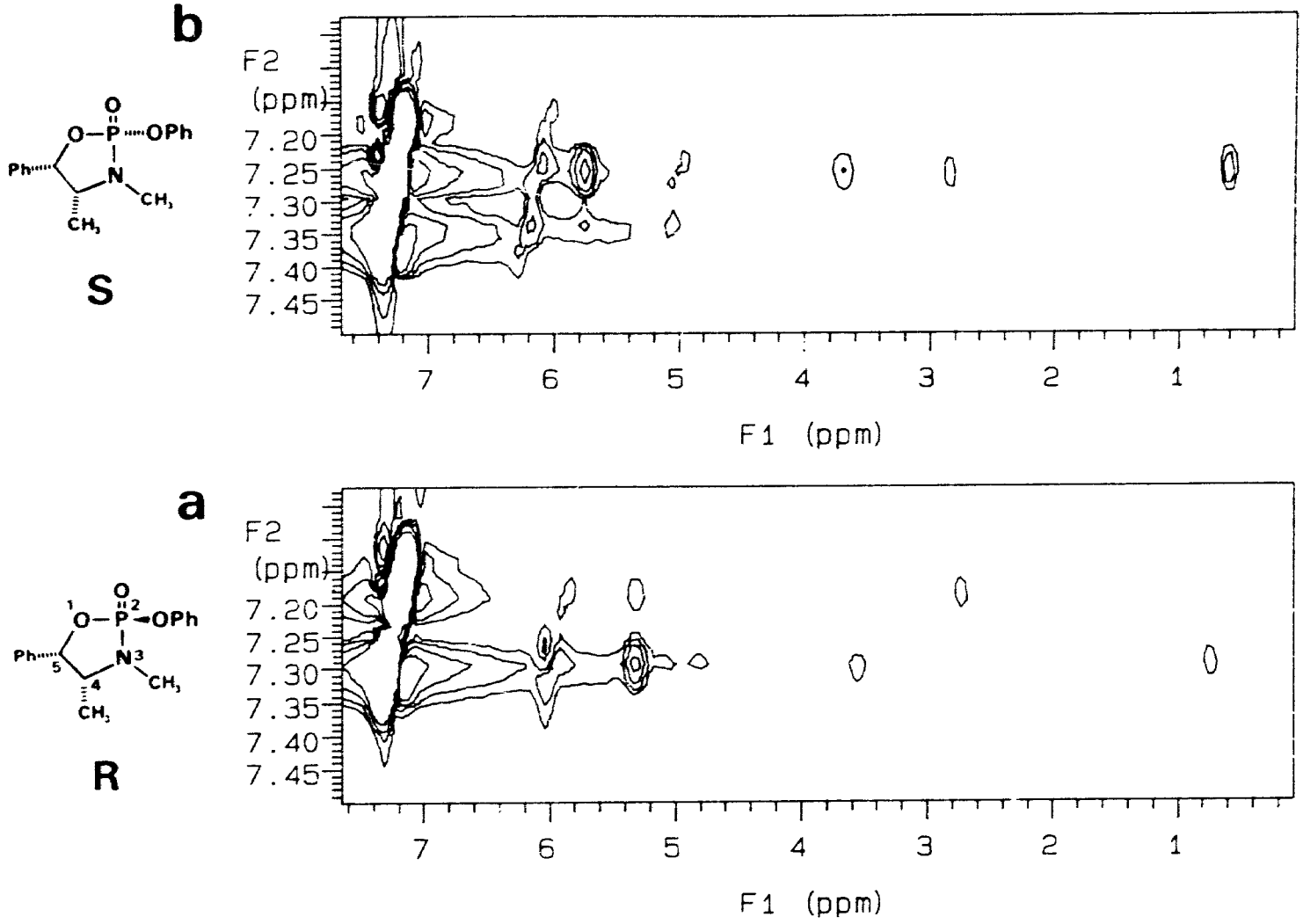


Figure 1. Comparison of the aromatic regions of the NOESY spectra for the minor (1a) and major (1b) diastereomers of 2-phenoxy-1,3,2-oxazaphospholidine-2-one (data is not symmetrized).

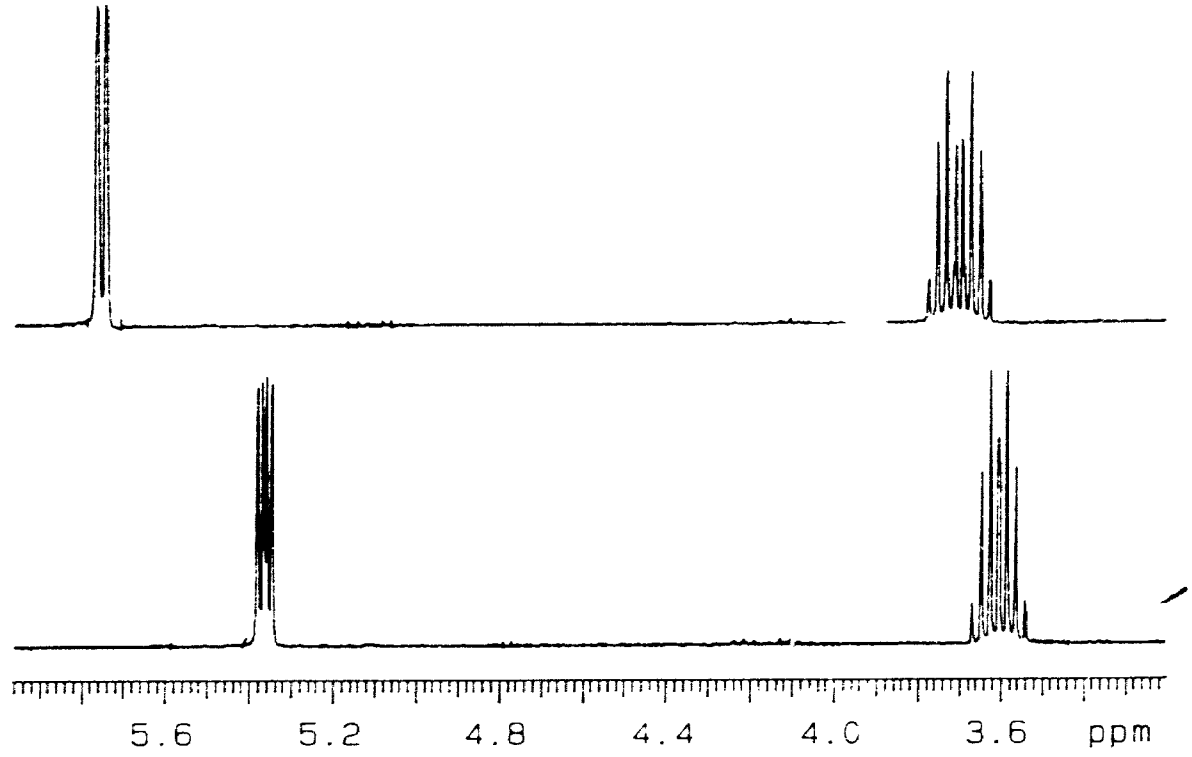


Figure 2. In the 1D NMR spectra, a distinct deshielding of the H-5 proton (**1a**, $\delta$ 5.362 , doublet of doublets; **1b**, $\delta$ 5.752 doublet) for the diastereomers of 2-phenoxy-1,3,2-oxazaphospholidine-2-one is observed. In **1b**, the P=O is *cis* to H-5; **1a** has a *trans* P=O. From this analysis, **1a** is assigned the 2*R* absolute configuration and **1b** the 2*S* configuration.

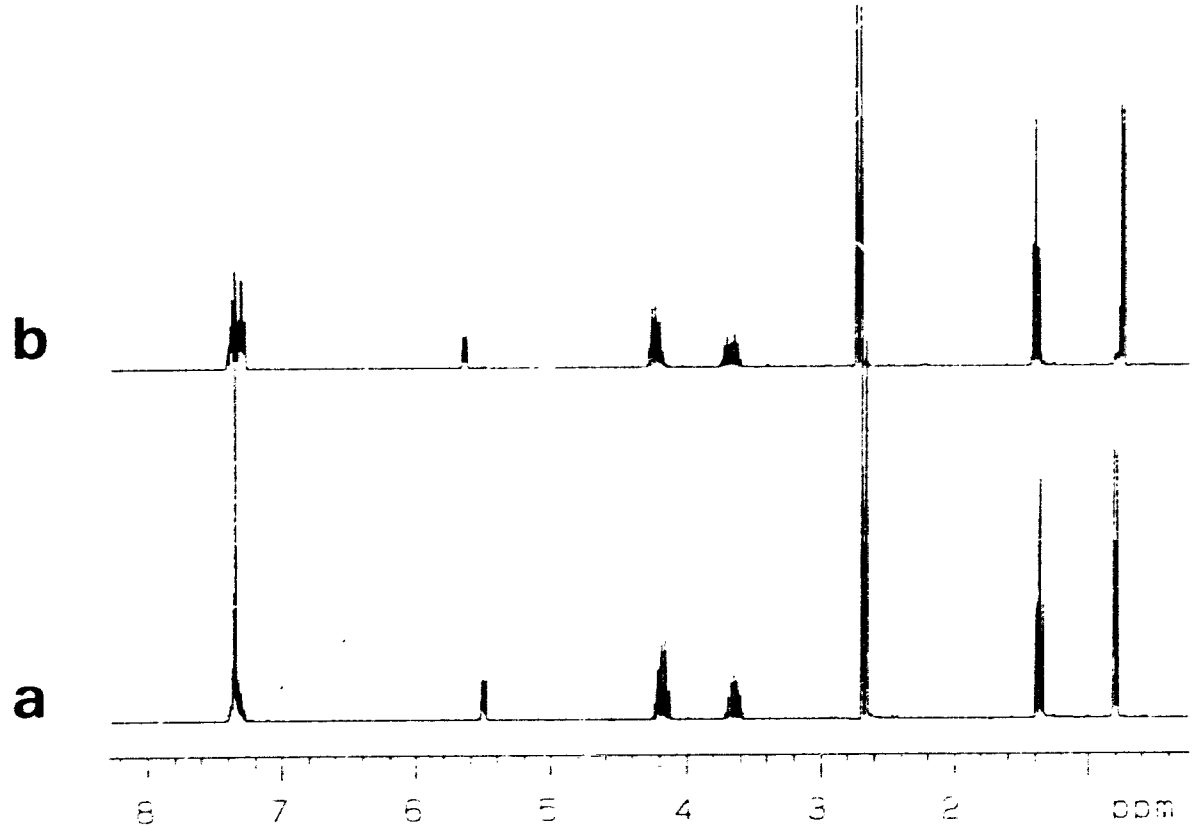


Figure 3. Comparison of the 300 MHz $^1$H NMR spectra of the diastereomers of 2-ethoxy-1,3,2-oxazaphospholidine-2-one showing the distinct downfield shift for the H-5 protons; $\delta$ 5.638 (**2b**) and $\delta$ 5.501 (**2a**). In **2b**, where H-5 is deshielded (P=O *cis*), the configuration is assigned as 2*R*; **2a** is assigned as the 2*S* configuration.

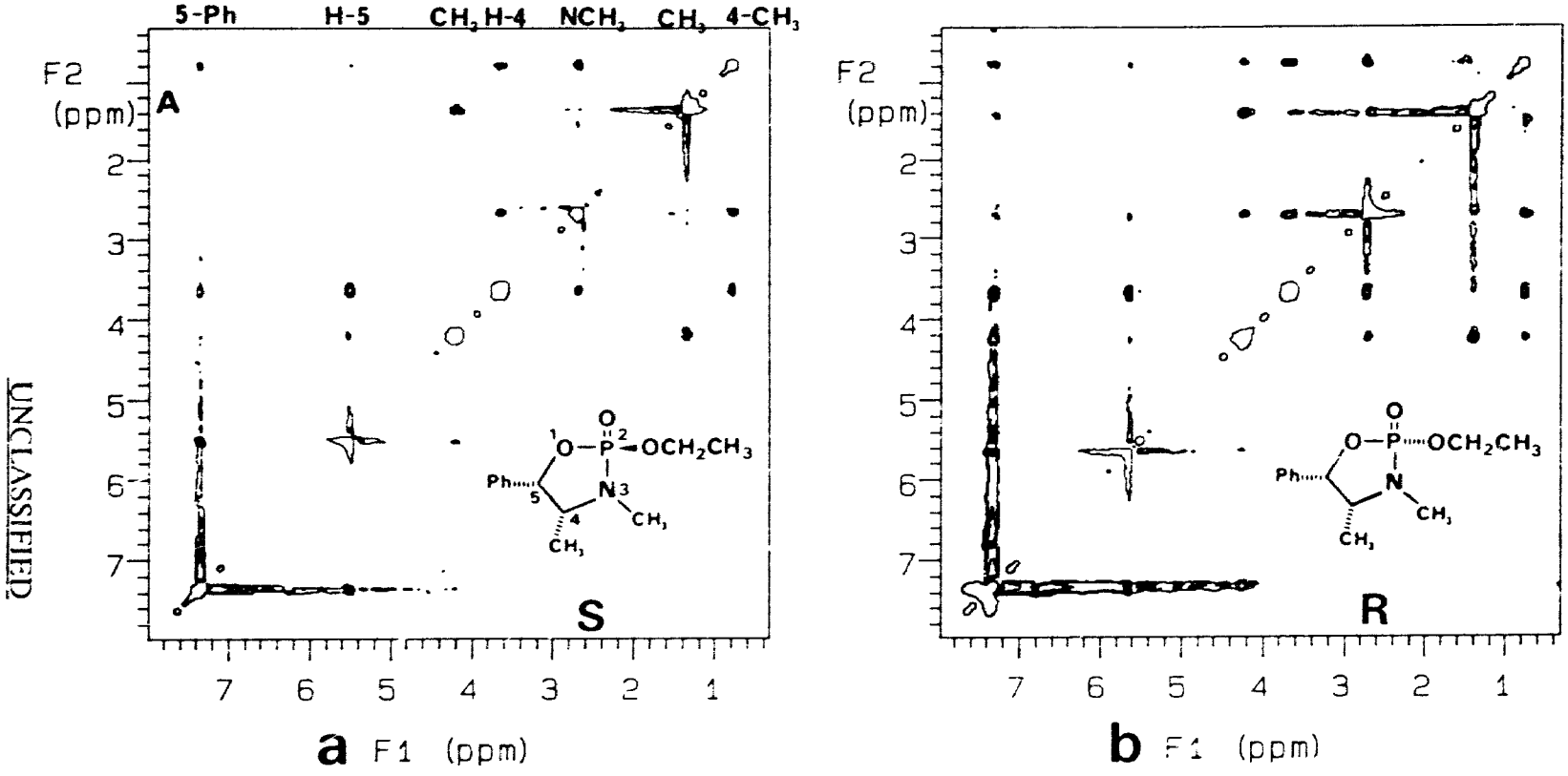


Figure 4. Comparison of the NOESY spectra of 2-ethoxy-1,3,2-oxazaphospholidine-2-one (data is symmetrized). The NOESY spectrum of **2b**, where the 2-ethoxy group is *trans* to H-4,5, clearly shows a number cross-peaks expected for this conformation. Cross-peaks are observed between the 2-$OCH_2CH_3$ methylene protons and the 5-phenyl, 4-$NCH_3$, and the 4-$CH_3$, clearly establishing the configuration of the 2-ethoxy group.

# SEARCH AND RETRIEVAL OF 13C NMR DATA[1]

DERYCK A. ROSS

DIRECTORATE OF SCIENTIFIC INFORMATION SERVICES

RESEARCH AND DEVELOPMENT BRANCH

DEPARTMENT OF NATIONAL DEFENCE

OTTAWA, CANADA

## I. INTRODUCTION

Roberts (1) and Jackman (2) have described the phenomenon of nuclear magnetic resonance. No further introduction needs to be given to this group.

From 1963 - 1965, I studied conformational effects on the chemical shifts of the carbinol carbon for the cis and trans isomers of 4-t-butyl-cyclohexanol (3). Further, a new approach to conformational analysis by 13C NMR was reported in 1966. (4).

The interpretation of the structures of complex organic molecules can be made by NMR spectroscopy (2). Besides 13C, other nuclei can be used in structure determinations by NMR, such as: 31P, 29Si, 19F, and 1H.

## II. RETRIEVAL OF 13C NMR DATA IN THE DEFENCE LITERATURE. THE DSIS EXPERIENCE

I now turn to what was retrieved from an SDI profile on NMR and molecular structure. This represents 15 years of retrievals by this profile in the defence literature. The concept map of the profile is shown on the next page.

Tague and Austin have described the transition from librarian to information scientist on educational grounds (5). They believe that prior distinction in the profession are disappearing.

1 This paper was presented at the 1990 Annual CAIS Conference at Queen's University, Kingston, Ontario, 26 May 1990

# DSIS NMR SDI PROFILE

**Subject area:** NMR and Stereochemistry

**Concept Map:**

**A. OR Logic**

Magnetic resonance )
Magnetic Fields )
Spin spin interactions )
Coupling(interaction) )
Couplings )
Coupling constants )
Spin lattice relaxation)
Coupling (interaction) )

and logic

**B. OR Logic**

(Stereochemistry
(Molecular Structure
(Steric hindrance
(Chemical equilibrium
(Free energy
(Carbon isotopes
(Vicinal
(Geminal
(Karplus
(Conformation

I wrote earlier about defence scientific information and the user-provider interface (6). The paper describes the work of the information scientist in the Directorate of Scientific Information Services (DSIS).

In 1975, I made the transition to information scientist and constructed my own SDI (selective dissemination of information) profile on NMR data and molecular structure determination.

This paper describes some results of the profile, which has now run for fifteen (15) years, without undue change. The following, therefore, are some key questions to be answered concerning this profile:

a) What numbers have been retrieved, ie, how many "hits" in 15 years"

b) What is the percentage relevancy?

c) What percent of the nuclei are 13C nuclei?

d) What other nuclei in the papers are retrieved?

e) What percent are Defence Purposes Only, and what percent are unlimited?

f) Where do our retrievals come from? ie, university, government labs, industry.

g) Are we missing anything if we do not search the defence literature?

## (a) WHAT NUMBERS HAVE BEEN RETRIEVED?

The total number of "runs" or passes per year with the profile is equal to the total number of tapes of the US Defense Technical Information Center (DTIC) matched with my profile. There are twenty-four (24) tapes each year, and the profile has run for 15 years. The total number of runs is, therefore, 360. This is shown in Table 1. The total number of retrievals of the profile was found to be 180. One hit is retrieved, therefore, every second run (Table 1).

## (b) WHAT IS THE PERCENTAGE RELEVANCY?

There were two boxes of microfiche collected and viewed. These are denoted "Box I" and "Box II". Please see Table 2). (SDI) Profile results). Seventy-four (74) of these microfiche were found to be relevant to my requirements - for which the criteria included: spectra given, molecular structure assessed, NMR used etc - while seventy-nine (79) were not: twenty-seven (27) did not have microfiche but were assessed by printout. Most of these were Defence Purposes Only fiche for which I had no legitimate need-to-know. Please see next viewgraph. These data are given in Table 2. The percentage relevancy was 41.0%. As there was some difficulty assessing the category for which microfiche were not available, if could be inferred that the relevancy was close to 1 in 2.

Thus, the profile was very precise, and the relevancy could not be enhanced much by making the profile broader. One could conclude that there was not a lot in the classified or limited defence literature on this topic.

## (c) WHAT PERCENTAGE OF NUCLEI ARE 13C NUCLEI?

Table 3 shows the individual results by "box" (Box I was relevant to my need; Box II was not relevant) for different nuclei. As we have seen earlier, 13C is not the only nucleus to undergo magnetic resonance. From the results in Table 3, it can be seen that from the relevant hits, the 13C nucleus data comprised 27.0% of the retrievals. The caption "multi-nuclear" should be interpreted with some caution, as it not only includes studies of other nuclei (1H, 29Si, 31P etc.) but also those cases where the actual nucleus examined could not be determined (ie NMR studies).

For "Box II" (irrelevant bits), this 27.0% had dropped to 11.4%, a not surprising result. Here the "catch-all" category had risen to 52.0%.

## (d) WHAT OTHER NUCLEI WERE STUDIED?

Table 4 shows the results in total. Almost as many papers used 1H as 13C nuclei in their NMR results. Together, they accounted for almost as many hits as, the "catch-all" category (multi-nuclear), and when combined these accounted for almost 80% of the retrievals. This table also shows the results for the other nuclei.

## (e) WHAT PERCENTAGE ARE DEFENCE PURPOSES ONLY, AND WHAT PERCENTAGE UNLIMITED PAPERS?

The totals for Box I and Box II for unlimited fiche (ADA fiche; NTIS fiche) was 158. The total Defence Purposes Only Fiche, for which a need-to-know would be required, was 22. This equals 12.2% DPO; 87.8% unlimited; nil classified. Please see Table 5).

## (f) WHERE DO THESE REPORTS COME FROM?

Table 6 shows graphically where these "hits" or printouts come from. Sixty-seven (67%) come from US universities (2-3); 17% come from the US military agencies, including FSTC and US Armed Forces translations of East block work; and 11% are from other sources, including Norway, France, Israel, and private US companies or organizations. Three (3%) come from Canada. (CRAD DRE's (DREO) and a Canadian University - York).

Much of the US Military sources are Defence Purposes Only sensitivity, and much of the US university work was funded by the US Armed Forces. Several of the retrievals are reprinted from journals.

## (g) ARE WE MISSING ANYTHING BY NOT SEARCHING THE DEFENCE LITERATURE?

From the foregoing, it can be discerned that very little is being retrieved with the current profile from the defence limited literature.

That concludes what I want to say about retrieval of 13C NMR data, let us now turn to the problem of searching the 13C NMR file on STN.

## III. Searching the 13C NMR File on STN[2]

STN International is operated in North America by Chemical Abstracts Service (CAS), a division of the American Chemical Society; in Europe by FIZ Karlsruhe; and in Japan, by JICST (The Japan Information Center of Science and Technology). All three are non-profit organizations. (7).

STN's special advantages include:

(a) advanced chemical structure searching;

(b) easy searching of comprehensive databases, such as Ca, IFIPAT, JICST, and NTIS;

2 Information about STN International is reprinted with the permission of the American Chemical Society.

(c) numeric searching capabilities;

(d) attentive, knowledgeable help desk staff and extensive on-line help messages;

(e) chemical reaction information, including access to multi-step reactions;

(f) thorough documentation, (7).

STN offers information in a variety of areas including chemistry, engineering, math, physics, geology, biotechnology, thermodynamics, energy, patents, and materials science. STN's bibliographic, structure, numeric, and full text databases complement and enhance one another (7).

Of interest to us to-day is the 13C NMR/IR File, only available through STN, from FIZ Karlsruhe in West Germany. From this database, one can identify chemical structures or substructures from the 13C NMR spectra (7).

In 13C NMR/IR, one will find some 88,000 13C NMR spectra for 71,400 compounds and 8,500 IR spectra for 8,300 compounds. Using 13C NMR/IR, one can easily identify organic chemical structures or sub-structures. 13C NMR/IR is produced by BASF Aktiengesellschaft and updated annually. (7).

The File is menu driven and a few illustrations of the output follow:

Users can connect to STN as usual, up to the point where selection of a port is required. Instead of x- the n- port must be chosen. Once connection to Karlsruhe is complete, the system will load and prompt for login ID and password. The successful connection results in the main menu appearing (8).

One can operate solely in text mode. (This is what I have done), but it is recommended that one have a standard video terminal (24 lines, 80 columns). If you wish to use graphic mode, you will need a terminal/software emulation that is supported by the program. The software emulation that can be used are: TGRAF, PCPLOT and STN Express (which DSIS has). Currently, supported graphic cards are Hercules and EGA.

The 13C NMR File gives information on "chemical shifts" and "coupling constants". This is a numeric database for use by chemists and is menu driven. 2D- of structures only is given; however, graphical representation is possible with different terminals and settings.

The IR File was not used in this report.

## IV. Conclusions

In conclusion, I have described briefly the phenomenon of nuclear magnetic resonance and the application of 13C NMR to structural problems in organic chemistry; I have described the results of my own SDI profile in the defence literature which covers NMR data and chemical structure; and I have taken you through a very brief tour of the 13C NMR File which is available on STN.

I conclude that there are ways for the information professional help the chemist through search and retrieval of 13C NMR data as shown.

## V. BIBLIOGRAPHY

1. Nuclear magnetic resonance: applications to organic chemistry, John D. Roberts 1959.

2. Applications of nuclear magnetic resonance spectroscopy in organic chemistry. L.M. Jackman 1964.

3. 13C NMR studies of some aliphatic and alicyclic compounds, D.A. Ross, M.Sc Thesis, University of Western Ontario, London, Ontario 1966.

4. A new approach to conformational analysis. Carbon - 13 nuclear magnetic resonance. G.W. Buchanan, D.A. Ross, and J.B. Stothers J. Am Chem Soc 88, 4301, (1966).

5. From librarian to information Scientist; Education directions for a changing profession. Jean Tague and Jill Austin, Can J. Information Science, Vol 11, No. 1, pg 24-40, 1986.

6. Defence Scientific Information. The user-provider Interface D.A. Ross, Can. J. Information Science, Vol 3 pg 158-175, May 1978.

7. Databases in Science and Technology. STN International, 1989.

8. 13C NMR/IR User Manual, May 1989.

## TABLE 1 % RECALL OF SDI PROFILE

Total No. of retrievals = 180

Total no. of SDI "runs"

24 ea. year

x 15 years = 360

Total no. hits/run = $\frac{180}{360}$ = 0.5

## TABLE 2 SDI PROFILE RESULTS

| | | | |
|---|---|---|---|
| Box I | Relevant Hits | 18 | |
| | Not Relevant Hits | 28 | |
| | No microfiche (printout only) | 12 | |
| | | 58 | Box I and Box II = 122 |
| | | | 58 |
| | | | 180 |
| Box II | Relevant Hits | 56 | |
| | Not Relevant Hits | 51 | |
| | No Microfiche (printout only) | | 122 |

Box I and Box II

| | No microfiche | Not relevant | Relevant | Total |
|---|---|---|---|---|
| Box I | 12 | 28 | 18 | 58 |
| Box II | 15 | 51 | 56 | 122 |
| Total | 27 | 79 | 74 | 180 |
| 100.0% | 15.0% | 44.0% | 41.0% | |

TABLE 3 INDIVIDUAL RESULTS SDI PROFILE

| | Box I * | | Box II + | |
|---|---|---|---|---|
| 13C | 20 | 27.0% | 9 | 11.4% |
| 1H | 10 | 13.5% | 18 | 22.8% |
| 19F | 3 | 4.0% | 1 | 1.3% |
| 29SI | 10 | 13.5% | 3 | 3.8% |
| 31P | 5 | 6.8% | 3 | 3.8% |
| 170 | 3 | 4.0% | 1 | 2.3% |
| 11B | 2 | 2.7% | 3 | 3.8% |
| Multi-nuclear | 21 | 28.4% | 41 | 51.9% |
| Total | 74 | 99.9% | 79 | 100.1% |

* Box I was "relevant hits".

\+ Box II was "not relevant to needs, hits".

TABLE 4 NUMBER OF RETRIEVALS BY NUCLEI

| Nucleus | Relevant | Not Relevant | Total | % |
|---|---|---|---|---|
| 13C | 20 | 9 | 29 | 19.0% |
| 1H | 10 | 18 | 28 | 18.3% |
| 19F | 3 | 1 | 4 | 2.6% |
| 29SI | 10 | 3 | 13 | 8.5% |
| 31P | 5 | 3 | 8 | 5.2% |
| 17O | 3 | 1 | 4 | 2.6% |
| 11B | 2 | 3 | 5 | 3.3% |
| Multi-nuclear + | 21 | 41 | 62 | 40.5% |
| Total | 74 | 79 | 153 * | 100.0% |

* Not including the 27 which did not have microfiche with the SDI printout.

\+ A combination of nuclei including , e.g., 31P, 29SI, 13C, 1H etc.

## TABLE 5 SENSITIVITY OF RETRIEVALS

| | | | |
|---|---|---|---|
| Box I | Unlimited | 71 | |
| | Defence Purposes Only | 1 | |
| | Classified | - | |
| Box II | Unlimited | 79 | |
| | Defence Purposes Only | 1 | |
| | Classified | - | |
| Sheets (SDI) Only | Unlimited | 8 | |
| | Defence Purposes Only | 20 | |
| | Classified | - | |
| Total | Unlimited | 158 | 87.8% |
| | Defence Purposes Only | 22 | 12.2% |
| | Classified | - | |
| | | 180 | 100% |

TABLE 6 WHERE THE PRINTOUTS COME FROM

| | No. | % |
|---|---|---|
| US University | 120 | 66.6% |
| Can University | 2 | 1.1% |
| Can DRE | 3 | 1.6% |
| US Military incl. incl FSTC DPO | 31 | 17.2% |
| UK Origin | 5 | 2.8% |
| Other Including Israel, Norway, France | 20 | 11.1% |
| Total | 181 | 100.4% |

# GAS CHROMATOGRAPHY-MASS SPECTROMETRY: A TECHNIQUE FOR THE VERIFICATION OF CHEMICAL WARFARE AGENTS AND RELATED COMPOUNDS

Paul A. D'Agostino
Defence Research Establishment Suffield,
P.O. Box 4000, Medicine Hat, Alta., T1A 8K6.

## INTRODUCTION

Verification of chemical warfare agents and related compounds generally involve the following three steps:

1. Sample Collection

2. Sample Storage and Handling/Clean-up

3. Sample Analysis

The last step, sample analysis, while very dependent on representative sampling and adequate storage and clean-up, often requires detection and confirmation of the analyte of interest by capillary column gas chromatography-mass spectrometry (GC-MS). GC-MS is often the method of choice for chemical warfare agent analyses requiring a high degree of certainty, as this technique offers the analyst excellent sensitivity and specificity. This paper describes some considerations during sample analysis by GC-MS and illustrates the importance of GC-MS for the verification of organophosphorus and organosulfur compounds of chemical defence interest.

Prior to analysis of samples by GC-MS, consideration should be given to acceptable criteria for confirmation, the utility of mass spectral libraries (hardcopy or computer searchable) and the type of analysis required.

GC-MS criteria for confirmation can be broken down into the following three general levels depending on the evidence collected for a compound of interest (1,2).

1. Tentative Structural Assignment

   * Library match of acquired electron impact (EI) mass spectrum.

2. Confident Structural Assignment

   * Library match of acquired EI mass spectrum and one of chemical ionization (CI) data (especially in the absence of a molecular ion), accurate mass (± 0.005 u) on molecular ion or GC retention data.

3. Confirmed Structural Assignment

* EI, CI mass spectra (or accurate mass) and GC retention data acquired agrees with that of an authentic sample. Generally applicable for ng levels and above.

* Selected Ion Monitoring (SIM) on a minimum of three ions (often difficult for CI), molecular ion information and GC retention data acquired agrees with that of an authentic sample. Generally applicable for sub-ng levels.

Consideration should also be given to the use of specific GC detectors (e.g., FTIR, ECD, FPD, NPD) as this complementary data may lend support to the confirmation of a compound of interest. Good QA/QC practices, including replicate analyses with appropriate blanks and an estimate of method detection limit, should also be considered.

Mass spectral libraries, while common to most mass spectrometer data systems, should be used with discretion as blind acceptance of library data matches could lead to erroneous structural assignments. Nothing surpasses the availability of an authentic reference compound for confirmed structural assignment. Most data systems contain a computer searchable copy of the EPA/NIH Mass Spectral Data Base which contains more than 40,000 compounds of environmental or health interest. This library, while very comprehensive, does not contain all the compounds that may be encountered in environmental analyses. For this reason a number of specific libraries have been compiled and compilation of a working library by the user should be considered by every laboratory involved in the identification of specific compound classes. Examples of specific libraries follow:

* Mass Spectral Compilation of Pesticides and Industrial Chemicals - U.S. Food and Drug Administration (EI/CI data: hardcopy, 100+ compounds).

* Mycotoxins Mass Spectral Data Bank - U.S. Food and Drug Administration (EI data: hardcopy, 100+ compounds).

* DRES Mass Spectral Data Base of Compounds of Chemical Defence Interest (EI/CI data: hardcopy and computer searchable, 200+ compounds).

GC-MS analyses usually require either quantitation or qualitative identification of the analytes of interest. Qualitative identifications are usually accompanied by a semi-quantitative estimate of concentration (SD typically ± 20 to 50 % depending on analyte concentration) while quantitative identifications, often performed by SIM after full scanning EI confirmation, usually involve use of external or internal standards (SD typically ± 5 to 20 % depending on analyte concentration and quantitation method). Strong consideration should be given to $^{2}H$ or $^{13}C$ analogues for internal standard quantitation, as use of these compounds minimizes instrumental variability during a given set of analyses. At DRES conventional GC detectors, such as FID, are often employed for quantitation following GC-MS confirmation provided the sample matrix and analyte level are suitable.

GC-MS analyses generally fall into one of two categories depending on the information required. Target compound analyses include those where the analyst looks specifically for a compound(s) with little regard for other sample components. In this instance standards are usually available and confirmation is possible. The second type, broad spectrum analysis, requires the analyst to identify all of the sample components in a semi-quantitative or qualitative manner. This type of analysis is the most interesting type of GC-MS analysis, but is also the most time consuming and difficult as it usually involves the identification of numerous unknowns.

The DRES mass spectrometry laboratory is involved in the development of methods for the detection/confirmation of chemical warfare agents, their degradation products and related compounds in environmental (soil, air, water), product formulation and waste samples. This work supports the Canadian Forces in a peacekeeping or military role and more recently has been applied to problems associated with the verification of a proposed United Nations Treaty banning chemical weapons. Work in this regard has necessitated the development of GC-MS methods for chemical warfare agents as well as a number of other compound classes including ether/thioether macrocycles, explosives and hydrocarbons.

The typical philosophy followed during these analyses and the data acquired for previously characterized compounds and unknowns follows:

1. Previously Characterized Compounds (standard(s) available)

| | |
|---|---|
| * EI-MS | Structural/molecular ion |
| * CI-MS ($NH_3$, isobutane) | Molecular ion data |
| * GC Retention Data | Structural data/volatility |
| * GC-FID or GC-FPD | Quantitation/selectivity |

2. Unknowns

* Interpretation of GC, EI-MS and CI-MS data and supplement this data with GC-selective detection, GC-FTIR, accurate mass or CI-MS with deuterated gas ($ND_3$) data. Synthesis is used for confirmed structural assignments.

The following five DRES GC-MS applications illustrate typical approaches for the verification of compounds of chemical defence interest and illustrate some possibilities available to an analyst confronted with either target or broad spectrum analysis.

1. Soil samples (Iran/Iraq sample for mustard)
   - illustrates target compound analysis utilizing multiple GC columns and EI library searching.

2. Product formulations component identification (Tabun)
   -illustrates broad spectrum analysis utilizing multiple GC columns, $ND_3$ CI-MS and synthesis.

3. Aqueous (waste) samples (Mustard hydrolysis products)
   - illustrates broad spectrum analysis utilizing isobutane and $NH_3$ CI-MS, GC-FTIR, synthesis and sample derivatization.

4. Multinational Chemical Disarmament Round Robin Exercise (VX)
   -illustrates broad spectrum analysis utilizing $NH_3$ CI-MS, specific (GC-FPD) detection and GC-FID quantitation.

5. GC-MS/MS of air sample (Highly specific target compound method)
   -illustrates target compound method comparing GC-MS to GC-MS/MS.

## DISCUSSION

1. Soil samples (Iran/Iraq Sample for Mustard)

A 300 mg soil sample was received from the Iran/Iraq region as part of an multinational round robin analytical exercise designed to assess the capabilities of participating laboratories to identify chemical warfare agents in environmental samples. The soil sample was transferred into a PTFE-lined screw capped glass vial and extracted by ultrasonic vibration for 30 min at 25°C with 1 mL of "HPLC-grade" chloroform. The soil material was allowed to settle prior to analysis by GC-FID and GC-MS.

The soil extract was screened by GC-FID on both DB-1 and DB-5 columns and the retention indices of the sample components were calculated by co-injection of the extract with a $C_7$ to $C_{32}$ homologous series of n-alkanes. GC retention index values (mean ± SD; n=3) of 1124.8 ± 0.1 (DB-1) and 1174.1 ± 0.1 (DB-5) were within 2 units of GC retention index data previously acquired for sulfur vesicants, and enabled the tentative identification of the organosulfur vesicant, mustard, and several related organosulfur compounds (3,4).

Mustard (H) and the related organosulfur compounds were confirmed during GC-MS analysis under EI conditions (Figure 1) (5). The acquired EI mass spectrum for mustard was found to match (fit values approaching a perfect 1000) both the EI library data (Figure 2) and that acquired for authentic reference material. External standard quantitation, based on the response of mustard, was performed by GC-FID (Table 1).

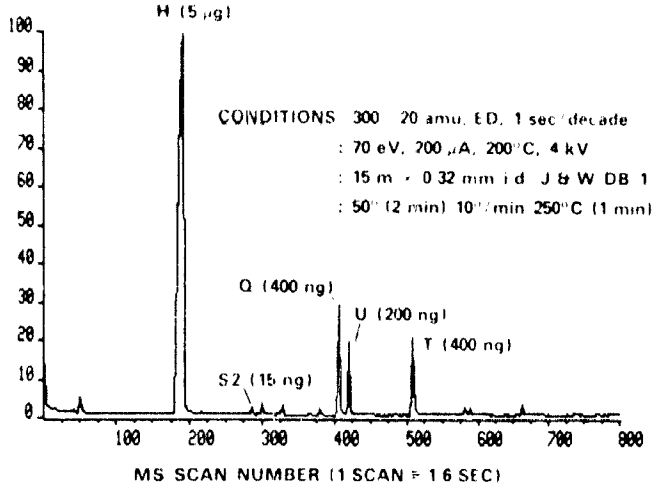


Figure 1
GC-MS chromatogram of extract of the equivalent of 0.24 mg of Iran/Iraq sample (SICA soil #1).

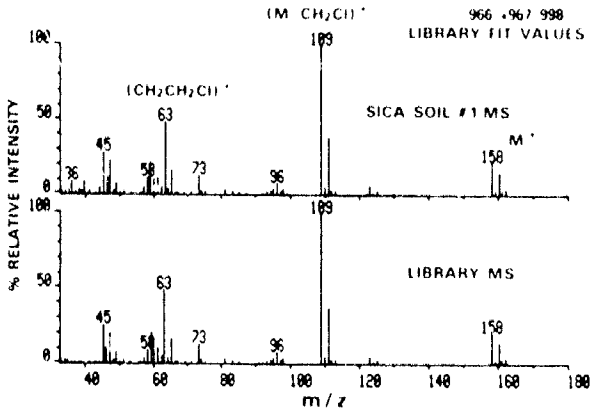


Figure 2
Comparison of EI mass spectrum of mustard from Iran/Iraq sample (SICA soil #1) to library data.

Table 1
Compounds identified in chromatogram (Figure 1) of extract of Iran/Iraq sample (SICA soil #1)

| COMPOUND | STRUCTURE | CONCENTRATION (mg g OF SOIL) |
|---|---|---|
| **SICA SOIL SAMPLE # 1** | | |
| MUSTARD (H) | Cl $CH_2CH_2$ S $CH_2CH_2$ Cl | 12.9 ± 0.2 (n = 3) |
| BIS(2 CHLOROETHYL) DISULFIDE (S2) | Cl $CH_2CH_2$ $S_2$ $CH_2CH_2$ Cl | 0.2* |
| SESQUIMUSTARD (Q) | 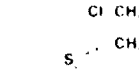 | 1.0* |
| 1,1 OXYBIS(2 (2 CHLOROETHYL) THIO)ETHANE) (T) | 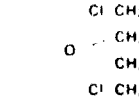 | 1.0* |

* ESTIMATE BASED ON FID RESPONSE OF MUSTARD

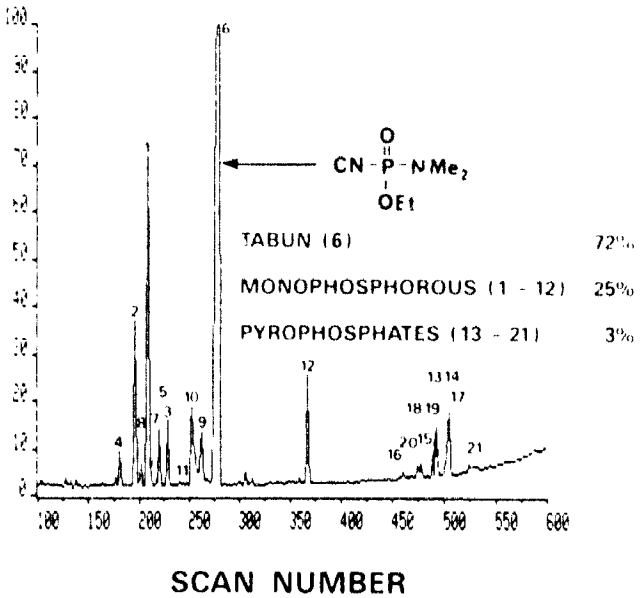


Figure 3
GC-MS chromatogram of munitions grade tabun sample (15 m x 0.32 mm ID J&W DBWAX).

2. Product formulations component identification (Tabun)

A munitions grade tabun formulation containing numerous impurities was provided for broad spectrum analysis. The sample was diluted with chloroform and analysed under several different chromatographic conditions in order to optimize resolution of the more than twenty monophosphorus and pyrophosphate compounds contained within the formulation. Use of the relatively polar DB-1701 and DBWAX columns allowed resolution of most of the components requiring identification.

Figure 3 illustrates the total-ion-current chromatogram obtained during GC-MS analysis of this sample using the DBWAX column. The EI data obtained enabled the identification of the principal sample component, tabun, and several related compounds. However most of the remaining sample components exhibited weak or no molecular ion information under EI conditions. An alternative "soft" ionization technique, chemical ionization (CI), was therefore necessary to confirm the molecular weight of these unknown sample components.

Figure 4 illustrates the EI, ammonia CI and deuterated ammonia CI mass spectra obtained for the organophosphorus chemical warfare agent, tabun. The EI mass spectrum contains a weak molecular ion and several structurally significant fragmentation ions. Molecular weight was confirmed by the presence of $(M+X)^+$ and $(M+NX_4)^+$ pseudo-molecular ions (where X = H during ammonia CI-MS and X = D during deuterated ammonia CI-MS).

Figure 5a illustrates the EI mass spectrum for an unknown that did not provide molecular ion information during EI analysis. Complementary molecular ion information, in the form of $(M+X)^+$ and $(M+NX_4)^+$ pseudo-molecular ions, was obtained during CI-MS analysis (Figure 5b and 5c). This compound also exhibited some structurally significant CI fragmentation ions that lend support to the identity of this unknown. Neutral losses of $C_3H_6$ were observed during ammonia CI-MS and these same losses, along with H/D exchange, were observed during deuterated ammonia CI-MS analysis. H/D exchange indicated the presence of an active hydrogen site (i.e., OH) in the CI fragmentation ion. Interpretation of this and supporting MS and GC data enabled confident structural assignment of diisopropyl ethyl phosphate. Several other sample components were synthesized to enable confirmed structural assignments.

The interpretation of the acquired GC, EI, ammonia CI and deuterated ammonia CI data enabled the identification of tabun and nineteen tabun impurities, including twelve organophosphorus and pyrophosphate compounds previously unreported in tabun (6). Deuterated ammonia CI-MS data was particularly useful as this technique provided both molecular ion information and evidence for the presence of active hydrogen sites in CI fragmentation ions. Consideration should also be given to the use of deuterated ammonia CI-MS as a detection technique in situations where the pseudo-molecular ions formed during ammonia CI-MS are masked by the chemical matrix.

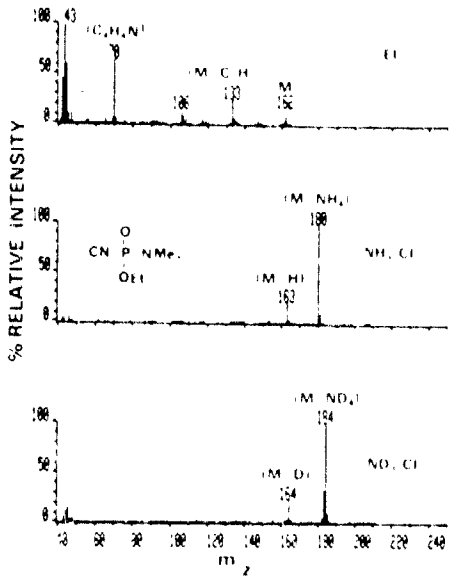


Figure 4
a) EI, b) ammonia CI and c) deuterated ammonia CI mass spectra of tabun.

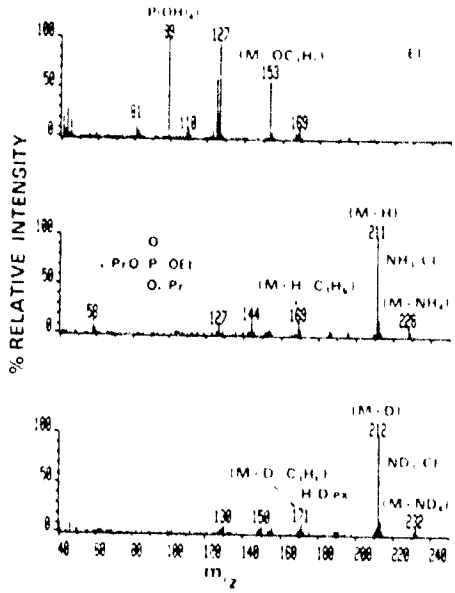


Figure 5
a) EI, b) ammonia CI and c) deuterated ammonia CI mass spectra of diisopropyl ethyl phosphate.

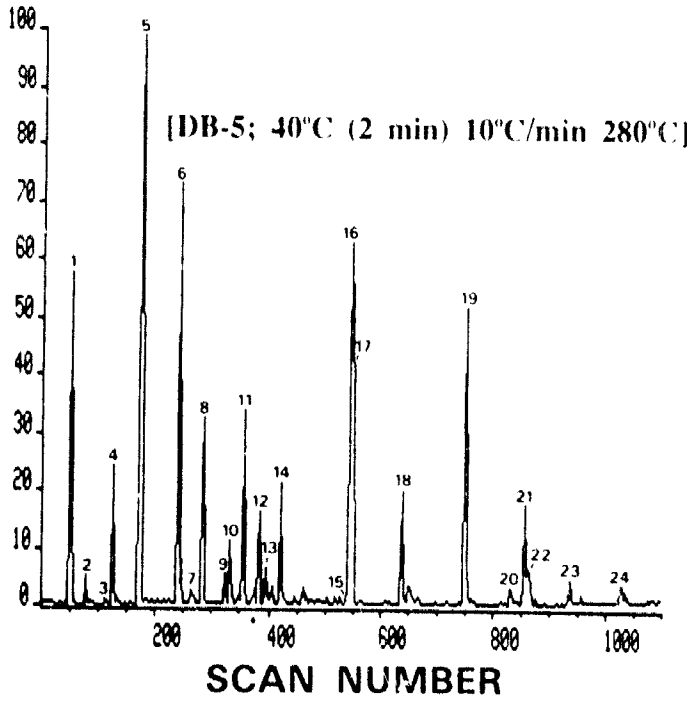


Figure 6
GC-MS chromatogram of hexane extract of aqueous (waste) sample (15 m x 0.32 mm J&W ID DB-5).

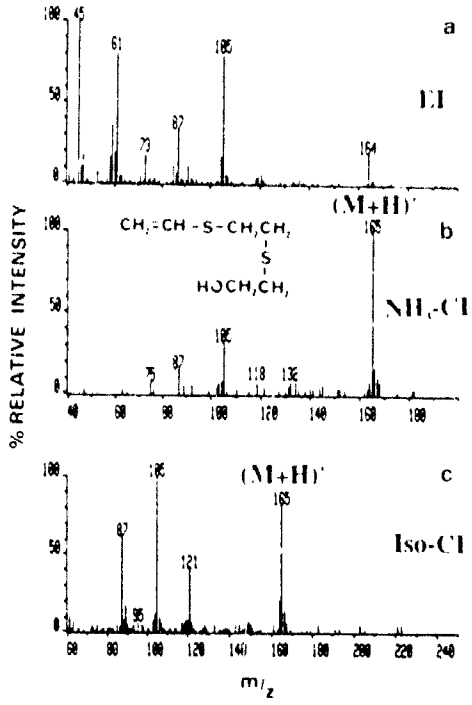


Figure 7
a) EI, b) ammonia CI and c) isobutane CI mass spectra of (2-hydroxyethylthio)ethyl vinyl sulfide.

3. Aqueous (waste) samples (Mustard hydrolysis products)

Hexane extracts of more than twenty aqueous samples were analysed for sulfur vesicant content. Mustard and the related vesicants, sesquimustard and bis[(2-chloroethylthio)ethyl] ether, were not detected in any of the hexane extracts. However, a number of sample components related to the decomposition of munitions grade mustard were observed during GC analysis. The identity of these sample components and the development of methods for their detection would be valuable for both the monitoring of chemical weapons destruction and for the verification of chemical agent use.

Figure 6 illustrates the GC-MS total-ion-current chromatogram obtained for a hexane extract of the sample selected for detailed study. Numerous components, including several of identical molecular weight, were detected during chromatographic analysis. Synthesis of the vinyl alcohol related to mustard, (2-vinylthio)ethanol, and interpretation of other EI and CI data suggested the presence of other vinyl alcohol compounds such as (2-hydroxyethylthio)ethyl vinyl sulfide (Figure 7). However sample components of the same molecular weight often exhibited similar EI and CI ions and identification was not possible without synthesis or additional spectroscopic support. GC-FTIR was selected as this technique could provide structural information which would enable the identification of vinyl alcohols or other components of the same molecular weight as these compounds.

Six ether/thioether macrocycles were identified by interpretation of both FTIR and mass spectral data. The presence of macrocycles was suspected following GC-FTIR analysis as the IR spectra of several of the sample components, including 1-oxa-4,7-dithionane, were similar to that of 15-crown-5, a crown ether tabulated in the Aldrich neat library. The ether/thioether macrocycles identified in this study have been synthesized by Dann et al (7) and Bradshaw et al (8,9). However, the full EI and CI mass spectra of these compounds have not been published. Figure 8 illustrates the EI and ammonia and isobutane CI data acquired for one ether/thioether macrocycle, 1-oxa-4,7-dithionane.

Three vinyl alcohols, related in structure to the sulfur vesicants mustard, sesquimustard and bis[(2-chloroethyl)ethyl] ether were also eventually identified. The vinyl alcohol, related to mustard, (2-vinylthio)-ethanol, was synthesized using the method developed by Nosyreva et al (10) and confirmed in this sample by comparison of the acquired chromatographic, mass spectral and FTIR data with that obtained for the synthetic standard. The EI mass spectra of the two higher molecular weight vinyl alcohols, related to sesquimustard and bis[(2-chloroethyl)ethyl] ether, exhibited fragmentation ions at m/z 45, 61, 86, 87 and 105 due to $(C_2H_5O)^+$ or $(CHS)^+$, $(C_2H_5S)^+$, $(C_4H_6S)^{+\cdot}$, $(C_4H_7S)^+$ and $(C_4H_9SO)^+$ respectively. The molecular weight of both vinyl alcohols was confirmed by the presence of $(M+H)^+$ pseudo-molecular ions during ammonia CI analysis of the aqueous sample extract.

Further evidence for the presence of vinyl alcohols in the aqueous extracts was provided after trimethylsilyl derivatization of the sample extract. Figure 9 illustrates the total-ion-current chromatogram obtained after derivatization with bis(trimethyl-

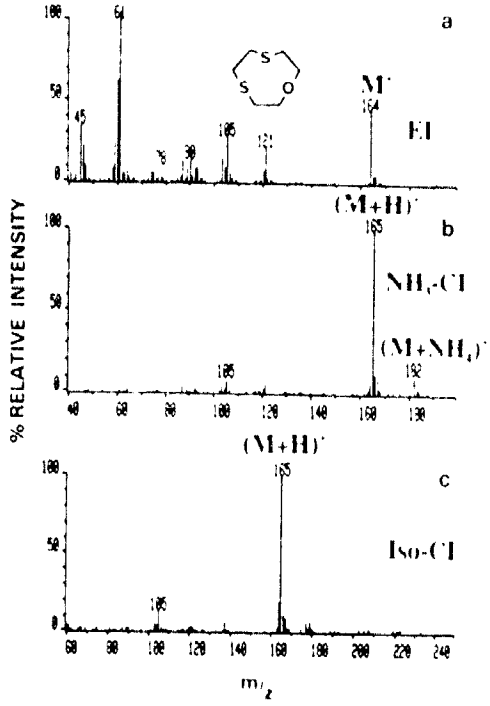


Figure 8
a) EI, b) ammonia CI and c) isobutane CI mass spectra of 1-oxa-4,7-dithionane.

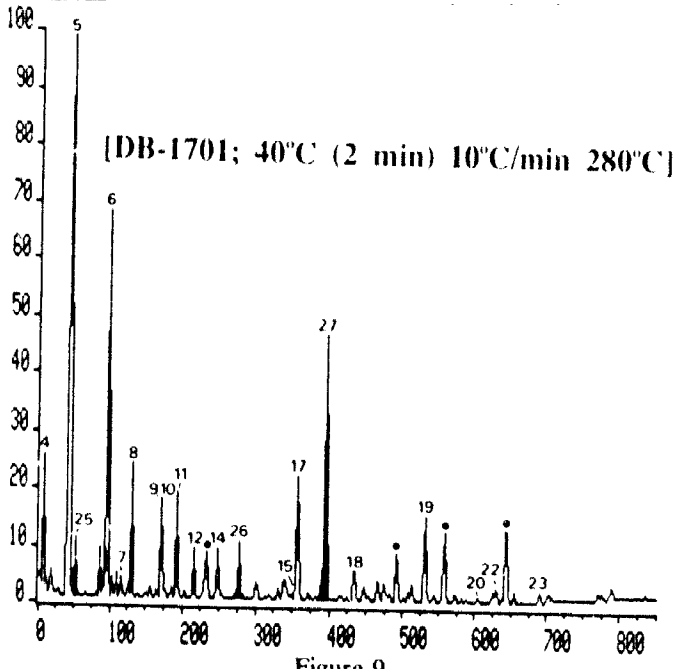


Figure 9
GC-MS chromatogram of TMS derivatized hexane extract of aqueous (waste) sample (15 m x 0.32 mm J&W ID DB-1701; Vinyl alcohols: 25, 26 and 27).

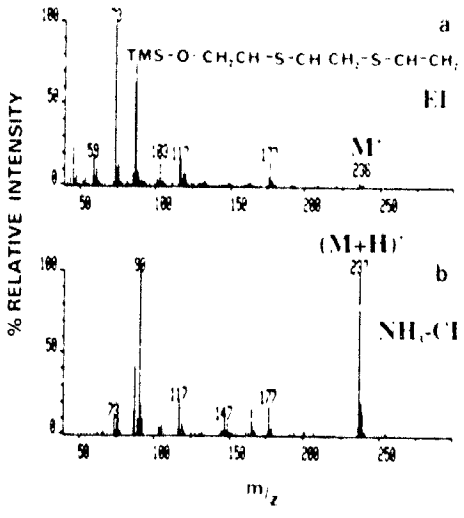


Figure 10
a) EI and b) ammonia CI mass spectra of TMS derivative of (2-hydroxyethylthio)ethyl vinyl sulfide.

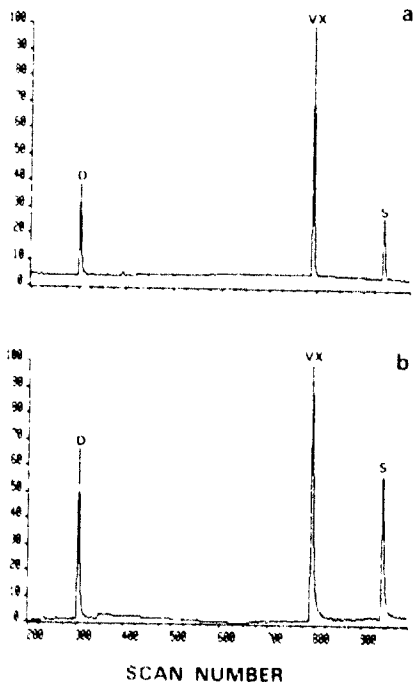


Figure 11
GC-MS chromatograms of dichloromethane extract of round robin sample under a) EI and b) ammonia CI conditions (15 m x 0.32 mm J&W ID DB-1701).

silyl)trifluoroacetamide (BSTFA) catalyzed with 1% trimethylchlorosilane according to the method of Butts (11). Chromatographic components due to macrocyclic compounds were observed, while underivatized vinyl alcohols were not. Three trimethylsilyl (TMS) derivatives, indicated by shading in Figure 9, were detected in place of the vinyl alcohols. Figure 10 illustrates the EI and ammonia CI mass spectra acquired for one of these TMS derivatives, (2-hydroxyethylthio)ethyl vinyl sulfide.

Interpretation of the mass spectral, FTIR, chromatographic and trimethylsilyl derivatization data acquired in this study enabled the identification of nineteen sulfur vesicant related compounds, including a number of ether/thioether macrocycles and vinyl alcohols not previously associated with the decomposition of mustard. The new EI and CI data acquired for the ether/thioether macrocycles, vinyl alcohols and their trimethylsilyl derivatives should prove valuable to other researchers confronted with the analysis of samples containing mustard or other sulfur vesicants (12).

4. Multinational Chemical Disarmament Round Robin Exercise (VX)

Four soil samples that may have been spiked with a chemical warfare agent(s) and related degradation products were received by DRES as part of an international round robin exercise designed to evaluate national laboratory capabilities. The participating laboratories in Canada, Australia, Finland, Norway, Switzerland, Sweden, The Netherlands, United Kingdom and Federal Republic of Germany were given the samples blind and asked to report in a semi-quantitative manner the presence of any CW agents or degradation products in the soil samples.

Portions of each soil sample were extracted sequentially with hexane and dichloromethane and analysed by GC-FID and GC-MS under EI and ammonia CI conditions. Diethyl methylphosphonate, VX and bis[2-(diisopropylamino)ethyl] disulfide were tentatively identified on the basis of GC-FID retention data in both the hexane and dichloromethane extracts of three of the four soil samples.

Figure 11 illustrates the GC-MS chromatograms obtained for one of the dichloromethane extracts of the soil samples and Figures 12 and 13 illustrate the EI and ammonia CI data acquired during these analyses. Pseudo-molecular ion data was considered essential as the EI mass spectra of all three compounds exhibit little or no molecular ion information. The EI (Figure 12) and ammonia CI (Figure 13) mass spectra obtained for these three major sample components agreed well with previously published data (13) and served as a basis for confirmation. The presence of phosphorus and sulfur in these compounds was confirmed during capillary column GC-FPD analysis.

VX and two VX related compounds, diethyl methylphosphonate and bis[2-(diisopropylamino)ethyl] disulfide, were confirmed using GC-MS and GC-FPD, and quantitated by GC-FID (Table 2) in three of four soil samples distributed by Finland as part of a multinational round robin exercise (14).

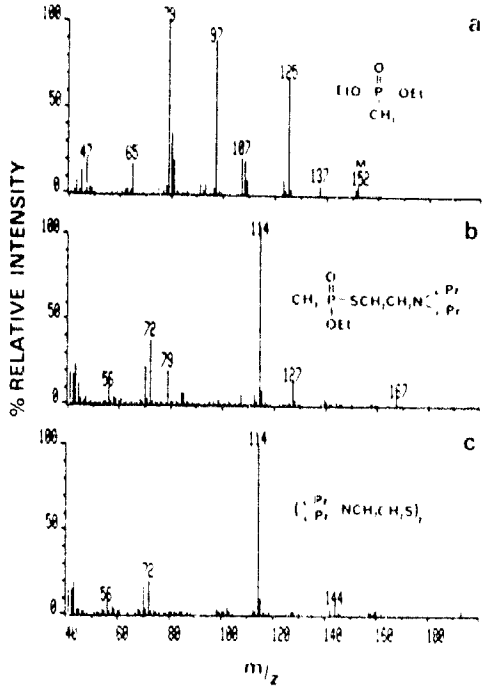


Figure 12
EI mass spectra of a) diethyl methylphosphonate, b) VX and c) bis[2-(diisopropylamino)ethyl] disulfide obtained during analysis of round robin sample.

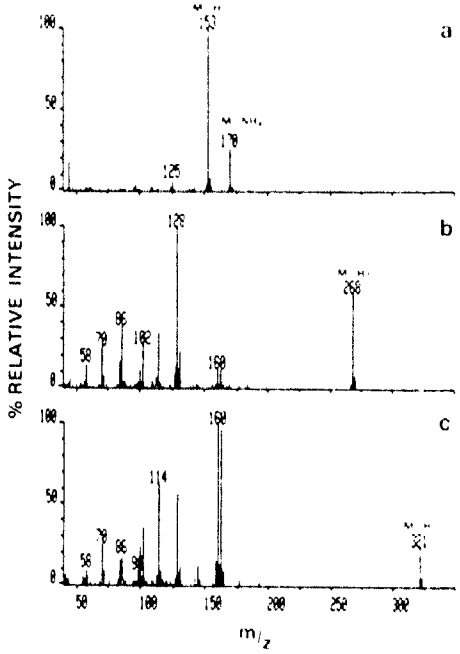


Figure 13
Ammonia CI mass spectra of a) diethyl methylphosphonate, b) VX and c) bis[2-(diisopropylamino)-ethyl] disulfide obtained during analysis of round robin sample.

Table 2
Principal soil sample components identified by Canada during multinational round robin exercise.

| Soil Sample No. | Concentration[1] (ug/g) | | |
|---|---|---|---|
| | D | VX | S |
| 2 | 2.6 | 16 | 11 |
| 15 | 3.1 | 38 | 7.7 |
| 29 | 2.3 | 8.7 | 10 |
| 31 | ND | ND | ND |

[1] Based on FID response of VX; [2]D: Not Detected, <0.5 ug/g.
D: Diethyl methylphosphonate
S: Bis[2-(diisopropylamino)ethyl] disulfide

Table 3
Comparison of detection limits for spiked airborne sample extracts (FS: Full Scanning, RIM: Reaction Ion Monitoring, SIM: Selected Ion Monitoring)

| Method | Detection Limit[1] | | |
|---|---|---|---|
| | Sarin | Soman | Mustard |
| GC-MS (EI; FS) | 20 ng | 20 ng | 20 ng |
| GC-MS/MS (EI; RIM) | 70 pg | 60 pg | 30 pg |
| GC-MS (CI; FS) | 5 ng | >5 ng | N/A |
| GC-MS (CI; SIM) | 40 pg | >500 pg | N/A |
| GC-MS/MS (CI; RIM) | 15 pg | 80 pg | N/A |

[1] Interpretable mass spectrum for full scanning methods and S/N ratio of 5:1 for SIM and RIM methods.

5. GC-MS/MS of air sample (Highly specific target compound method)

A capillary column gas chromatographic study using FID, MS and MS/MS detection was initiated with the principal objective being the development and evaluation of these methods for the verification of sarin, soman and mustard in a complex airborne matrix. The air sampled during this study contained the volatile components of diesel exhaust and was very similar in composition to battlefield air sampled onto charcoal during a recent interlaboratory analytical exercise. Charcoal from exposed C2 Canadian respirator canisters was solvent extracted and spiked at several levels to allow evaluation of these analytical methods for the trace detection of the sarin, soman and mustard. The development of suitable confirmation methods for chemical warfare agents adsorbed onto charcoal under realistic conditions would be valuable in a Chemical Weapons Convention verification role as charcoal mask canisters represent a possible retrospective sampling device.

Figure 14 illustrates GC-MS chromatograms obtained for the charcoal extract (Figure 14a) and chemical warfare agent spikes of this extract at the 20 ng (Figure 14b) and 2 ng (Figure 14c) levels. Recognizable full scanning EI mass spectra were only possible at the 20 ng level for all the spiked chemical warfare agents due to the complexity of this airborne extract.

200 to 500 pg of chemical warfare agent standard were routinely detected during full scanning EI-MS operation, but the presence of the diesel exhaust components severely hampered trace confirmation of the chemical warfare agents. Selected ion monitoring under EI conditions typically improves sensitivity by about two orders of magnitude over full scanning so that low picogram levels may be verified. However, this technique was not applicable at a resolution of 1-2000 due to chemical noise. For this reason no detection limits were estimated. Higher resolution (e.g., 10,000) selected ion monitoring under capillary column GC-MS conditions, while not readily achieved on our instrument, may reduce the matrix chemical noise so that lower levels of the chemical warfare agents may be confirmed during GC-MS(EI) analysis.

Hesso and Kostiainen (15) reported the daughter spectra for the pseudo-molecular ions formed during ammonia chemical ionization of sarin, soman, tabun and VX. The utility of reaction ion monitoring (RIM) for the detection of chemical warfare agents in a complex or environmental matrix, while mentioned, was not demonstrated. The inability of conventional GC-MS(EI) to confirm trace levels of chemical warfare agents in a real environmental matrix prompted investigation into application of MS/MS instrumentation for the trace detection of chemical warfare agents in a complex matrix.

The daughter spectrum of the molecular ion (m/z 158) for H was acquired under collisional activated dissociation (CAD) conditions, which, while perhaps not optimal, did provide significant lower mass ions for use in a reaction ion monitoring experiment. The use of a higher mass ion, such as the molecular or higher mass fragmentation ion, for the acquisition of daughter spectra is usually preferred to minimize potential interferences. Daughter ions of m/z 158 at m/z 63, 73, 96, 109 and 123 were observed by scanning the

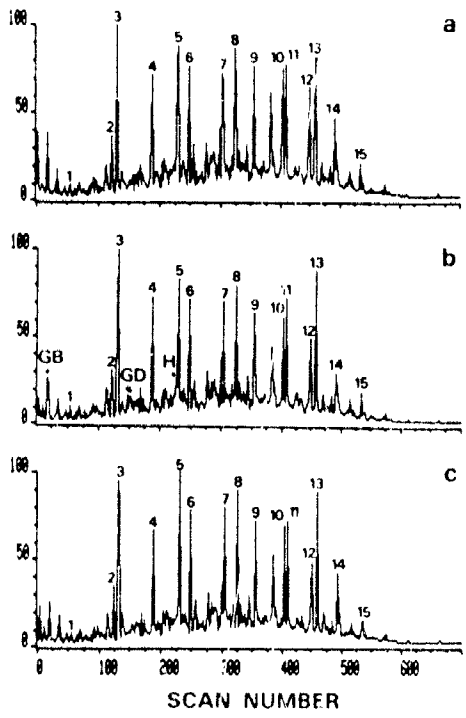


Figure 14
GC-MS (full scanning EI) chromatogram of a) dichloromethane extract of airborne sample and the same extract spiked with b) 20 ng and c) 2 ng of sarin (GB), soman (GD) and mustard (H) (15 m x 0.32 mm ID J&W DB-5).

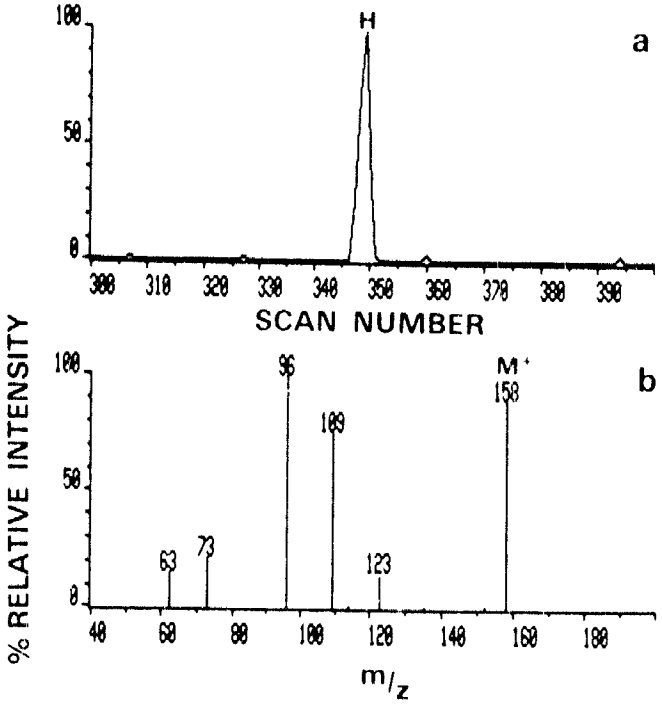


Figure 15
a) Collisional activated dissociation chromatogram of daughters of m/z 158 obtained during GC-MS/MS analysis of mustard (H) (15 m x 0.32 mm ID J&W DB-5). b) Daughter spectrum of H.

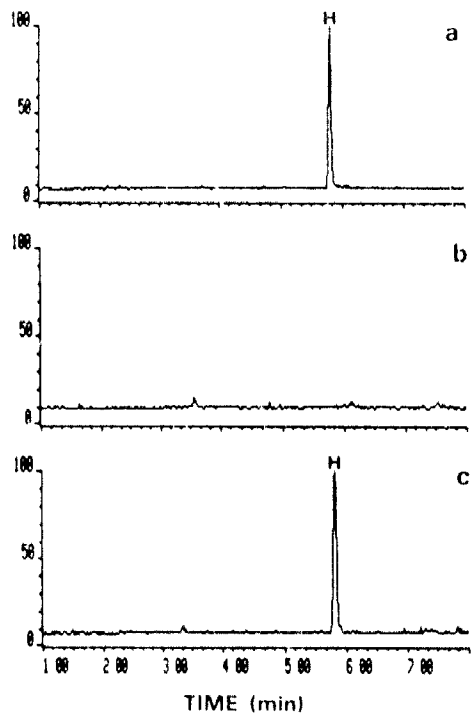


Figure 16
Reaction ion monitoring chromatograms for m/z 158 to m/z 109 transition for a) 500 pg mustard (H), b) dichloromethane extract of airborne sample and c) the same extract spiked with 500 pg H (15 m x 0.32 mm ID J&W DB-5).

quadrupole after CAD at 58 eV using air (Figure 15). Both the m/z 158 to 109 (loss of $CH_2Cl$) and m/z 158 to 96 (loss of $C_2H_3Cl$) transitions were considered suitable and monitored during reaction ion monitoring of mustard (H) in the diesel exhaust extract. Figure 16 illustrates the RIM chromatograms obtained for the m/z 158 to 109 transition for 500 pg of H standard, the charcoal extract, and the charcoal extract spiked with 500 pg of H. H was easily confirmed without any interference in the presence of more than twice as much sample extract (i.e., $5 \times 10^{-4}$ cubic meters of diesel exhaust air) as was used during GC-FID and GC-MS(EI) evaluation. The signal-to-noise ratio for 500 pg of H (S/N greater than 80:1) was independent of the matrix and virtually identical for both the standard (Figure 16a) and spiked extract (Figure 16c). A conservative method detection limit of 30 pg (S/N=5:1) was estimated for H based on these findings.

Table 3 lists the results of a comparison of GC-MS and GC-MS/MS airborne extract detection limits for three chemical warfare agents under EI and ammonia CI conditions. In all cases the use of MS/MS resulted in enhanced detection limits and enabled low picogram verification of these compounds in the presence of numerous chemical interferences common to the battlefield (16,17).

## CONCLUSIONS

The following summary of several approaches recently utilized at the Defence Research Establishment Suffield illustrate applications where GC-MS was used to solve a number of target compound and broad spectrum analyses. Typically GC, EI and CI data were acquired to confirm the presence of the compounds of interest. However, several instances have also been highlighted where supplementary data such as GC-FTIR, GC-FPD and derivatization played an important analysis role. Data has been extracted from several formal publications and further details regarding these GC-MS analyses may be obtained from the references provided.

## REFERENCES


1. R.F. Christman, Environ. Sci. Tech., 16, 1982, 143A.

2. NATO Panel concerned with battlefield sampling and identification of chemical warfare agents.

3. P.A. D'Agostino and L.R. Provost, J. Chromatogr., 331, 1985, 47.

4. P.A. D'Agostino and L.R. Provost, J. Chromatogr., 436, 1988, 399.

5. P.A. D'Agostino and L.R. Provost, Biomed. Environ. Mass Spectrom., 15 1988, 553.

6. P.A. D'Agostino, L.R. Provost and K.M. Looye, J. Chromatogr., 465, 1989, 271.

7. V.V. Nosyreva, S.V. Amosova and B.A. Trofimov, Zh. Org.Khim., 19, 1983, 2044.

8. J.R. Dann, P.P. Chiesa and J.W. Gates Jr., J. Org. Chem., 26, 1961, 1991.

9. J.S. Bradshaw, J.Y. Hui, B.L. Haymore, J.J. Christensen and R.M. Izatt, J. Hetercyclic Chem., 10, 1973, 1.

10. J.S. Bradshaw, J.Y. Hui, Y. Chan, B.L. Haymore, R.M. Izatt and J.J. Christensen, J. Heterocyclic Chem, 11, 1974,

11. W.C. Butts, Anal. Biochem, 46, 1972, 187.

12. P.A. D'Agostino, L.R. Provost, A.S. Hansen and G.A. Luoma, Biomed. Environ. Mass Spectrom., 18, 1989, 484.

13. P.A. D'Agostino, L.R. Provost and J. Visintini, J. Chromatogr., 402, 1987, 221.

14. P.A. D'Agostino, L.R. Provost, T.W. Sawyer and M.T. Weiss, DRES Memorandum No. 1331, April 1990.

15. A. Hesso and R. Kostiainen, "Tandem Mass Spectrometry: A Potential Method for Detection and Identification of Chemical Warfare Agents". Proc. 2nd. Int. Symp. Protection Against Chemical Warfare Agents, Stockholm, Sweden, 15-19 June 1986, 257-260.

16. P.A. D'Agostino, L.R. Provost, J.F. Anacleto and P.W. Brooks, J. Chromatgr., 504, 1990, 259.

17. P.A. D'Agostino, L.R. Provost and P.W. Brooks, received and under review by J. Chromatogr.

UNCLASSIFIED

# KINETICS AND MECHANISMS OF THE HYDROLYSIS AND OXIDATION OF HD AND VX

Linda L. Szafraniec, William T. Beaudry, Dennis K. Rohrbaugh,
Leonard J. Szafraniec, J. Richard Ward and Yu-Chu Yang
U.S. Army Chemical Research, Development and Engineering Center
Aberdeen Proving Ground, Maryland 21010-5423

The acquisition of two high field spectrometers (200 and 400 MHz) has given us the opportunity to apply NMR spectroscopy to systematically study the kinetics and mechanisms of the hydrolysis and oxidation of HD and VX. This elegant and powerful technique has allowed us to follow the dynamic formation and disappearance of reactive intermediates, to identify products from these reactions, and to quantitate these products in situ as a function of time.

Our studies showed that the hydrolysis of 2-chloroethyl sulfides (e.g. HD) can be complicated by the formation of dimeric sulfonium chloride salts and that HD can form reversibly from its hydrolysis products. VX, on the other hand, was shown to hydrolyze by three parallel pathways at neutral pH. Rates for cleavage of the P-S, P-O-C, and S-C bonds were determined and P-O-C cleavage was shown to predominate.

When our investigations of the oxidation reactions of 2-chloroethyl sulfides showed that the reactivity of the sulfide increased with the nucleophilicity of the sulfur atom, we chose a selective sulfur oxidant and determined the competitive oxidation rates for HD and its various simulants. We also showed that the sulfur atom in the phosphonothiolates (e.g., VX) was much less susceptible to attack than the sulfur atom in HD derivatives. Indeed, VX , itself, was found to oxidize by two separate mechanisms depending on the nature of the solvent system.

Through these studies on the hydrolysis and oxidation of HD and VX, we have determined the controlling factors required for the detoxification of these compounds. While our use of NMR to investigate the mechanisms of decontamination of CW agents is fairly recent (1986), our findings have resulted in redirecting current research/development efforts in chemical decontamination at CRDEC.

UNCLASSIFIED

# KINETICS AND MECHANISMS OF THE HYDROLYSIS AND OXIDATION OF HD AND VX

Linda L. Szafraniec, William T. Beaudry, Dennis K. Rohrbaugh,
Leonard J. Szafraniec, J. Richard Ward, and Yu-Chu Yang

Chemical Research, Development and Engineering Center
Aberdeen Proving Ground, Maryland 21010-5423, U.S.A.

## INTRODUCTION

Traditionally, studies at CRDEC on the decontamination of chemical warfare (CW) agents have focused on determining the rate of decomposition of the agent in various decontaminating solutions or on determining the amount of residual agent present on a surface after employing a particular decontamination protocol. Typically, the chemical analyses of the samples were performed using fluorometric, titrimetric, colorimetric, enzymatic, or gas chromatographic (GC) procedures; bioassay methods have also been used to determine the amount of agent present. Product identification was usually accomplished by isolation of the pure compounds after decontamination was complete or, in some cases, by chemical intuition.

The acquisition of two high field (200 and 400 MHz) spectrometers has given us the opportunity to apply NMR spectroscopy to systematically study the kinetics and mechanisms of the hydrolysis and oxidation of HD and VX. This elegant and powerful technique has allowed us to follow the dynamic formation and disappearance of the reactive intermediates, to identify (in conjunction with mass spectrometry, MS) the products formed from these reactions, and to quantitate these products in situ as a function of time.

The purpose of this paper is to review the recent work in decontamination that has been carried out at CRDEC and to emphasize the role that NMR has played in these investigations.

## EXPERIMENTAL PROCEDURES

General Procedure: Depending on the substrate, $^{1}H$, $^{13}C$, or $^{31}P$ NMR was used to monitor the hydrolysis and oxidation reactions at 19-21 $^{o}C$. For very fast reactions, $^{1}H$ NMR was used for substrate concentrations of 0.0005M in $D_2O$. Typically, a weighed amount of substrate was placed into a 5-mm o.d. Pyrex NMR tube. The appropriate reagents were prepared in a separate vial, and an aliquot of this solution was then pipetted into the NMR tube. The tube was quickly capped, wrapped with Parafilm and shaken to ensure complete mixing of the reactants. The NMR tube was placed in

the spectrometer, and spectra were recorded periodically using either a Varian XL-200 or a Varian VXR-400S FTNMR system. Quantitative data were obtained by digital integration of the peak areas of interest. All reaction products were identified by $^{13}C$ and $^{1}H$ and/or $^{31}P$ NMR. GC/MS and Direct Exposure Probe (DEP) mass spectrometry were used to assist and confirm the NMR identifications. Specific details of the experimental procedures may be found in the appropriate references.

## RESULTS AND DISCUSSION

### Hydrolysis of HD

The hydrolysis of HD, bis(2-chloroethyl) sulfide, and its monochloro analogs, 2-chloroethyl methyl sulfide (CEMS) and 2-chloroethyl ethyl sulfide (CEES), have been extensively studied,[1-4] and it was shown that the first step in the hydrolysis is the formation of a transient ethylene sulfonium cation. This cation then reacts quickly with water to form the 2-hydroxyethyl sulfide and HCl. Studies in our laboratory and others[3,5] sometimes showed $H^+$ concentrations lower than expected suggesting that the 2-hydroxyethyl sulfide and HCl were not the only products being formed. In 1946, Stein and coworkers[6] prepared and isolated various sulfonium salts from reactions of HD with thiodigycol (TG) in water. It was thought that the formation of these salts (I and II, Scheme 1) might be responsible for the low $H^+$ concentrations being observed. However, the presence of sulfonium salts in reacting mixtures of HD or other 2-chloroethyl sulfides with water at ambient temperatures had never been reported. Indeed, literature reports[6-8] indicated that the concentration of sulfonium salts in solutions of 2-chloroethyl sulfides should be negligible especially at the dilute concentrations ($10^{-3}$ to $10^{-4}$M) used in most kinetic studies.

Identification of Sulfonium Salts.[9,10] The sulfonium salt, I (EHT, R=Et), was first identified by NMR in samples of CEES in water that had been allowed to come to equilibrium for 40 days; 22 mol% EHT and 78 mol%

Scheme 1

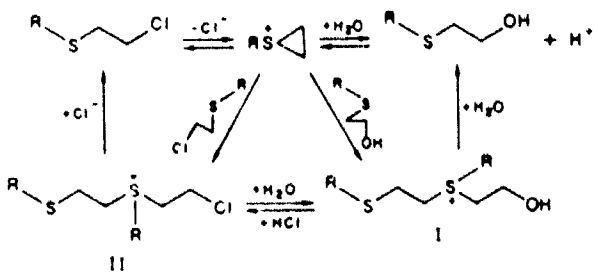

II I

Scheme 2

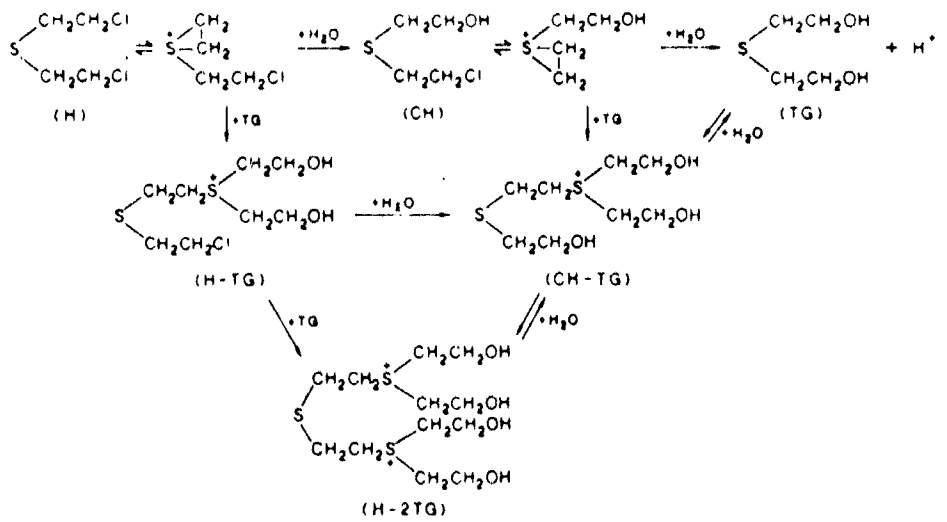


2-hydroxyethyl ethyl sulfide (HEES) were found. A 1:1 (vol) solution of CEES and water that was over 2 years old also showed 78 mol% EHT present. Subsequently, EHT was observed in water-acetone solutions containing 12-75 vol% acetone, in aqueous solutions buffered to pH 10, and in a microemulsion[11] of pH ~9 that was being considered as a decontaminating medium. I (MHT, R=Me) was also observed for solutions of CEMS in the same solvent systems, and two of the sulfonium salts of HD, itself, the H-2TG and CH-TG proposed by Stein et al. (Scheme 2) were detected in the aqueous phase of a two-phase mixture of equal volumes of HD and water. Of particular importance is that using C-13 enriched CEMS, we were able to determine that even at 0.001M, ~20% of the substrate reacted to form the MHT sulfonium salt in pure water and ~11% went to form MHT in a 50 vol% aqueous acetone solution. This observation indicates that even at fairly dilute substrate concentrations, the kinetics for hydrolysis of 2-chloroethyl sulfides are complicated by the formation of the dimeric sulfonium chloride salts. The $^{1}H$ and $^{13}C$ NMR spectral parameters for all of the sulfonium ions have been reported and were determined using APT and both hetero- and homonuclear correlated 2-D experiments.[9,10]

Product Profiles of 2-Chloroethyl Sulfides.[12,13] Figure 1 shows the reaction profile of a 0.17M solution of CEES in 50 vol% aqueous acetone. As can be seen, the CEES initially reacts with itself to form II (ECT, R=Et), which is subsequently hydrolyzed via a dithiane disulfonium ion to I, EHT. Similarly, when $^{1}H$ NMR was used to monitor the dissolution and product profile of CEMS in pure water, II ( MCT, R=Me ) was first formed

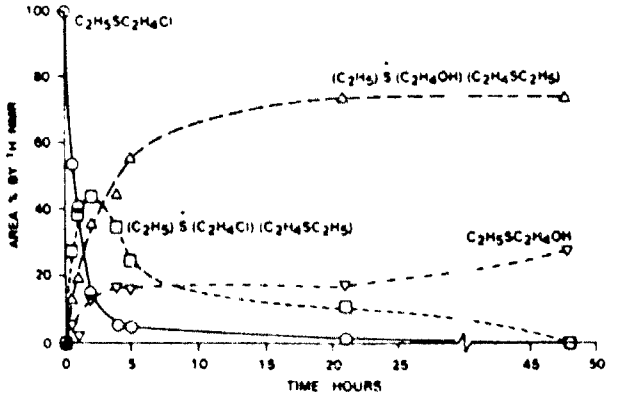


**Figure 1.** Hydrolysis of CEES in 50 vol % $(CD_3)_2CO$-water at 20 °C.

then hydrolyzed relatively quickly (in ~1 day) to form the more stable I, MHT (Figure 2). I was found to be stable for at least a day, slowly hydrolyzing to 2-hydroxyethyl methyl sulfide (HEMS) via an $S_N2$ mechanism at a rate dependent on $[OH^-]$. At higher concentrations of CEMS and CEES where the $[H^+]$ was also relatively high, the amount of I reached an equilibrium and remained in solution for years (see above).

Reverse Reactions.[13,14] In solutions containing 2-hydroxyethyl sulfides and excess HCl, $^1H$ and $^{13}C$ NMR were used to show that all of the sulfide was slowly converted to I at 20 °C (~83% in 5 days). The dimerization mechanism includes protonation followed by dehydration (Scheme 1), and the rate determining step is believed to be the formation of the ethylene sulfonium cation. In TG/HCl solutions, $^{13}C$ NMR showed that CH-TG formed first. Subsequently, a small amount of H-2TG was detected providing the first direct evidence for the reverse reactions shown in Scheme 2 and for the presence of equilibria in acidic HD solutions. Furthermore, in the HCl solution, I (EHT) was found to thermally decompose to CEES showing that, at elevated temperatures, HD is not produced by direct substitution of the two hydroxy groups in TG as reported in past literature,[15,16] but rather from the decomposition of the intermediate sulfonium salts, CH-TG and H-2TG, which form readily in TG/HCl solutions.

Reaction Rates and the Effect of a Strong Nucleophile.[13,17] The rates of hydrolysis of CEES under different conditions are shown in Table 1. As can be seen, a decrease in solvent polarity retards the rate as does an increase in chloride ion concentration. At high substrate concentrations (0.17M), not only is the chloride ion effect significant, but the kinetics are complicated by the formation of the dimeric sulfonium chloride salts, I and II. However, as Table 1 shows, a powerful

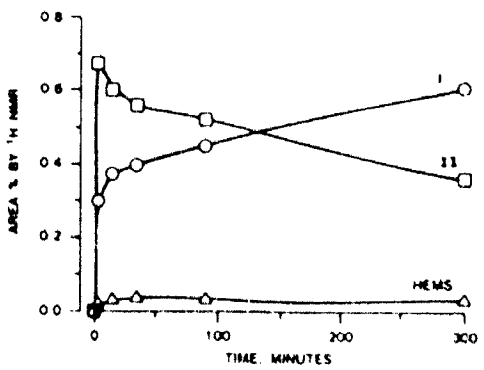


**Figure 2.** Dissolution and hydrolysis of 0.2 M CEMS in water at 20 °C.

nucleophile (e.g. thiosulfate) can effectively capture the transient ethylene sulfonium ion intermediate formed during the initial step of hydrolysis, completely eliminating the formation of I and II and enhancing the observed rate so that it approaches the first order limiting rate observed for dilute solutions. The $^{1}H$ and $^{13}C$ NMR parameters of the thiosulfate products of CEES and HD have been reported,[13,14] and it was shown that for HD, both chlorines were replaced to form $Na_2[S_2O_3C_2H_4)_2S]$.

Thus, our NMR studies have proven that the hydrolysis of 2-chloroethyl sulfides proceeds via the mechanism depicted in Scheme 1. The hydrolysis approaches a simple, first-order $S_N1$ mechanism only when the substrate is predissolved in an organic solvent and when the concentration is below 0.001M. At higher substrate concentrations, the presence of a strong nucleophile is required for the simple $S_N1$ mechanism minus side reactions to predominate.

Hydrolysis of VX.

The hydrolysis reactions of VX and its dimethylamino analog [S-(2-dimethylaminoethyl) O-ethyl methylphosphonothiolate] were easily followed using $^{31}P$ NMR.[18] Unlike previous studies in which the hydrolysis reactions were monitored at fixed pH values and the products were isolated for identification,[19] we were able to simulate the fate of VX in actual field conditions by quantitatively monitoring the acid products in situ for the phosphonothiolates in water minus any buffer to control pH.

The reaction profile for VX is shown in Figure 3. The most striking result is that the primary product is the toxic S-(2-diisopropylaminoethyl) methylphosphonothioic acid formed from P-O-C cleavage. Ethyl methylphosphonic acid (P-S cleavage) and O-ethyl methylphosphonothioic acid (S-C cleavage) were the other two phosphorus

Table 1. Reaction Half-Lives for the Disappearance of CEES at 20 °C.

| solvent | substrate concn, M | products | $t_{1/2}$, min |
|---|---|---|---|
| water | $4 \times 10^{-4}$ | HEES and HCl | 1.4[a] |
| water | $3 \times 10^{-4}$ and 0.05 M NaCl | HEES and HCl | 2.7[b] |
| 50 vol % acetone | $4 \times 10^{-4}$ | HEES and HCl | 14[a] |
| 50 vol % acetone | $3 \times 10^{-4}$ and 0.05 M NaCl | HEES and HCl | 132[b] |
| 50 vol % acetone | 0.17 | I, II, HEES, and HCl | 42[c,d] |
| 50 vol % acetone | 0.17 and 0.2 M $Na_2S_2O_3$ | $C_2H_4SC_2H_4S_2O_3Na$ and NaCl | 13[d] |

*a* Reference 3. *b* Reference 13. *c* Apparent first-order rate assumed. *d* Rate followed by NMR.

products observed. Similar results were obtained for the dimethyl analog: P-O-C cleavage predominated. However, S-C cleavage was not observed which is consistent with the hypothesis that this mechanism involves formation of an immonium ion.[19] The tertiary amine with two methyl groups is expected to be less basic than a comparable amine with two isopropyl groups making formation of the immonium ion less likely.

The rates of hydrolysis for VX and its dimethyl analog are shown in Table 2. The $^{31}P$ NMR data gave excellent first order fits for both compounds even though the pH dropped from ~9 to ~7.5 over the course of the reaction. This result casts doubt on the strong pH dependence of the hydrolysis of V-agents previously reported in the literature.[19] Indeed, contrary to the findings of Epstein et al., that P-S cleavage is the only hydrolysis pathway at pH values above 10, we observed 22% P-O-C cleavage using $^{31}P$ NMR for the reaction of 0.05M VX with 2N NaOH in an aqueous solution of 10 vol% 2-propanol (necessary to solubilize the VX under alkaline conditions). This result and the fact that the toxic phosphonothioic acids were found to be very stable ($t_{1/2}$ ~ 12-14 days at pH 12.5) almost precludes hydrolysis as an effective reaction to detoxify V-agents.

Table 2. Rate Coefficients for the Hydrolysis of VX and S-(2-Dimethylaminoethyl) O-Ethyl Methylphosphonothiolate, 0.5% Solutions. (k, $hr^{-1}$, x $10^3$)

| Compound | Overall Rate | P-O-C Cleavage | P-S Cleavage | S-C Cleavage |
|---|---|---|---|---|
| VX | 12.1 +/- 0.7 | 6.5 | 4.4 | 1.2 |
| Dimethyl Analog | 7.8 +/- 0.8 | 5.5 | 2.3 | - |

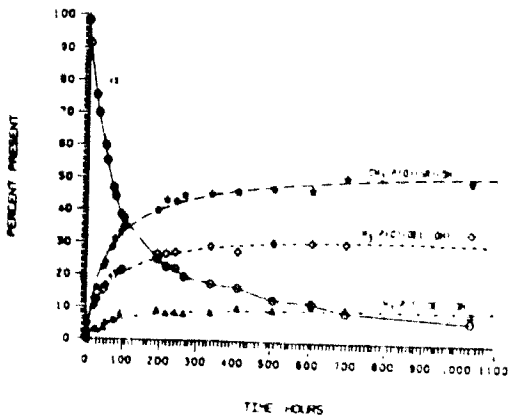

Figure 3. Hydrolysis of 0.5% VX Followed by $^{31}P$ NMR.

Oxidation of HD,[20,21]

HD can be detoxified by oxidation to either the sulfoxide or sulfone. Since the sulfone has been reported to exhibit some vesicant toxicity,[16,22] the sulfoxide product has been our goal in the oxidative detoxification of HD. Recently, N-sulfonyloxaziridine derivatives were presented as a new class of neutral organic oxidants that quickly and selectively oxidize bivalent sulfides to sulfoxides in organic solvents.[23,24] Using $^{13}C$ NMR, we showed that oxaziridine was able to convert HD to its sulfoxide in less than 2 min at 20 °C in $CDCl_3$. No sulfone was observed even when excess oxaziridine was used, and the chlorines in HD did not provide any additional oxidation sites for reaction.

Several laboratories are currently engaged in studying oxidation reactions that may eventually be used to detoxify HD. Since these laboratories can only test simulants, it was of interest to determine the oxidative reactivity of these compounds compared to HD, itself. Table 3 shows the competitive oxidation rates for various bivalent sulfides including HD. The data were obtained using $^{1}H$ NMR to determine the ratio of sulfoxide products formed when two sulfides are allowed to compete for a limited amount of the selective oxidant, oxaziridine. The results show that oxidative reactivity increases as the nucleophilicity of the sulfur atom increases. Whereas CEMS and CEES are excellent HD simulants for hydrolysis (see above), they oxidize ~5 times faster than HD and are, therefore, not the best simulants for studying oxidation. 2-Chloroethyl phenyl sulfide, which was found to have almost the same oxidative rate as HD, is more appropriate.

In addition to the competition rates, a first-order rate constant for 2-chloroethyl phenyl sulfide in the presence of excess oxaziridine was

**Table 3. Competition Oxidation Rates of Bivalent Sulfides.**

| Sulfide | | Competition Oxidation Rate |
|---|---|---|
| $(ClCH_2CH_2)_2S$ | (HD) | 1.0 |
| $C_2H_5SCH_2CH_2Cl$ | (CEES) | 4.8 |
| $(C_2H_5)_2S$ | | 23 |
| $(n\text{-}C_4H_9)_2S$ | | 9.6 |
| $(C_6H_5)_2S$ | | 0.96 |
| $C_6H_5SCH_2CH_2Cl$ | | 0.92 |
| $C_6H_5SCH_2CH_2Br$ | | 1.8 |
| $C_6H_5SCH_2CH_2OH$ | | 4.0 |
| $CH_3SCH_2CH_2Cl$ | (CEMS) | 4.2 |
| $CH_3SCH_2CH_2OH$ | (HEMS) | 10 |
| $i\text{-}C_3H_7SCH_2CH_2Cl$ | | 5.0 |
| $i\text{-}C_4H_9SCH_2CH_2Cl$ | | 5.0 |
| $n\text{-}C_4H_9SCH_2CH_2Cl$ | | 5.0 |
| $i\text{-}C_5H_{11}SCH_2CH_2Cl$ | | 5.4 |

determined. $^1H$ NMR was used to monitor the oxidation of a dilute (0.0005M) solution of the sulfide; the observed first-order rate constant was found to be 0.11 +/- 0.01 $min^{-1}$ at 18 °C ($t_{1/2}$ = 6.5 +/- 0.6 min). This was the first time an absolute first-order rate constant was determined for the oxidation of a sulfide by an oxaziridine! Furthermore, using the competition rates in Table 3, all of the rate constants for the various sulfides studied can be calculated. Thus, HD reacts with oxaziridine with the same rate constant as that measured above.

Further studies using NMR to elucidate the oxidation mechanisms of 2-chloroethyl sulfides are planned. Indeed, a recent study[25] showing that 2-chloroethyl sulfides are more readily oxidized by DMSO than dialkyl sulfides (opposite to that observed for oxaziridine, above) emphasizes the need to carefully evaluate the mechanism of oxidation before selecting a simulant for study.

VX Oxidation.

Recent studies show that hydrolysis, the usual method for detoxifying organophosphorus agents both in the laboratory and in the field, is unacceptable for VX because the rate is slow and a toxic product is often produced (see above). Oxidation would appear to be a viable alternative; however, little information is available. Consequently, a systematic study using multinuclear FTNMR was initiated in our laboratory in order to elucidate the mechanism of VX oxidation and to determine the controlling factors required for its oxidative detoxification.[26] The oxidants used included the stable, commercial peroxygen compounds m-chloroperoxybenzoic

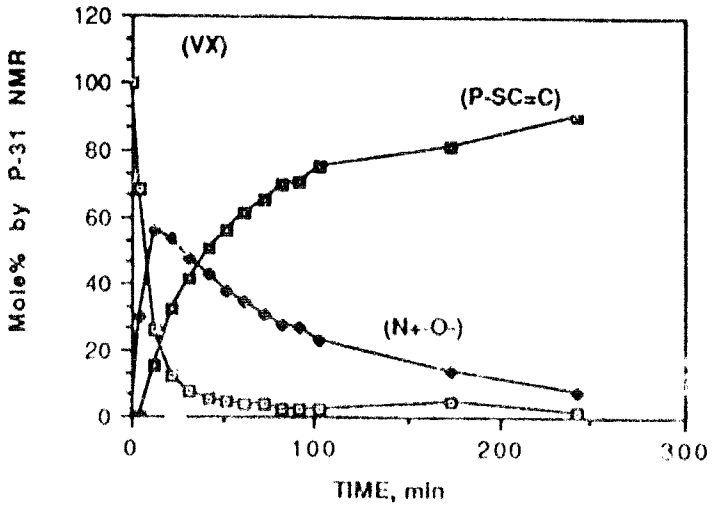


Figure 4. Oxidation of VX ($10^{-2}$M) by Oxaziridine.

acid and OXONE (active component $HSO_5^-$) as well as the selective oxidant, oxaziridine. The solvent systems used were pure water, 50 vol% aqueous t-butanol, pure t-butanol and $CDCl_3$. In all cases, VX oxidation was compared with that of O,S-diethyl methylphosphonothiolate in order to determine the effect of the diisopropylamino moiety in VX on the mechanism of oxidation.

Oxidation of the Nitrogen. In our first experiments, the reaction of VX with oxaziridine in $CDCl_3$ was monitored by $^{31}P$ NMR; the reaction profile is shown in Figure 4. VX was oxidized at the nitrogen to its N-oxide which subsequently decomposed at ambient temperature via a cis-elimination (Cope reaction) to form O-ethyl S-vinyl methylphosphonothiolate ($t_{1/2}$~85 min). Simultaneous oxidation of the secondary product, hydroxylamine, occurred so that 2 moles of oxidant were required for each mole of VX. Similarly, the N-oxide was the initial product formed when VX was oxidized by m-chloroperoxybenzoic acid in pure t-butanol as well as in 50 vol% aqueous t-butanol. In the pure alcohol, the N-oxide decomposed to the S-vinyl product fairly rapidly, ($t_{1/2}$ ~2 hrs at 20 °C), whereas only 10% of the N-oxide decomposed in 27 hrs in 50 vol% aqueous t-butanol.

Oxidation of the Sulfur. In the presence of excess oxidant in 50 vol% t-butanol, the sulfur in the N-oxide was also oxidized. Immediate hydrolysis of the P-S bond occurred, and the final products were identified as ethyl methylphosphonic acid and diisopropylaminosulfonic acid N-oxide which subsequently decomposed. Oxidation at the sulfur was confirmed by examining the reaction of O,S-diethyl methylphosphonothiolate with m-chloroperoxybenzoic acid in 50 vol% t-butanol. At neutral and acid pH, this compound is stable to hydrolysis; but, in the presence of

excess oxidant, it quickly formed ethyl methylphosphonic acid and ethylsulfonic acid ($t_{1/2}$=1.0 min).

In the absence of water, stable intermediates were observed by $^{31}P$ NMR for both VX and the diethyl methylphosphonothiolate. These intermediates (believed to be the P-$S^{+}$-$O^{-}$ compound or its reactive equivalent) subsequently reacted to form several products. The major product, in both cases, was the P,P'-diethyl dimethyldiphosphonate which is known to be quite toxic. Thus, the presence of water or some innocuous nucleophile is required to prevent the formation of toxic products and achieve detoxification.

In aqueous solutions, both phosphonothiolates reacted with excess oxidant directly in one step to form the phosphonic and sulfonic acids; no intermediates were detected by NMR indicating that the subsequent hydrolysis step is faster than the oxidation step. When OXONE (pH=2.3) was used to oxidize VX in water, reaction occurred quickly ($t_{1/2}$=19 min) with no oxidation at the nitrogen observed (confirmed by $^{13}C$ NMR). This was attributed to the fact that the nitrogen was protonated in the OXONE solution and not available for reaction. Thus, oxidation at the sulfur occurred immediately with subsequent hydrolysis to the phosphonic and sulfonic acids. In addition, the OXONE solution had the added advantage of increased solubility for VX due to protonation of the nitrogen to form a water soluble salt.

Multiple Paths of VX Oxidation. Based on our NMR investigations, a scheme for VX oxidation was proposed (Scheme 3) that details two separate reaction mechanisms. The first mechanism involves oxidation of the nitrogen in neutral solutions to form the N-oxide, which decomposes at ambient temperature in organic solvents via a Cope elimination reaction but which is stable in polar solvents and can be further oxidized at the sulfur. The second mechanism involves oxidation of the sulfur in polar acidic solutions followed by nucleophilic attack at the P-S bond and subsequent oxidation of the sulfide product. In the two extreme cases, organic solvents promote the reactions in the direction of $k_{-1}$, $k_N$, and $k_c$ (rate of the Cope reaction; negligible in polar solvents); whereas aqueous acidic solutions promote the reactions in the directions of $k_1$, $k_{VHS}$, and $k_D$. This second pathway is the only one leading to complete detoxification of VX.

## CONCLUSION

We have found NMR to be particularly suited to studying the decontamination of CW agents. Many of the solvent systems are aqueous, and the reactions can easily be monitored by $^{13}C$ or $^{31}P$ NMR without any interferences from the water. In addition, many of the products from these reactions are either acids, salts or pyrophosphate compounds and do not readily chromatograph. NMR allows us to follow not only the

UNCLASSIFIED

**Scheme 3**

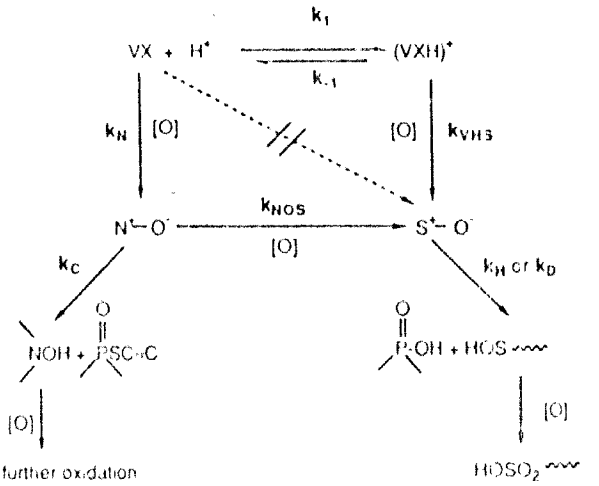


disappearance of the agent but, also, the appearance of these various products so that a complete reaction profile can be obtained. Furthermore, the NMR investigations can be carried out at agent concentrations closer to those expected for field conditions (0.1-0.01M) allowing us to observe interactions which may not exist at the dilute concentrations required by some other analytical methods.

Through our NMR studies on the hydrolysis and oxidation of HD and VX, we have determined the controlling factors required for the detoxification of these compounds. While our use of NMR to investigate the mechanisms of decontamination of CW agents is fairly recent (1986), our findings have resulted in the redirection of current research and development efforts in chemical decontamination at CRDEC.

## REFERENCES

1. Bartlett, P. D.; Swain, C. G. *J. Am. Chem. Soc.* **1949**, *71*, 1406-1415.
2. McManus, S. P.; Neamati-Mazraeh, N.; Hovanes, B. A.; Paley, M. S.; Harris, J. M. *J. Am. Chem. Soc.* **1985**, *107*, 3393-3395.
3. Yang, Y.-C.; Ward, J. R.; Luteran, T. *J. Org. Chem.* **1986**, *51*, 2756-2759.
4. Yang, Y.-C.; Ward, J. R.; Wilson, R. B.; Burrows, W.; Winterle, J. S. *Thermochim. Acta* **1987**, *114*, 313-317.
5. Blandamer, M. J.; Golinkin, H. S.; Robertson, R. E. *J. Am. Chem. Soc.* **1969**, *91*, 2678-2683.
6. Stein, W. H.; Moore, S.; Bergmann, M. *J. Org. Chem.* **1946**, *11*, 664-674.
7. Stein, W. H.; Fruton, J. S.; Bergmann, M. *J. Org. Chem.* **1946**, *11*, 692-703.

8. Davies, J. S. H.; Oxford, A. E. *J. Chem. Soc.* **1931**, 224-236.
9. Yang, Y.-C.; Szafraniec, L. L.; Beaudry, W. T.; Ward, J. R. "Sulfonium Chlorides Derived from 2-Chloroethyl Sulfides. I. Formation and Nuclear Magnetic Resonance Identification in Water." CRDEC-TR-88008, October 1987. Unlimited Distribution.
10. Yang, Y.-C.; Szafraniec, L. L.; Beaudry, W. T.; Ward, J. R. *J. Org. Chem.* **1987**, *52*, 1638-1640.
11. The microemulsion consisted of 16.5 wt% $C_{16}H_{33}N^{+}(CH_3)_3Cl^{-}$, 11.6 wt% $(n\text{-}C_4H_9)_4N^{+}(OH^{-})$, 7.4 wt% $C_2Cl_4$ and 1.4 wt% $(C_8H_{17})_4N^{+}Cl^{-}$ in water and buffered by saturation with $CO_2$ gas.
12. Yang, Y.-C.; Szafraniec, L. L.; Beaudry, W. T.; Ward, J. R. "Sulfonium Chlorides Derived from 2-Chloroethyl Sulfides. II. Effects of Solvent and Substrate Concentration." CRDEC-TR-034, February, 1989. Unlimited Distribution.
13. Yang, Y.-C.; Szafraniec, L. L.; Beaudry, W. T.; Ward, J. R. *J. Org. Chem.* **1988**, *53*, 3293-3297.
14. Yang, Y.-C.; Szafraniec, L. L.; Beaudry, W. T. "Sulfonium Chlorides Derived from 2-Chloroethyl Sulfides. IV. Formation from Protonated 2-Hydroxyethyl Sulfides." CRDEC-TR-198, August, 1990. Unlimited Distribution.
15. Welti, D.; Whittaker, D. *J. Chem. Soc.* **1962**, 3955-3960.
16. *Organic Chemistry of Bivalent Sulfur*; Reid, E. E., Ed.; Chemical Publishing: New York, 1960; Vol. II, Chapter 5.
17. Yang, Y.-C.; Szafraniec, L. L.; Beaudry, W. T.; Ward, J. R. "Nucleophile-Assisted Hydrolysis of Mustard. CRDEC-TR-216, September 1990. Unlimited Distribution.
18. Szafraniec, L. J.; Szafraniec, L. L.; Beaudry, W. T.; Ward, J. R. "On the Stoichiometry of Phosphonothiolate Ester Hydrolysis." CRDEC-TR-212, July 1990. Unlimited Distribution.
19. Epstein, J.; Callahan, J. J.; Bauer, V. E. *Phosphorus* **1974**, *4*, 157-163.
20. Yang, Y.-C.; Szafraniec, L. L.; Beaudry, W. T.; Davis, F. A. "Simulation of HD Reactivity. I. Competition Rates of Oxidation of HD with Simulants." CRDEC-TR-186, May 1990. Unlimited Distribution.
21. Yang, Y.-C.; Szafraniec, L. L.; Beaudry, W. T.; Davis, F. A. *J. Org. Chem.* **1990**, *55*, 3664-3666.
22. Anslow, W. P., Jr.; Karnofsky, D. A.; Val Jager, B.; Smith, H. W. *J. Pharmacol. Exptl. Therap.* **1948**, *93*, 1-9.
23. Davis, F. A.; Jenkins, R. H., Jr.; Yocklovich, S. G. *Tetrahedron Lett.* **1978**, 5171-5174.
24 Davis, F. A.; Billmers, J. M.; Gosciniak, D. J.; Towson, J. C.; Bach, R. D. *J. Org. Chem.* **1986**, *51*, 4240-4245.
25. Hsu, F.-L.; Szafraniec, L. L.; Beaudry, W. T.; Yang, Y.-C. *J. Org. Chem.* **1990**, *55*, 4153-4155.
26. Yang, Y.-C.; Szafraniec, L. L.; Beaudry, W. T.; Rohrbaugh, D. K. *J. Am. Chem. Soc.* **1990**, *112*, 6621 6627.

# CATALYTIC $O_2$-OXIDATION OF ALKYL SULFIDES TO SULFOXIDES USING DIOXO-RUTHENIUM PORPHYRINS: A $^1H$ NMR INVESTIGATION

Nimal Rajapakse and Brian James

Department of Chemistry, University of British Columbia

Vancouver, B.C., V6T 1Y6.

## INTRODUCTION

There remains extreme interest in using air or dioxygen for selective catalytic oxidation of organic compounds,[1-3] partly due to the growing environmental concerns in the use of classical oxidizing agents such as permanganate and dichromate. We have initiated studies on $O_2$-oxidation of a range of organic substrates, with a particular aim of selective oxidation of sulfides to sulfoxides, a reaction of some industrial importance.[4,5] Also, the oxidation of the vesicant mustard, bis-2-chloroethyl sulfide, to the sulfoxide is investigated as a means of chemical detoxification.[6]

In nature, certain enzyme systems accomplish selective oxidation of a wide range of substrates utilizing dioxygen from air. These mono- and di-oxygenase type biological systems, which incorporate one or both oxygen atoms of $O_2$ into substrates, respectively, operate via direct activation of dioxygen by iron-porphyrin centers. Many recent major advances in $O_2$-oxidation chemistry have originated from increased understanding of the ubiquitous monooxygenase enzyme Cytochrome P-450. The active-site of this enzyme consists of an iron-protoporphyrin moiety coordinated to the protein chain via a thiolate anion of a Cysteine amino-acid residue. The mechanism of P-450 oxidation is presented here illustrating key steps in the catalytic cycle (Scheme 1) that operate by reductive-activation of dioxygen according to the Eq. 1.

$$\text{Substrate 'S'} + O_2 + 2H^+ + 2e \longrightarrow S(O) + H_2O \qquad (1)$$

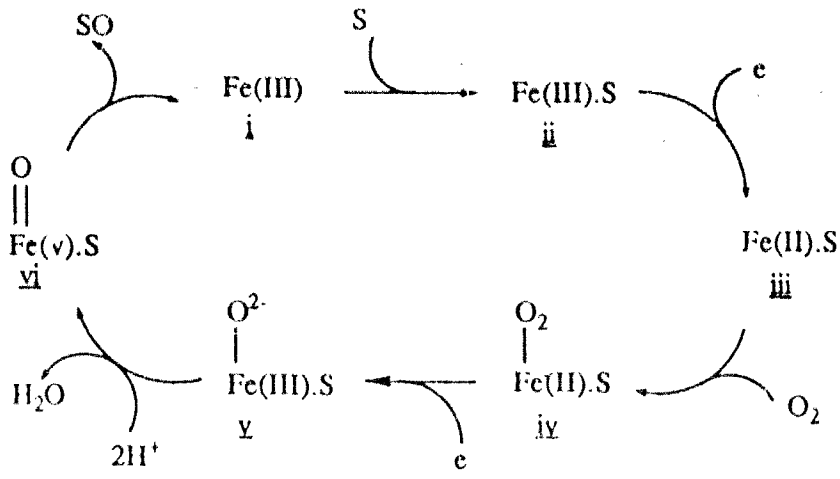


Scheme 1 Catalytic cycle proposed for P-450 oxidations.

1. Binding of the substrate 'S' to the resting enzyme [low-spin Fe(III)], i, to give high-spin enzyme-substrate complex ii
2. One-electron reduction to give a high-spin Fe(II) species iii
3. Binding of $O_2$ to form formally Fe(II)-$O_2$ species iv
4. A second one-electron reduction to form Fe(III)-$O_2^{2-}$ species v
5. Cleavage of the O-O bond generating 'Fe(v)=O' species vi and a molecule of $H_2O$
6. A two-electron oxidation of the substrate S to form SO and to regenerate the resting Fe(III) enzyme.

In recent years, notable progress has been made toward mimicking these biological systems using protein-free metal-porphyrin model complexes.[3,7-11] Among these are some ruthenium porphyrin complexes capable of catalytic oxidation of alkenes to epoxides,[12-14] alkyl sulfides to sulfoxides,[15-17] tertiary phosphines to phosphineoxides,[18] and also phenols and alcohols.[16]

The present paper gives further details of our alkyl sulfide oxidations using ruthenium porphyrins reported recently,[15,16] and the results of initial studies on oxidation of the mustard simulant 2-chloroethyl ethyl sulfide, $CE_2S$.

EXPERIMENTAL METHODS

Nuclear magnetic resonance spectra were recorded using a Bruker WH-400 (400 MHz) or a Varian XL-300 (300 MHz) instrument operating in FT mode. The $^1H$ nmr spectra were referenced to residual solvent peak for $C_6H_6$ at 7.18 ppm, $CH_2Cl_2$ at 5.32 ppm, $CHCl_3$ at 7.25 ppm or $C_6H_5CH_3$ at 2.09 ppm (TMS = 0.00 ppm). Electronic absorption spectra were recorded on a Perkin-Elmer 552A instrument equipped with a thermoelectric temperature controller.

The carbonyl species Ru(TMP)(CO) (TMP= the dianion of 5,10,15,20-tetramesitylporphyrin) was prepared from $Ru_3(CO)_{12}$ and the free-base porphyrin $H_2TMP$ according to a literature procedure.[19] The carbonyl species was converted to the bis(acetonitrile) complex by a standard photolysis procedure described elsewhere.[20,21] Addition of $O_2$ to benzene or toluene solutions of the bis(acetonitrile) species rapidly generates *in situ* solutions of trans-Ru(TMP)$(O)_2$,[18,21] and complete removal of solvent from such solutions give quantitative yields of spectroscopically pure Ru(TMP)$(O)_2$. The corresponding Ru(OCP)$(O)_2$ [OCP= the dianion of 5,10,15,20-tetra(2,6-dichlorophenyl)porphyrin] was synthesized by analogous routes via $Ru_3(CO)_{12}$ and $H_2OCP$ [22] precursors.

The reactions of Ru(Porp)$(O)_2$ with the sulfides were monitored against time by $^1H$ nmr ([Ru]= ~$5\times10^{-3}$ M in $C_6D_6$) or by UV-visible spectroscopy ([Ru]= ~$3\times10^{-6}$ M in $C_6H_6$) after adding appropriate amounts of the sulfide using a micro-syringe. The S-bonded sulfoxide complexes, Ru(Porp)$(OSR_2)_2$, were isolated following the oxidation reaction or by the reaction of Ru(Porp)$(CH_3CN)_2$ species with the sulfoxide in excess; the sulfoxide complex was obtained by evacuating the reaction mixture to dryness or by chromatography on Activity II alumina using $CH_2Cl_2$ as elutant following hexane to remove excess sulfoxide. All isolated sulfoxide complexes have been characterized especially using $^1H$ nmr and UV-visible spectroscopy, and give satisfactory elemental analyses; for Ru(TMP)$(OSCE_2)_2$, Calculated(found): C= 66.08(66.21), H= 6.06(6.12), N= 4.82(4.67), S=5.51(5.46). Data for other species have been listed elsewhere.[23]

## RESULTS AND DISCUSSION

The oxidation of alkyl sulfides diethyl-, di-n-propyl-, di-n-buytyl-, decylmethyl-, and 2-chloroethyl ethyl-sulfide by $Ru(Porp)(O)_2$ complexes (Porp= TMP, OCP) were studied.

Addition of the alkyl sulfide $R_2S$ to the solutions of $Ru(Porp)(O)_2$ (Porp= TMP, OCP) results initially in the formation of the bis-O-bonded species $Ru(Porp)(\underline{O}SR_2)_2$,[15] via a process kinetically first-order in Ru and $R_2S$; clean isosbestic points are observed in the UV-visible spectra and detailed $^1H$ nmr studies show unambiguously that $Ru(Porp)(\underline{O}SR_2)_2$ is the initial product. The bis-O-bonded species subsequently converts to the 'mixed' species $Ru(TMP)(\underline{O}SR_2)(O\underline{S}R_2)$ and finally to the bis-S-bonded derivative $Ru(TMP)(O\underline{S}R_2)_2$. A mechanism involving electrophilic attack by the O=Ru=O moiety on $:SR_2$ is proposed for the oxidation (Scheme 2).[15]

Monitoring the reaction of $Ru(TMP)(O)_2$, 1, ($\sim 5 \times 10^{-3}$ M) and $Et_2S$ ($\sim 2 \times 10^{-2}$ M) in $C_6D_6$ at 20 °C by $^1H$ nmr allows for observation of 3, 4 and 5; the spectrum of 5 is shown in Figure 1 and that of a mixture of 3 and 4 in the high-field region is shown in Figure 2. Spectral assignments are given in Table 1. The relative intensities of the singlets for the pyrrole protons in 8.5 - 8.7 ppm range readily reveals the proportions of 3 - 5 present. For 5, the $CH_2$ protons of $Et_2SO$, as in the free ligand,[20] are seen to be magnetically inequivalent, and appears as multiplets (approximately sextets centered at $\delta$= -1.47 and -2.08 in $CD_2Cl_2$) as the AB moiety of an $ABX_3$ system; the $CH_3$ protons approximate as a triplet ($\delta$= -1.10). The spectrum shown in Figure 2 under the conditions given pertains to a mixture of 3 and 4 before appreciable amounts of 5 are formed; by using selective decoupling and integration intensities, the peaks are assigned as shown in the figure. The $CH_2$ protons of the O-bonded $OSEt_2$ in 3 and 4, appear as quartets (coupled to adjacent $CH_3$) and thus theoretically expected magnetic inequivalency is not observed, which is not unprecedented for O-bonded $OSEt_2$ systems.[24] The $CH_3$ protons of 3 appear as the expected triplet, while in 4, the two types of $CH_3$ groups appear as partially overlapping triplets. The $CH_2$ protons of the S-

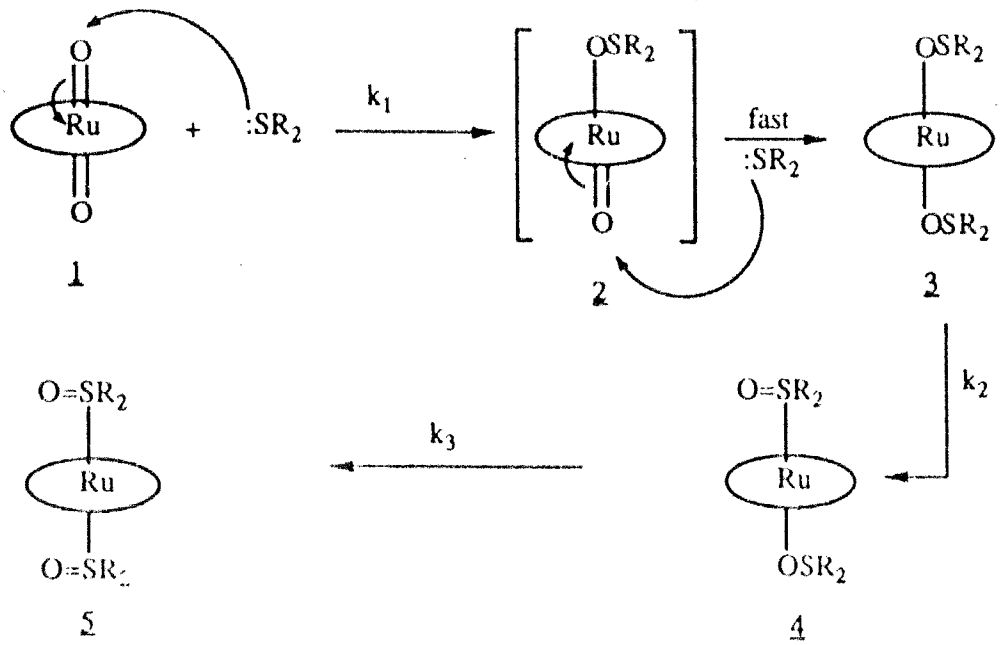


Scheme 2 Proposed mechanism for the oxidation of alkyl sulfides by $Ru(Porp)(O)_2$ species Porp= TMP, OCP; $k_1 >> k_2 > k_3$.

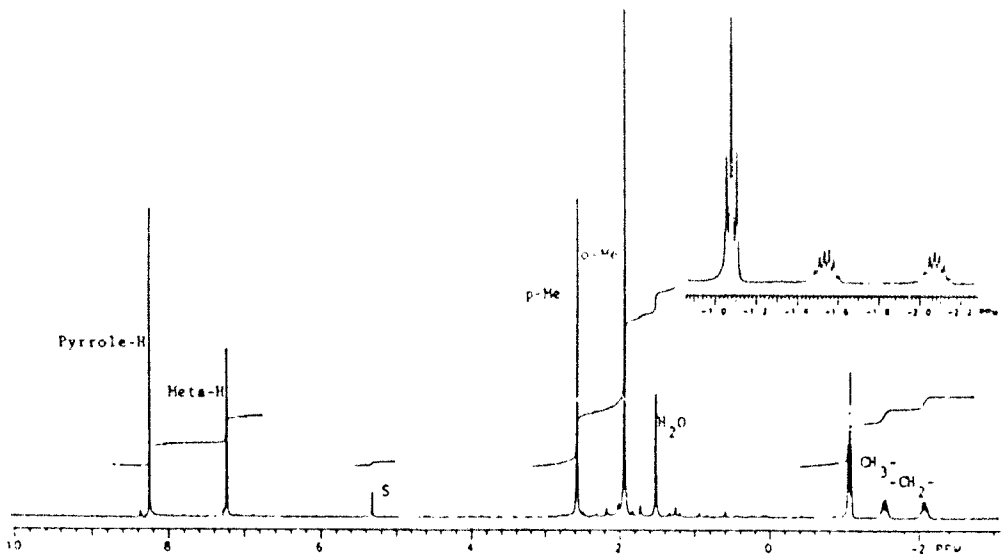


Figure 1 Room temperature $^1H$ nmr spectrum (300 MHz) of isolated Ru(TMP)(OSEt$_2$) in $CD_2Cl_2$.

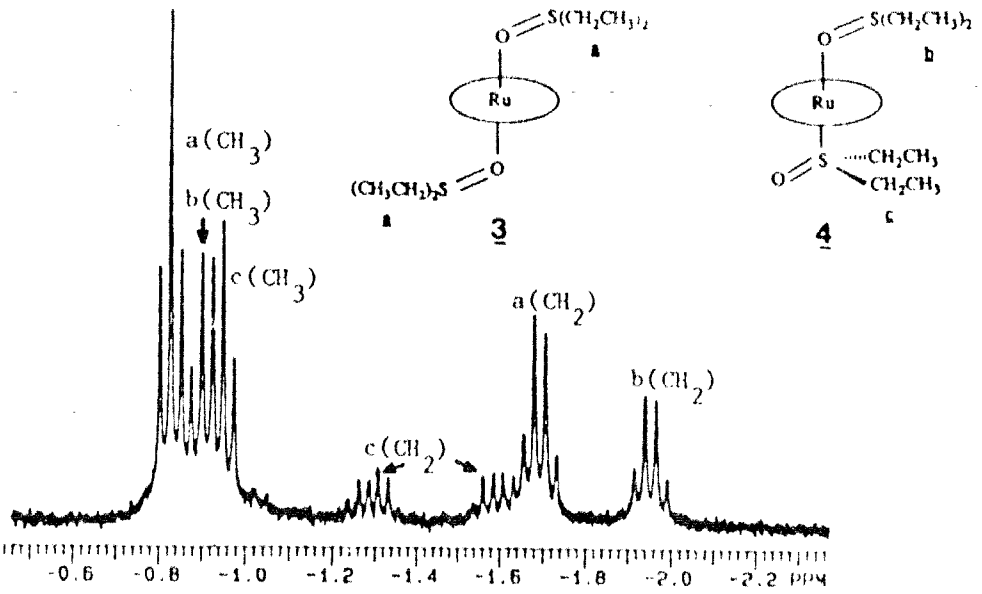


Figure 2 High-field portion of a $^1H$ nmr spectrum of a mixture of 3 and 4 in $C_6D_6$.

Table 1 $^1H$ nmr data[a] for Ru(TMP)$(O)_2$, and $Et_2SO$ complexes of Ru(TMP).

| | Porphyrin | | | | Axial Ligand | |
|---|---|---|---|---|---|---|
| Complex | Pyrrole-H | Meta-H | p-Me | o-Me | $CH_3$[c] | $-CH_2-$ |
| 1 | 9.01 | 7.14 | 2.45 | 1.86 | - | - |
| 3 | 8.50 | ~7.2[b] | 2.50 | 2.24 | -0.80 | -1.66(q) |
| 4 | 8.60 | ~7.2[b] | 2.50 | 2.30 | -0.90 | -1.30(m) |
| | | | | 2.14 | -0.95 | -1.58(m) |
| | | | | | | -1.96(q) |
| 5 | 8.64 | ~7.2[b] | 2.50 | 2.20 | -1.02 | -1.44(m) |
| | | | | | | -1.80(m) |

a- room temperature in $C_6D_6$, all singlets unless mentioned otherwise.
b- under residual solvent peak.
c- triplet, m- complex multiplet, q- quartet.

bonded sulfoxide within 4, as in 5, are magnetically inequivalent and appear as multiplets ( $\delta$ = -1.30 and -1.59). The presumed intermediate 2 is not observed during the process 1 ---> 5 via 3 and 4.

Above reactivity pattern is also observed in the oxidation of di-n-propyl-, di-n-butyl and decylmethyl- sulfides. In the oxidation of the mustard simulant 2-chloroethyl ethyl sulfide, ($CE_2S$), the expected bis-S-bonded sulfoxide species is not formed. However, this species is isolated following the reaction of $Ru(TMP)(CH_3CN)_2$ with excess $CE_2SO$. The high-field portion of the $^1H$ nmr spectrum of some bis-S-bonded sulfoxide complexes are shown in Figure 3. These complexes are substitution inert and unreactive toward $O_2$. The limited catalytic $O_2$-oxidation (a maximum of 15 turnovers for $Et_2S$ in 15 h at 65 °C) is thus pictured as ocurring via 3 with $O_2$ replacing the more labile O-bonded sulfoxide[25] to regenerate 1. At the end of this catalysis, the TMP ligand has clearly undergone degradation indicated by the loss of nmr signals for porphyrinic species.

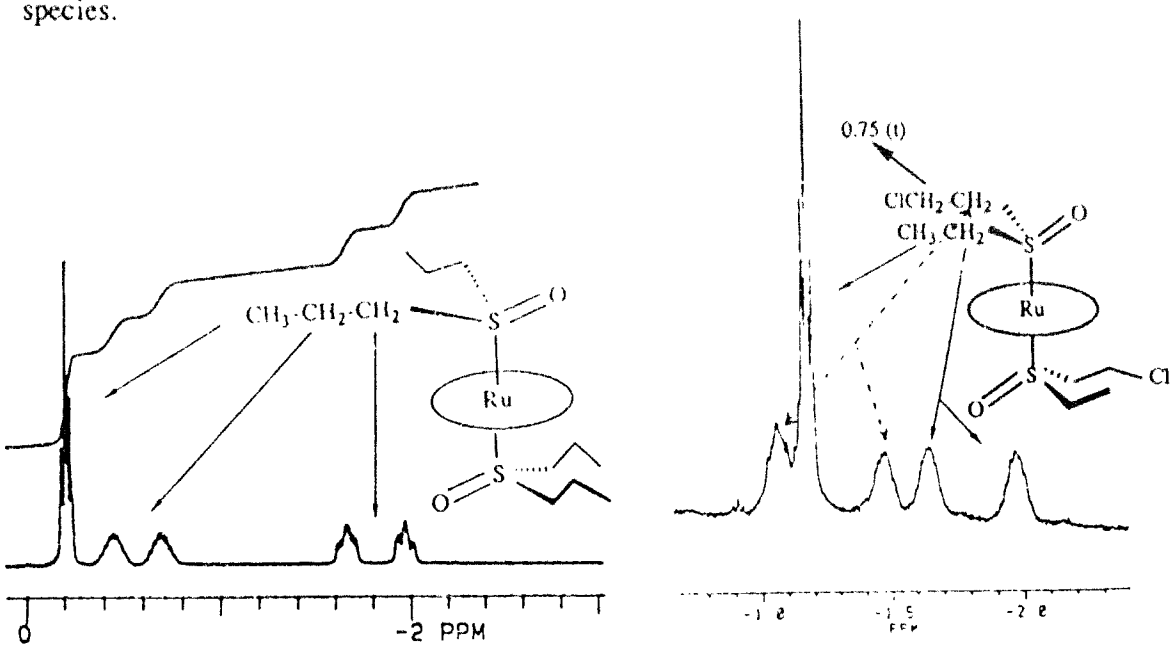


Figure 3 High-field portion of the $^1H$ nmr spectra of $Ru(TMP)(OS^nPr_2)_2$ and $Ru(TMP)(OSCE_2)_2$.

The oxidation resistant dioxo-porphyrin species $Ru(OCP)(O)_2$ is a much more effective catalyst for the sulfide oxidation; more than 30 turnovers are produced in the oxidation of $Et_2S$ at 100 °C under $O_2$ (1 atm), producing sulfoxide and sulfone in 4:1 ratio with no loss of the porphyrin.

The sulfide $CE_2S$ is also oxidized by $Ru(Porp)(O)_2$ (Porp= TMP, OCP) species, but slowly. The $^1H$ nmr data for $CE_2S$, $CE_2SO$ (prepared also by $H_2O_2$ oxidation of $CE_2S$) and their Ru(Porp) complexes are given in Table 2. It should be noted that the O-atom transfer to $CE_2S$ and subsequent isomerizations are much slower compared to those observed in $Et_2S$ oxidation.

Table 2 $^1H$ nmr data [a] for $CE_2S$, $CE_2SO$ and their Ru(Porp) complexes.

| | $CH_3$- [b] | $(CH_3)CH_2$ | $CH_2(CH_2)Cl$ | $CH_2Cl$ |
|---|---|---|---|---|
| $CH_3CH_2SCH_2CH_2Cl$ | 0.90 | 2.05 (q) | 2.45 (t) | 3.20 |
| $CH_3CH_2S(O)CH_2CH_2Cl$ | 0.85 | 2.00 (m) | 2.20, 2.40 (m) | 3.40, 3.70 (m) |
| $Ru(TMP)(\underline{O}SCE_2)_2$ [c] | -0.96 | -1.90 (q) | -1.44 (t) | 0.82 (t) |
| $Ru(TMP)(\underline{O}SCE_2)$. | -1.08 | * | * | * |
| $(O\underline{S}EC_2)$ [c] | -1.12 | -1.76, -2.16 (m) | * | * |
| $Ru(TMP)(O\underline{S}CE_2)_2$ | -1.20 | -1.63, -1.95 (m) | -1.05, -1.46 (m) | 0.75 (t) |
| $Ru(TMP)(SCE_2)_2$ | -0.96 | -1.88 (q) | -1.40 (t) | 1.22 (t) |
| $Ru(OCP)(\underline{O}SCE_2)_2$ [c] | -0.90 | -1.66 (q) | -1.18 (t) | 1.25 (t) |

a- in $C_6D_6$ at room temperature; b- triplet, c- *in situ* species; q- quartet; m- complex multiplet; *- not assigned.

## CONCLUSIONS

The incorporation of O-atoms of $O_2$ to alkyl sulfides via oxo-ruthenium porphyrins is demonstrated. A dioxygenase type activity, i.e. transfer of both O-atms of $O_2$ to substrate is observed and these systems operate via reactive 'M=O' moieties acting as O-atom donors and do not appear to effect outer-sphere ($O_2^{2-}$ type) activation of dioxygen. The O-atom transfer reactions are catalytic, but turnovers are limited. The low catalytic activity is attributed to the strong coordination of sulfoxide ligand to the metal center. Incorporation of the electron withdrawing substituent Cl into the porphyrin ligand increases both the reaction rate and the temperature at which the reaction can be carried out without the degradation of the catalyst. Other porphyrins substituted with electron withdrawing, non-oxidizable substituents such as F and Cl (e.g. Perfluoro-tetraphenyl porphyrin) are now being considered as candidates for more effective catalytic oxygenations.

## ACKNOWLEDGEMENTS

Many helpful discussions with Prof. D. Dolphin, University of B.C., and Dr. C. Boulet, DRES, are gratefully acknowledged. We also thank Natural Sciences and Engineering Research Council of Canada and Department of National Defence, Canada for financial support, and Johnson Matthey Ltd. for the loan of ruthenium.

REFERENCES


1. T.J. Collins (ed.), Report of the International Workshop on Activation of Dioxygen Species and Homogeneous Catalytic Oxidations, Galzignano, Italy, 1984.
2. L.L. Ingraham and D.L. Meyer, Biochemistry of Dioxygen, Plenum, New York, 1985.
3. A.E. Martell and D.T. Sawyer (eds.) Oxygen Complexes and Oxygen Activation by Transition Metals, Plenum, New York, 1988.
4. L. Roecker, J.C. Dobson, W.J. Vinning and T.J. Meyer, Inorg. Chem. 26, 779(1987).
5. D.P. Riley, M.R. Smith and P.E. Correa, J. Am. Chem. Soc., 110, 177(1988)
6. W.P. Anslow Jr., D.A. Karnofsky, B. Val Jager, H.W. Smith, J. Pharmacol. Exp. Ther., 93, 1 (1948).
7. J.T. Groves and T.J. McMurry in Cytochrome P-450. Structure, Mechanism and Biochemistry (P. Ortiz de Montellano, ed.), Plenum, New York, 1986, Chap.1.
8. B.R. James, in Fundamental Research in Homogeneous Catalysis, Vol. 1, (A.E. Shilov, ed.), Gordon and Breach, New York, 1986, p. 309.
9. D. Mansuy, Pure Appl. Chem., 59, 759 (1987).
10. I. Tabushi, Coord. Chem. Rev., 86, 1 (1988).
11. T.C. Bruice, Aldrichimica Acta, 21, 87 (1988).
12. J.T. Groves and R. Quinn, J. Am. Chem. Soc., 107, 5790 (1985).
13. J.C. Marchon and R. Ramasseul, J. Chem. Soc. Chem. Commun., 298 (1988); idem , J. Mol. Catal. 51, 29 (1989).
14. M. Tavares, R. Ramasseul and J.C. Marchon, Catal. Lett., 4, 163 (1990).
15. N. Rajapakse, B.R. James and D. Dolphin, Catal. Lett., 2, 219 (1989).
16. N. Rajapakse, B.R. James and D. Dolphin, Stud. Surf. Sci. Catal., 55, 109 (1990).
17. B.R. James, A. Pacheco, S.J. Rettig and J.A. Ibers, Inorg. Chem. 27, 2414 (1988).
18. J.T. Groves and K-H. Ahn, Inorg. Chem., 26, 3831 (1987).
19. D.P. Rillema, J.K. Nagel, L.F. Barringer and T.J. Meyer, J. Am. Chem. Soc., 103, 56 (1981).
20. M.J. Camenzind, B.R. James, D. Dolphin, J.W. Sparapany and J.A. Ibers, Inorg. Chem., 27, 3054 (1988).
21. M.J. Camenzind, B.R. James and D. Dolphin, J. Chem. Soc. Chem. Commun., 1137 (1986).
22. P.S. Traylor, D. Dolphin and T.G. Traylor, J. Chem. Soc. Chem. Commun., 279, 1984.
23. N. Rajapakse, Ph.D. Thesis, Dept. of Chemistry, University of British Columbia, 1990.
24. W. Kitching, C.J. Moore and D. Doddrell, Inorg. Chem., 9, 541(1970).
25. J.A. Davies, Adv. Inorg. Chem. Radiochem., 24, 115(1981).

# THE FORMATION OF PYROPHOSPHATES IN THE OXIDATION OF PHOSPHONOTHIOLATES

D. Ralph Leslie*
Materials Research Laboratory, DSTO,
P.O. Box 50, Ascot Vale, Vic. 3032,
Australia.

and

William T. Beaudry, Linda L. Szafraniec, Dennis K. Rohrbaugh
U.S. Army Chemical Research, Development and Engineering Center
Aberdeen Proving Ground, Maryland 21010-5423

## INTRODUCTION

The chemical oxidation of phosphorothiolates (1) has been the subject of a number of studies which have emphasized the identification of intermediates in the reaction sequence.[1-6] Interest in the process was initiated by the desire to identify the potent in vivo phosphorylating species that are proposed to form via oxidative bioactivation of thiophosphorus insecticides. Although phosphorothiolates are activatated by bio-oxidation, the proposed active species are very labile and are readily hydrolysed. Our interest lies in the potential of oxidation to detoxify phosphonothiolates, such as VX. Chemical oxidation (Scheme 1) is believed to involve the initial formation of a reactive S-oxide (2) which rearranges to a phosphinyloxysulfenate (3), possibly via a phosphoranoxide. Subsequent oxidation of 3 ultimately produces the phosphinyloxysulfonate (4) which is stable in the absence of nucleophilic species.

Scheme 1

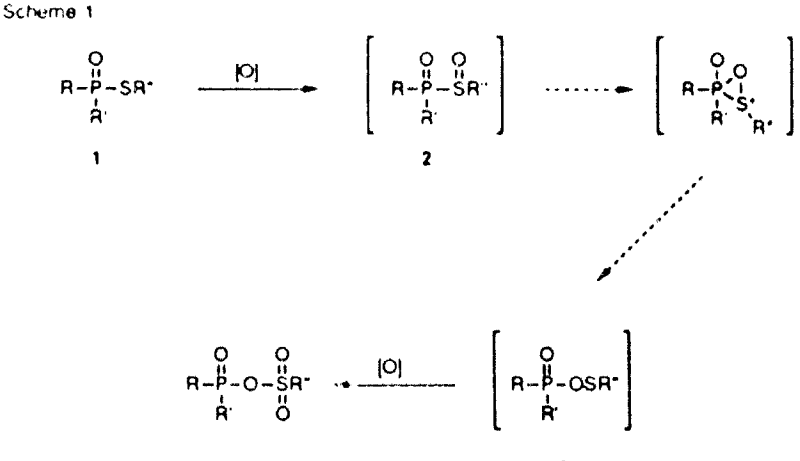

When the oxidation is performed in the absence of an added nucleophilic species, in addition to 4, a significant fraction of the symmetrical pyrophosphate (5) is observed.[3,6] This is undesirable in a procedure that is intended to detoxify the thiophosphorus species because of the toxicity that may be associated with pyrophosphates. For example, the pyrophosphate formed during the oxidation of VX has a $LD_{50}$ (i.v., rabbit) only ten times that of VX itself.[7] Formation of 5 is assumed to result from the reaction of one of the species 2-4 with the free acid (6) (eq 1), in turn formed by hydrolysis of 2, 3 or 4 by adventitious water in nominally dry solvents.[8] While investigating the oxidation of phosphonothiolates,[7] we observed that the formation of pyrophosphates was enhanced by efforts to reduce the amount of water in the reaction, although this should reduce the formation of the intermediate acid. Hence the current study was undertaken.

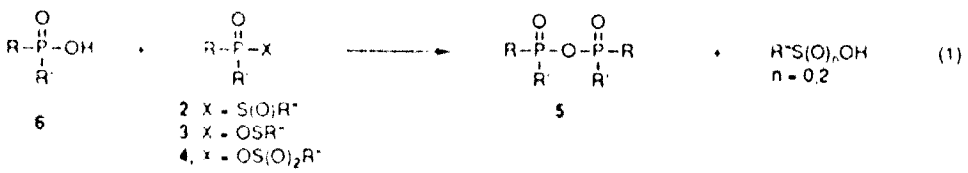


RESULTS AND DISCUSSION

For ease of investigation, we desired a reaction that would yield the pyrophosphate as the major, if not exclusive, product. The reactions of several combinations of substrate and oxidant, including those of VX, O,O-diethyl-S-phenyl phosphorothioate, O,S-diethyl methylphosphonothioate or O,S-dimethyl phosphoramidothioate (7) with *m*-chloroperbenzoic acid or 2-phenylsulfonyl-3-(4-nitrophenyl)oxaziridine (8) were screened. Our interest in the last of the substrates may appear incongruous; phosphoramidothioates are not obvious choices as models for phosphonothiolates. The sulfoxide formed by oxidation of this compound is, however, the only one for which NMR data have been reported. In the report, S-methyl $^{13}C$ labelled (7) was oxidized with *m*-chloroperbenzoic acid and the $^{13}C$ spectrum of the reaction mixture was interpreted as evidence for formation of a stable sulfoxide.[5] Unfortunately, no $^{31}P$ NMR data were reported. We repeated the reaction with the intention of obtaining the substituent effect of the sulfoxide moiety on the $^{31}P$ chemical shift. This would assist the identification of intermediates that may form in the oxidation reactions.

Our attempts to oxidize (7) with *m*-chloroperbenzoic acid resulted in mixtures of products (as determined by $^{31}P$ NMR), all of which had $^{31}P$ shifts consistent with phosphoramidic acids or pyrophosphates formed therefrom. There was no evidence for sulfoxide formation. Oxidation with 2-phenylsulfonyl-3-(4-nitrophenyl)oxaziridine (8), a milder reagent, gave only a single product ,which we identified as a pyrophosphate. Thus, we used this combination of substrate and oxidant in this study.

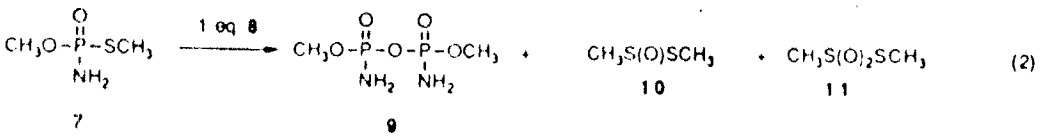


(2)

Reaction of 7 with one equivalent of 8 in dry, ethanol-free chloroform yielded P,P'-dimethyl diamidodiphosphate (9) in greater than 95% yield (50% conversion of 7) after 2 hours at 18°C (eq 2). The identity of the pyrophosphate was determined by its $^{31}P$ NMR spectrum ( δ1.21 and 1.43 for the diastereomers[9]), GC/MS and direct exposure probe MS of the reaction mixture (CI, M+1=205). The S-methyl moiety was present in the final reaction mixture as S-methyl methanethiosulfinate (10), S-methyl methanthiosulfonate (11) and a third unidentified product ($^{1}H$ NMR: δ3.22; $^{13}C$ NMR δ38.3).[10] The structures of products 10 and 11 were confirmed by comparison of their NMR spectra ($^{1}H$ and $^{13}C$) and GC/mass spectra (CI) with authentic material prepared by oxidation of dimethyl disulfide.[11,12] Thiosulfonate 11 has previously been isolated from the *m*-chloroperbenzoic acid oxidation of 7.[1,13] Neither methane sulfinic nor methane sulfonic acid were formed during the reaction. The absence of these acids is evidence that only one oxygen is transferred to the phosphorothiolate sulfur. Thus the involvement of more highly oxidized species in pyrophosphate formation can be excluded. This is important, since one of the proposed pathways for pyrophosphate formation is blocked if more than one oxygen atom is transferred to the phosphorothiolate sulfur. We also noted the formation of S-ethyl ethanethiosulfinate and S-ethyl ethanethiosulfonate in the oxidation of O,S-diethyl methylphosphonothioate, suggesting a common mechanism for pyrophosphate formation from both compounds.

The concomitant formation of the dimethyl disulfide oxidation products, 10 and 11, and pyrophosphate 9 suggested an alternate mechanism for the formation of 5 (Scheme 2). Oxidation of 7, followed by rearrangement, first yields the mixed phosphoramidic/sulfenic acid anhydride, 3a. Subsequent nucleophilic attack upon the anhydride by the phosphorothiolate sulfur of a second molecule of 7 could then lead to the pyrophosphate and dimethyl disulfide. If the phosphinyloxysulfenate was oxidized to the sulfinate or sulfonate, then this mechanism could not operate. The susceptibility of the phosphorothiolate sulfur to oxidation by oxaziridine 8 is evidence of its nucleophilicity. The mechanism for oxidation by this reagent involves attack by a nucleophilic substrate on the electrophilic oxygen of the oxaziridine ring.[14]

The presence of dimethyl disulfide (12) required by Scheme 2 was confirmed by GC/MS, but its concentration was insufficient for detection by $^{1}H$ NMR spectroscopy. Similarly, diethyl disulfide was detected by GC/MS in the reaction of O,S-diethyl methylphosphonothioate. In a

Scheme 2

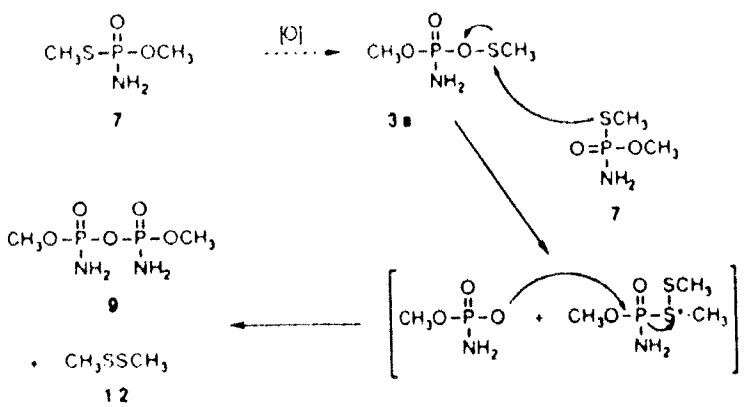

separate experiment, dimethyl disulfide was found to react with one equivalent of 8 in less than 15 minutes at 18°C to give 10. Addition of excess 8 resulted in formation of 11. $^{1}H$ and $^{13}C$ NMR spectra of the reaction also revealed that the unidentified product formed from the S-methyl moiety in the oxidation of 7 is also present in the oxidation of dimethyl disulfide by 8.

Scheme 2 is appealing because it accounts for all of the products formed in the reaction, and does not require the involvement of water. Our procedure for the oxidation reaction must result in a very low concentration of water since the addition of 1 equivalent of water to the reaction after all the oxidant was consumed and pyrophosphate formation had ceased, resulted in hydrolysis of three quarters of the pyrophosphate formed within 1 hour. Without the addition of water no hydrolysis is observed in the same period.

Provided a catalytic amount of water is present, the series of reactions shown as Scheme 3 also accounts for the products. As the final step of the sequence, methane sulfenic acid (13) dimerizes to S-methyl methanethiosulfinate (10), returning one equivalent of water to the reaction. Alkyl sulfenic acids have been postulated as transient species in a variety of organic transformations, and their fleeting existence during the pyrolysis of alkyl thiosulfonates has been confirmed by trapping as the addition product (14) with ethyl acrylate (eq 3).[15,16] In the absence of a trapping agent, alkyl sulfenic acids dimerize as shown in Scheme 3.[15,16] The detection of dimethyl disulfide in the reaction is consistent with the reported disproportionation of 10 to dimethyl disulfide and 11.[17]

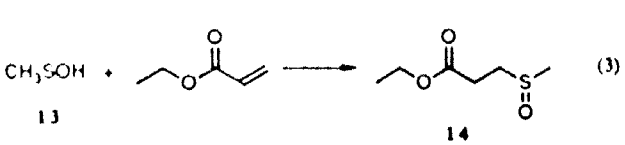

(3)

Scheme 3

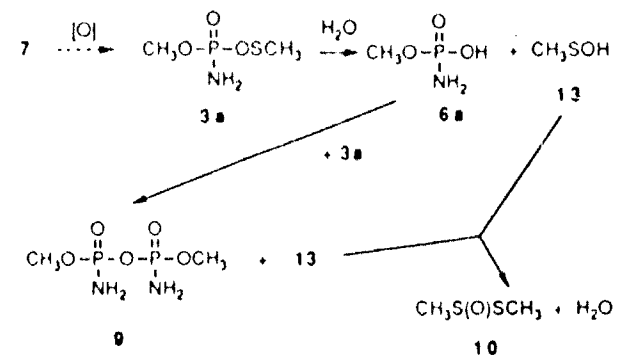


Since formation of pyrophosphate 9 in Scheme 3 requires generation or the free acid **6a**, addition of a different phosphorus acid to the reaction should result in the formation of a mixed pyrophosphate. By itself, this would not prove the involvement of acid **6a** in the formation of the symmetrical pyrophosphate. However, we reasoned that if the free acid was involved then the presence of a pool of a different acid (nucleophile) should result in the accumulation of **6a** in solution. When reaction of 7 with one equivalent of 8 was repeated with 0.2 equivalents of isopropyl methylphosphonic acid (15) added to solution, both the symmetrical and mixed pyrophosphates, 9 and 16 respectively, formed. Identification of 16 relied upon its $^{31}P$ and $^{1}H$ NMR spectra.[18] In addition, acid **6a** accumulated in solution (Figure 1). After completion of

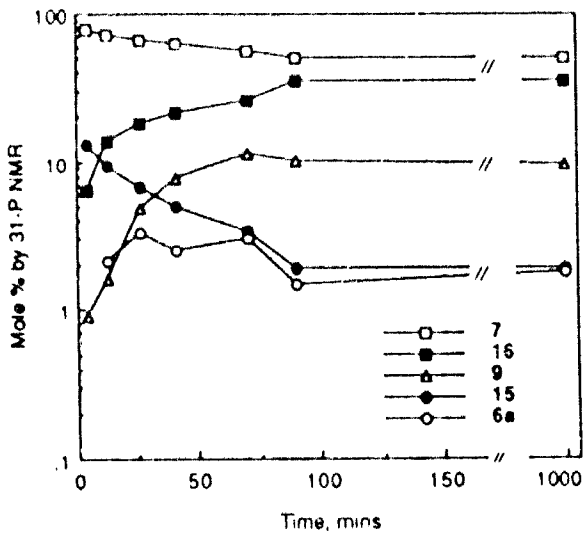


**Figure 1.** Oxidation of O,S-dimethyl phosphoramidothioate (7) by (8) in the presence of 0.2 eq of 2-methylethyl methylphosphonic acid (15).

the reaction, $^{1}H$ and $^{13}C$ NMR spectra of the reaction mixture indicated that S-methyl methanethiosulfinate (10), S-methyl methanthiosulfonate (11) and the unidentified product ($^{1}H$ NMR: δ3.22; $^{13}C$ NMR: δ38.3) were present in approximately the same proportions observed in the reaction without the pool of free acid. Since the fate of the S-methyl moiety is the same in both reactions, a common pathway for formation of 9 and 16 is implicated.

The alternate explanation, that 16 forms via nucleophilic substitution of the symmetric pyrophosphate 9 by acid 15 (eq 4) was discounted for the following reasons. Firstly, the presence of 16 soon after initiation of reaction and at a much higher concentration than 9 may be used to argue against this possibility (Figure 1). Secondly, when the above reaction was repeated with the same amount of free acid 15 added *after* all of the oxidant was consumed and pyrophosphate formation was complete, subsequent generation of the mixed pyrophosphate was slow. After 16 hours, the concentration of the mixed pyrophosphate was only two thirds that of 9. Thus the involvement of the free acid 6a in formation of the symmetrical pyrophosphate 9 has been demonstrated.

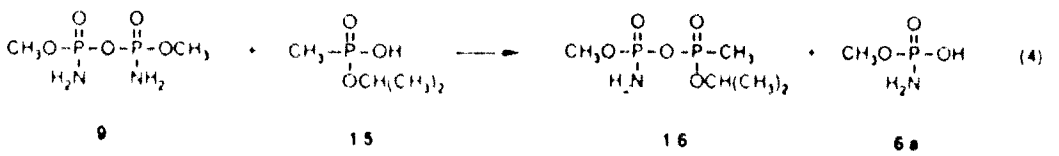

9 15 16 6a (4)

The products observed in the reaction with the added acid are also consistent with Scheme 2, provided the added phosphorus acid could displace the phosphoramidate anion from the proposed transient ion-pair. Demonstration of the involvement of methane sulfenic acid in the reaction is necessary to differentiate between the alternate pathways. To this end, the oxidation of 7 was repeated in the presence of 20 equivalents of ethyl acrylate. An intense ion at m/z 165, which was absent in control experiments, was detected by direct exposure probe CI/MS of the reaction solution. This is consistent with the protonated molecular ion of ethyl 3-methylsulfinylpropionate (14), the methane sulfenic acid/ethyl acrylate adduct. Formation of 14 was confirmed by the $^{1}H$ and $^{13}C$ NMR spectra of the reaction mixture which contained resonances identical to those obtained for an authentic sample of 14 prepared by thermal decomposition of methyl methanethiosulfinate (10) in ethyl acrylate.[15,16] Methane sulfenic acid has therefore been shown to form during the reaction. The involvement of the free acid 6a and the transitory presence of methane sulfenic acid indicate that formation of the symmetric pyrophosphate 9 by oxidation of O,S-dimethyl phosphoramidothioate (7) occurs, at least in part, via the sequence of reactions given as Scheme 3.

Trapping of the highly reactive methane sulfenic acid was expected to limit its concentration in solution thereby preventing dimerization to 10 and subsequent oxidation to 11. In turn, this removes water from the

reaction manifold thereby inhibiting formation of **9** by the mechanism shown in Scheme 3. Although the methane sulfenic acid/ethyl acrylate addition product formed when the oxidation of 7 was performed with the trapping agent present, the major products from the S-methyl moiety of 7 were still the dimethyl disulfide oxidation products, 10 and 11. The dominant phosphorus containing product in this reaction was pyrophosphate **9** (>95% yield, 45% conversion).

These observations suggest that formation of **9** also occurs via Scheme 2. Support for this mechanism may be elicited from the oxidation of 7 by **8** in the presence of ethyl acrylate (20 eq) and methanol (2.5 eq). The major phosphorus product from this reaction is O,O-dimethyl phosphoramidate (17), formed by displacement of methane sulfenic acid from **3a** by methanol.[19] Formation of methane sulfenic acid was confirmed by the presence of 14 in the reaction solution. S-methyl methanethiosulfinate (10) was not detectable by GC/MS in this solution. Thus, in the presence of ethyl acrylate, methane sulfenic acid does not dimerize. Formation of 10 in the oxidation of 7 by **8**, in the presence of ethyl acrylate, could not then have occured by this process.

In summary, the formation of P,P'-dimethyl diamidodiphosphate (9) in the oxidation of O,S-dimethyl phosphoramidothioate (7) does not require the involvement of water. Scheme 2 provides a plausible mechanism for the pyrophosphate formation, consistent with all the experimental observations.

## EXPERIMENTAL

O,S-Dimethyl phosphoramidothioate (7) (>98%) was obtained from the EPA Pesticide Repository, ethyl acrylate (>99%) from Chem Services, 2-(phenylsulfonyl)-3-(4-nitrophenyl)oxaziridine (8) was prepared at Drexel University and chloroform was dried over 5A molecular sieves prior to use. 2-Methylethyl methylphosphonic acid (15) was available within the laboratory (CRDEC) and had a purity of greater than 95% by NMR.

Reactions were performed in 5 mm NMR tubes by mixing aliquots of standard chloroform solutions of the reactants which were stored over molecular sieves. Typically, 8-10 mg of 7 was oxidized with ca. 1 equivalent of 8, giving a concentration of each reactant of about 0.05 M. $^{31}P$, $^{1}H$ and $^{13}C$ NMR were used to monitor the reactions. Spectra were recorded at probe temperature (ca. 20°C) using either a Varian VXR-400S or XL-200 FTNMR Specrometer operating at 400 or 200 MHz respectively for $^{1}H$. $^{31}P$ spectra were referenced to external 85% $H_3PO_4$, while $^{13}C$ and $^{1}H$ spectra were referenced to the solvent ($CHCl_3$, $^{13}C$ NMR: $\delta$77.2; $^{1}H$ NMR: $\delta$ 7.27). Gas chromatography/mass spectrometry (GC/MS) and direct exposure probe (DEP) mass spectrometry were performed using a Finnigan model 5100 GC/MS equipped with a 25 m x 0.25 mm i.d. fused silica GB-1 column coated with 0.25 $\mu$m dimethylpolysiloxane (Analabs, North Haven, CT). Reagent gas used for CI analysis was methane at a source pressure of 0.6 Torr.

## ACKNOWLEDGEMENTS

The authors are grateful to Dr. F.A. Davis of Drexel University for providing the 2-(phenylsulfonyl)-3-(4-nitrophenyl) oxaziridine; and Mr. L.J. Szafraniec of CRDEC for the 1-methylethyl methylphosphonic acid and O,S-diethyl methylphosphonothioate.

NOTES AND REFERENCES

1. Bellet, E.M., and Casida, J.E.; *J. Agr. Food Chem.*, 1974, 22, 207-211.

2. Segall, Y., and Casida, J.E.; In *Phosphorus Chemistry*; Quin, L.D., and Verkade, J., Eds.; ACS Symposium Series 171, American Chemical Society: Washington D.C., 1981; 337-340.

3. Segall, Y., and Casida, J.E.; *Tetrahedron Lett.*, 1982, 23, 139-142.

4. Segall, Y., and Casida, J.E., *Phosphorus Sulfur.*, 1983, 18, 209-212.

5. Thompson, C.M., Castellino, S., and Fukuto, T.R., *J. Org. Chem.*, 1984, 49, 1696-1699.

6. Bielawski, J., and Casida, J.E., *J. Agr. Food Chem.*, 1988, 36, 610-615.

7. Yang, Y-C., Szafraniec, L.L., Beaudry, W.T., and Rohrbaugh, D.K., *J. Amer. Chem. Soc.*, 1990, 112, 6621-6627.

8. Mixed anhydride 4 has been described as an exclusively sulfonating agent (refs. 2 and 4) which could not therefore form 5 by reaction with 6, or as both a phosphorylating and sulfonating agent (ref. 6). In dry methanol, 4 is exclusively phosphorylating (Dabkowski, W., Michalski, J., Radziejewski, C., and Skrzypczynski, Z.; *Chem. Ber.*, 1982, 115, 1636-1643).

9. The $^{31}P$ chemical shift for 9, presumed to have formed (although no supporting evidence for its presence was reported), in the 3-chloroperbenzoic acid oxidation of 7 has previously been reported as a single line at $\delta$ -6.53 or $\delta$ -5.74 ppm (ref 3). In our hands, oxidation of 7 with 3-chloroperbenzoic acid resulted in a mixture of products, including 9. The $^{31}P$ chemical shifts of diastereomeric 9 in this reaction solution were $\delta$ 1.6 and $\delta$ 1.2 ppm.

10 The $^{1}H$ and $^{13}C$ chemical shifts of the unidentified product do not correspond to those reported for any of the products detected in the 3-chloroperbenzoic acid oxidation of S-methyl methanethiosulfinate (11) (ref 12), although we found that it is formed in the oxidation of dimethyl disulfide by 8. This product is not amenable to GC separation as we were unable to detect it using GC/MS.

11. Allen, P., and Brook, J.W.; *J. Org. Chem.*, 1962, 27, 1019-1020.

12. Freeman, F., and Angeletakis, C.N.; *J. Amer. Chem. Soc.*, 1983, 105, 4039-4049.

13. Eto, M., Okabe, S., Ozoe, Y., and Maekawa, K.; *Pest. Biochem Phys.*, 1977, 7, 367-377.

14. Davis, F A., Billmers, J.M., Gosciniak, D.J., and Towson, J.C.; *J. Org. Chem.*, 1986, **51**, 4240-4245.

15. Block, E.; *J. Amer. Chem. Soc.*, 1972, **94**, 642-644.

16. Block, E., and O'Connor, J.; *J. Amer. Chem. Soc.*, 1974, **96**, 3929-3944.

17. Douglass, I.B.; *J. Org. Chem.*, 1959, **24**, 2004-2006.

18. NMR data for 16 (diastereomers): $^{31}P$ NMR: $\delta$ 22.8 (d, $^{2}J_{POP}$ = 24.5 Hz, $CH_3$-*P*-O-P-$NH_2$), 23.3 (d, $^{2}J_{POP}$ = 23.3 Hz, $CH_3$-*P*-O-P-$NH_2$), 1.48 (d, $^{2}J_{POP}$ = 24.5 Hz, $CH_3$-P-O-*P*-$NH_2$), 1.06 (d, $^{2}J_{POP}$ = 23.3 Hz, $CH_3$-P-O-*P*-$NH_2$); $^{1}H$ NMR: $\delta$ 1.38 (d, $^{2}J_{HCH}$ = 6.0 Hz, 3H, $(CH_3)_2$CH-O-P)), 1.38$_5$ (d, $^{2}J_{HCH}$ = 6.4 Hz, 9H, $(CH_3)_2$CH-O-P)), 1.69 (d, $^{2}J_{PCH}$ = 18.4 Hz, 3H, P-O-P-$CH_3$), 1.72 (d, $^{2}J_{PCH}$ = 18.4 Hz, 3H, P-O-P-$CH_3$), 3.85 (d, $^{3}J_{POCH}$ = 12.0 Hz, 3H, P-O-P-O$CH_3$), 3.85$_5$ (d, $^{3}J_{POCH}$ = 12.0 Hz, 3H, P-O-P-O$CH_3$), 4.89 (m, 2H, P-O-P-O$CH(CH_3)_2$).

19. Formation of (17) was confirmed by GC/MS: CI, M+1 = 126; and multinuclear NMR. $^{31}P$ NMR: $\delta$ 12.6 (septet, $^{3}J_{POCH}$ = 11.2 Hz); $^{1}H$ NMR: $\delta$ 3.75 (d, $^{3}J_{POCH}$ = 11.2 Hz); $^{13}C$ NMR: $\delta$ 53.3 (d, $^{2}J_{POC}$ = 5.6 Hz).

# NMR OF CALIXARENES

Paul D.Beer and Jonathan P.Martin
Department of Chemistry,
University of Birmingham

Andrew N.Trethewey
Chemistry and Decontamination Division,
Chemical Defence Establishment,
Porton Down, Salisbury.

In support of the CDE research programme, the analytical section requires real time monitoring of chemical agents and simulants in chamber and field trials. The work in support of this requirement centres on the use of host-guest chemistry as a possible monitoring probe. It is hoped that 'cavitands' with electro active centres may be electro-polymerised onto surfaces to provide specific probes. Calixarenes have a hydrophobic cavity which makes possible the inclusion of highly lipophilic molecules such as Di(2-chloroethyl) sulphide. The inclusion of Dimethyl sulphide is shown at low temperature with $^{1}$H nmr and $^{13}$C nmr. Molecular modelling interactions of the Di(2-chloroethyl) sulphide and substituted calixarenes are discussed.

## INTRODUCTION

At the Chemical Defence Establishment the analytical section has a requirement for real time monitoring of chemical agents and simulants for use in chamber and field trials. This work, in support of this requirement, centres on supra molecular interactions of a host gas type. In particular, it is hoped that a host for mustard gas could be produced and this work extrapolated to the development of a chemical detector. Figure 1 shows the essentials of a electro-chemical detector. The transducer here is an potentiometer, the interface is an electro active species and the zone of selective chemistry is the host molecule.

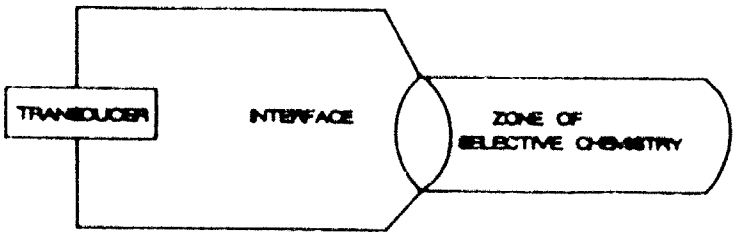


Figure 1 Schematic of electro-chemical detector.

Studies by P.Beer[1] et al and C.D.Hall[2] et al on the complexation of metal ions in redox active crown ether systems (Fig.2) showed selectivity to certain ions and also that the potential difference varied with the ionic radius of the included ions.

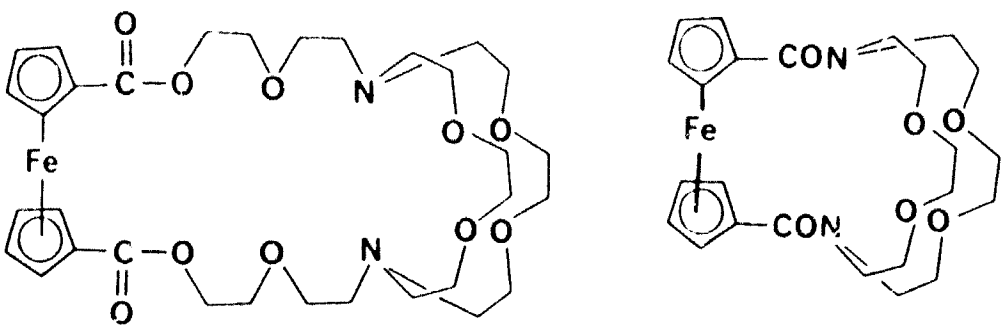


Figure 2 Electro active crown ethers capable of inclusion

1. P.D.Beer et al J.Org.Met.Chem. 1986,314.
2. C.D.Hall et al J.Chem.Soc.Chem.Comm. 1989,419.

This work suggested the possibility of an electro chemical system which could be designed to be stereo selective. These systems would need a hydrophobic capacity to complex the highly lipophilic molecules of interest such as Di(2-chloroethyl)sulphide. The literature abounds with potential hosts such as porphyrins, corrins, phthalocyanines, crown ethers, cryptands, spherands, lariat ethers and cyclodextrins. In this work, it was decided to investigate a class of compounds called calixarenes (1) as this group of compounds could be designed to have enforced cavities, are stable to pH over a wide range, and have a cavity size which can be changed.

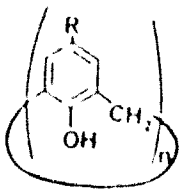


(1)

The name calixarene was brought into common usage by David Gutsche[3] who thought they looked like a vase hence the name calix from the Greek meaning cup. The calixarenes evolved from Bakelite chemistry. They arise from polymerisation of substituted phenols and formaldehyde with the presence of sodium hydroxide. Unlike Bakelite, these phenols are substituted in the four position forcing methylene groups to join the benzene ring from the two position on one ring to the six on the next ( Fig.2 ). This synthesis produces a range of calixarenes where n=4,5,6,7,8,9 but the major components are n=4,6 and 8[4]. The size of rings can be controlled. Lower temperature produces mostly the octamer while heating forces the octamer to de dimerise to give the tetramer and by using Rubidium hydroxide instead of sodium hydroxide as a template base the hexamer is produced as a major component. A retro Friedel Craft reaction dealkylates at the four positions to give the parent system.

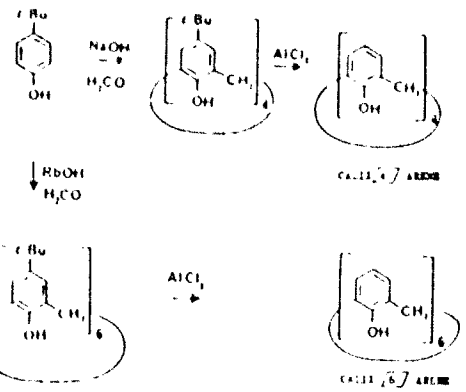


Figure 2 synthesis of unsubstituted calixarenes

3. C.D.Gutsne, The Calixarenes - Monographs On Macrocyclic Chemistry, Royal Society of Chemistry 1989.
4.C.D.Gutshe et al,J.Org.Chem.1986,51,742.

The conformation of the calixarenes is more defined for the tetramer than for the hexamer or octamer. The hexamer is fluctional at room temperature and there is evidence of the octamer forming two smaller rings by pinching in the middle of the large ring to form a figure of eight[5].

The conformation of the tetramer is more rigid and has been more thoroughly investigated. There are four major conformations possible for the calix[4]arenes[6] (Fig.3)

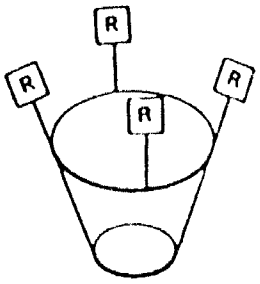


Cone

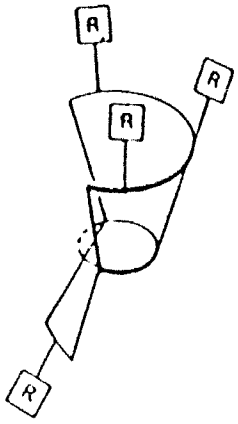


Partial Cone

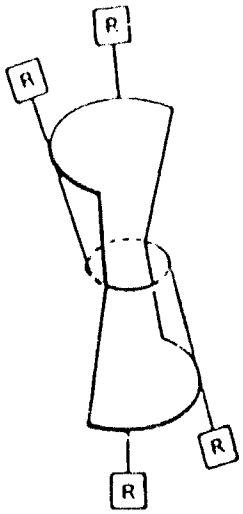


1,2-Alternate

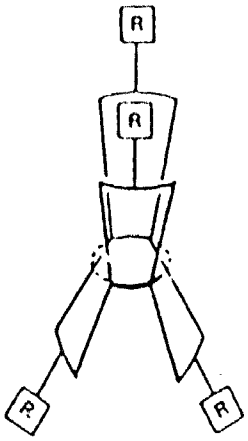


1,3-Alternate

Figure 3 The four major conformations of the calix[4]arenes

5. C.D.Gutshe et al,Tet. Lett. 1981,4763.
6. C.D.Gutshe et al, Tetrahedron,1983,39,409.

Substitution patterns can vary the conformations adopted. Substitution at a bottom rim will, in general, prevent inversion and so 'lock' the conformation in the full cone conformer. An X-Ray structure of a substituted calix[4]arene shows the full cone conformer in the solid state[7] (Fig.4).

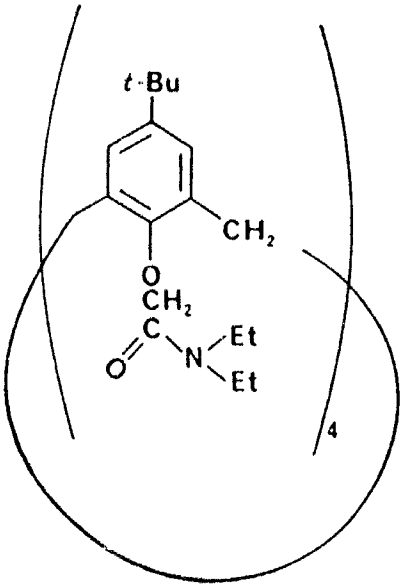


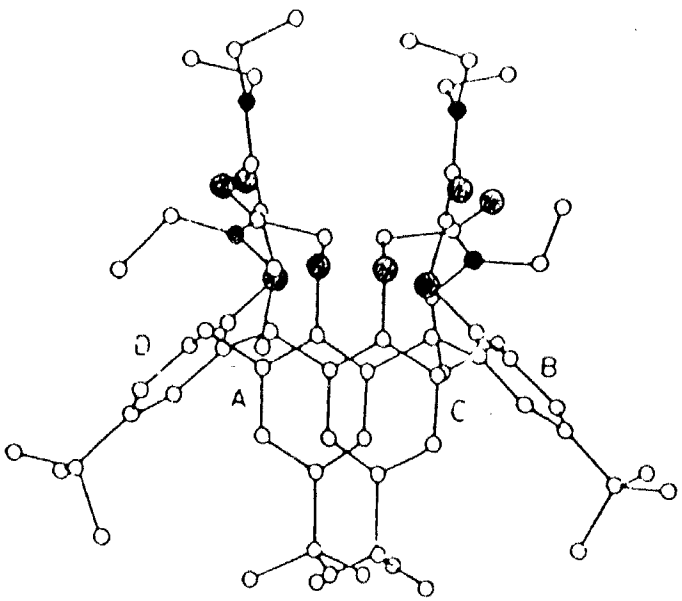


Figure 4 X-Ray structure of a substituted calix[4]arene

7.C.Calestani et al, J.Chem.Soc.Chem.Comm. 1987,344.

N.M.R. can be used to determine the predominant conformation adopted in the solution state. The ring methylenes give very useful information which can be related directly to the structure. The various possible adopted conformations and the N.M.R. patterns which these give rise to are seen in Fig.5.

| CONFORMATIONS | 1H NMR PATTERN |
|---|---|
| CONE | ONE PAIR OF DOUBLETS |
| PARTIAL CONE | TWO PAIRS OF DOUBLETS OR<br>ONE PAIR OF DOUBLETS AND ONE SINGLET |
| 1,2-ALTERNATE | ONE SINGLET AND TWO DOUBLETS |
| 1,3-ALTERNATE | ONE SINGLET |

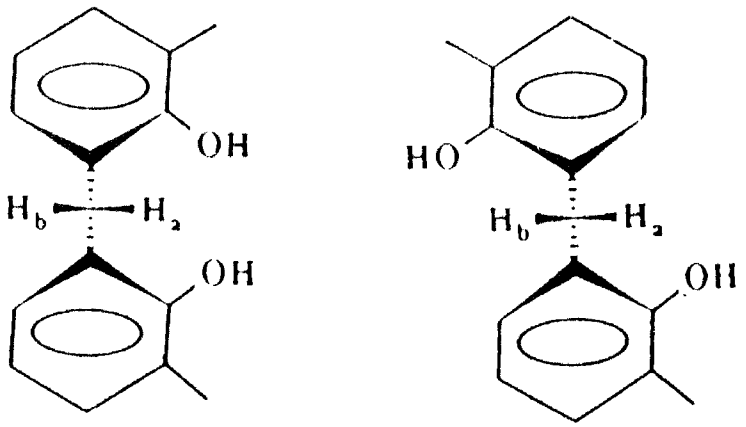


CONE
$\Delta$ = 0.9 +/- 0.2 ppm

1,3-ALTERNATE
$\Delta$ = 0.0 ppm

Figure 5 The structures and corresponding NMR patterns

$^1$H N.M.R. has been used to study the parent calix[4]arene. These studies show a coalescence point at ca. 50$^0$C indicating that below this point the full cone is adopted but above this temperature the system is fluctional[8].

8. A.Kammerer et al, Makromol. chem.1972,162,3317.

To study the inclusion phenomena a rigid full cone conformation was considered desirable as a start point. A calix[4]arene tetra substituted on the hydroxy function, which would be soluble in an organic solvent, was proposed and to this end the tetra tosyl calix[4]arene (2) was synthesised as well as the 1,3 bis ferrocenoyl calix[4]arene(3).

The a,b quartets seen in both $^{1}H$ N.M.R spectra suggest sterically locked full cone conformers for both compounds - see Fig.6 and 7. The full cone conformer is very stable for the bottom ring tetra substituted calix[4]arene. The a,b quartet for (2) does not coalesce in DMSO even at 170$^{0}$C.

$^{1}H$ N.M.R studies on neutral molecule inclusion suggested that a downfield shift will be observed for an included species as in the case of tert-butylamine[9]. Here the methyl resonances of the tert-butylamine experience a downfield shift of 0.28 ppm. On addition of a two fold excess of dimethyl sulphide to a chloroform solution of the tetra tosyl derivative(2), no shift of the methyl signal was observed. However, on cooling the system down to -58$^{0}$C, two signals could be observed (Fig.8). This indicates the presence of an inclusion phenomenon which is too fast to observe at room temperature. The same phenomenon is observed in the $^{13}C$ N.M.R spectra. It was supposed that this inclusion rate would be the same for the bis ferrocenoyl derivative and so to date this work has not been performed. Instead, data for the bis ferrocenoyl derivative obtained from X-ray data was used in molecular modelling work designed to see where an included molecule would sit in the cavity. For ease of modelling the Iron and bottom cyclopentene ring are not included. The results with di chloro methane and this system (Fig.9a) suggest that this molecule sits higher than was proposed for a molecule of this size. The results of modelling mustard and the bis ferrocenoyl derivative show an even weaker inclusion phenomenon( Fig 9b).

This brought about a reappraisal of the earlier sizing work and a calix[6]arene (4) derivative was modelled to study inclusion phenomena with this system. The calix[6]arene is not as conformationally rigid as the calix[4]arene and so for comparison the model has been 'computer' locked in the full cone conformer. These studies show that the included molecule sits further into the cavity ( fig 10).

This work is still ongoing and the results so far, while promising, have yielded more problems than answers. It is hoped to examine these calix[4]arene systems with cyclic voltametry and then under inclusion conditions. It may be that while the inclusion phenomenon is only weak, it is enough to give a detectable difference in the electro potential of the system. If this is not the case, the calix[5]arene and the calix[6]arenes will be studied as well.

9.C.D.Gutshe et al J.Amer.Chem.Soc.1985,107 6063.

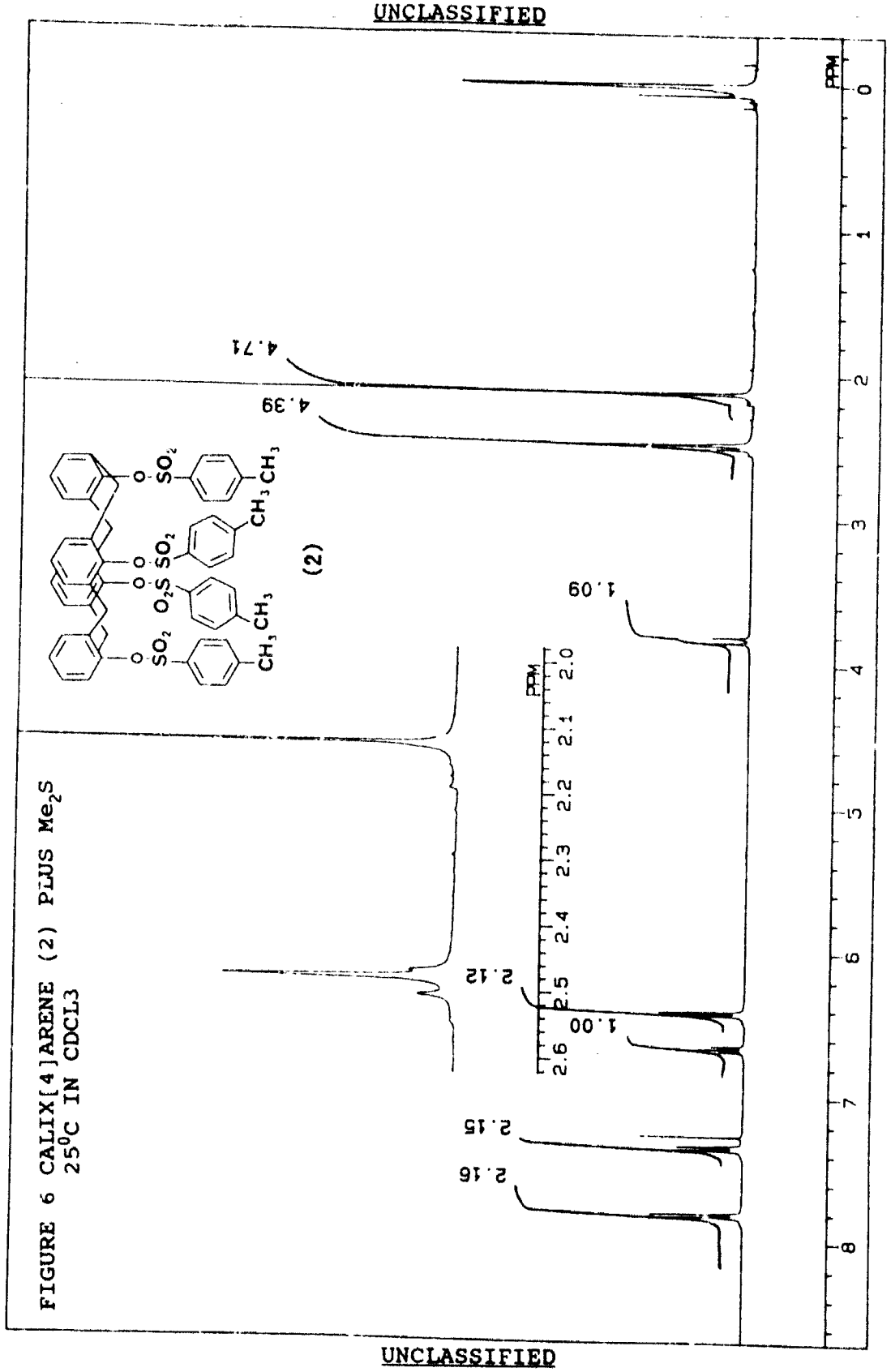


FIGURE 6 CALIX[4]ARENE (2) PLUS $Me_2S$
25°C IN CDCl3

UNCLASSIFIED

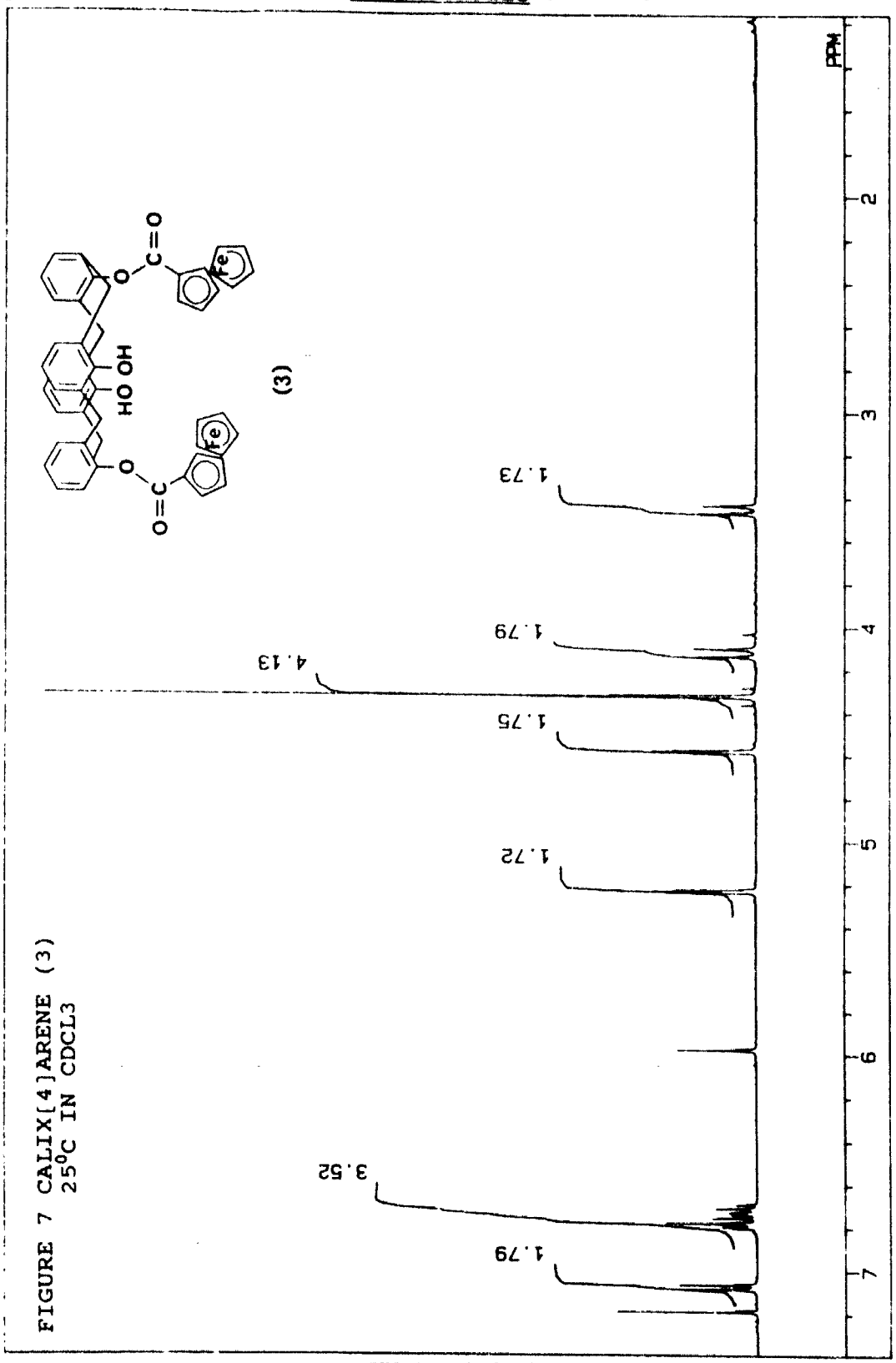


FIGURE 7 CALIX[4]ARENE (3)
25°C IN CDCL3

UNCLASSIFIED

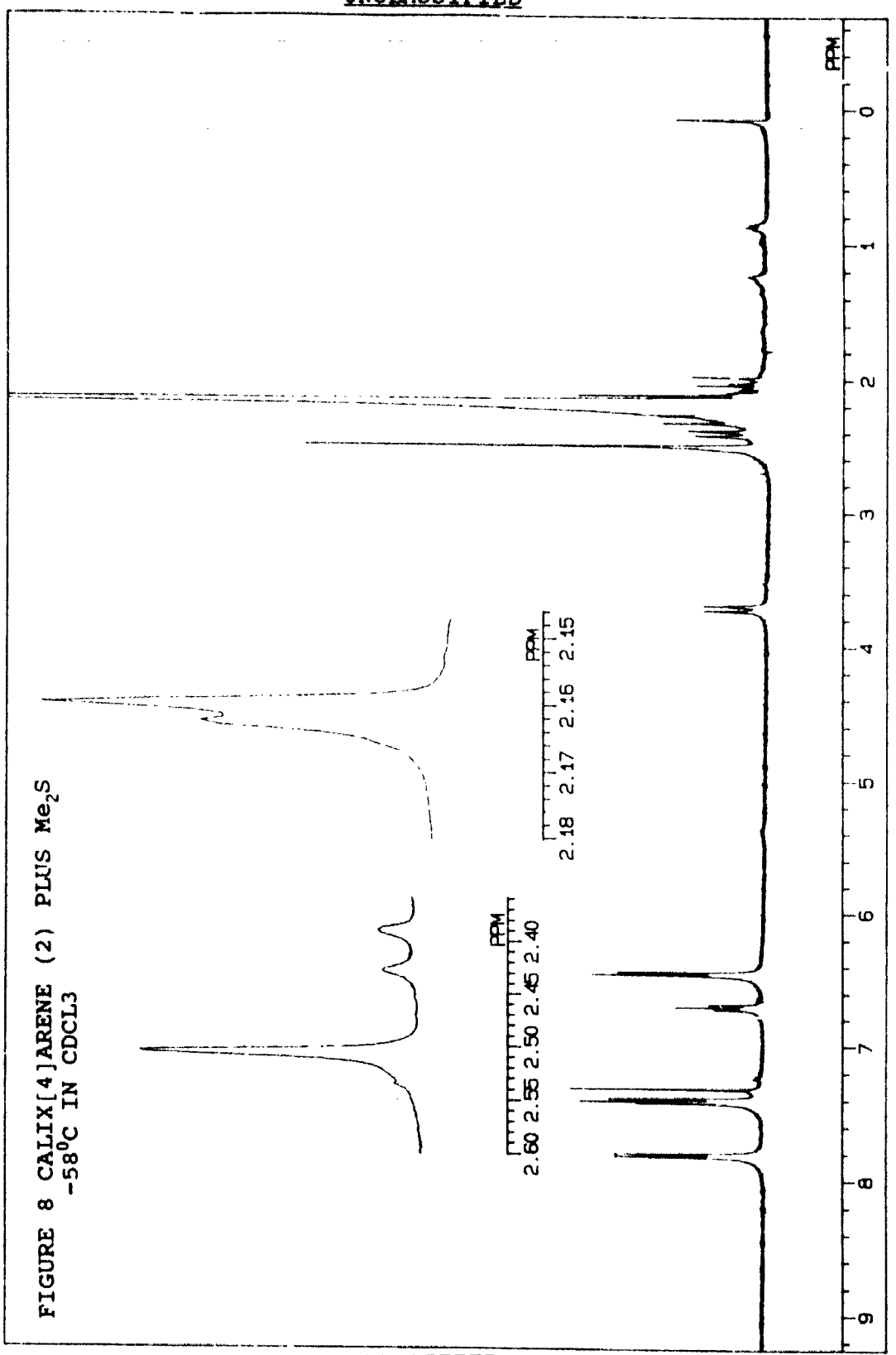


FIGURE 8 CALIX[4]ARENE (2) PLUS $Me_2S$
-58$^0$C IN CDCL3

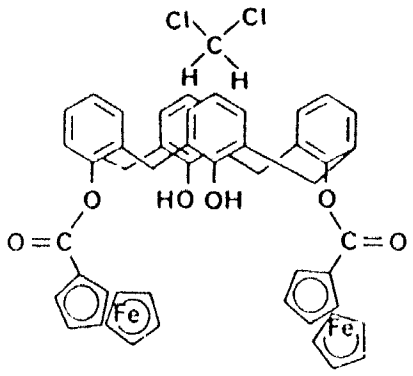


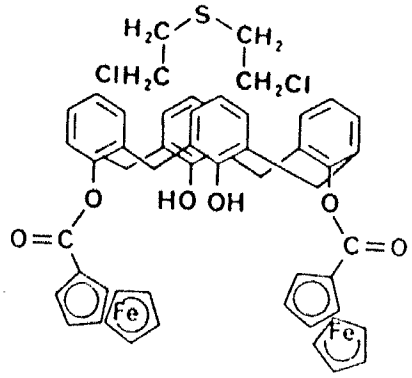


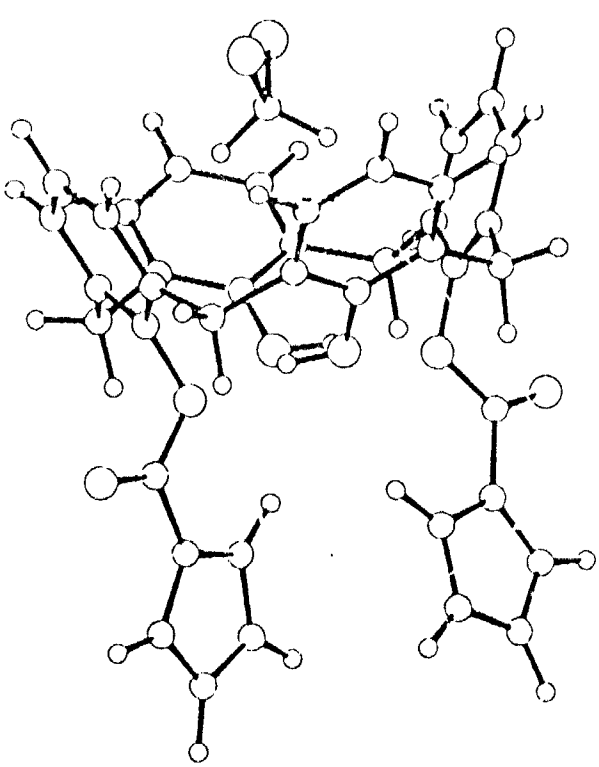

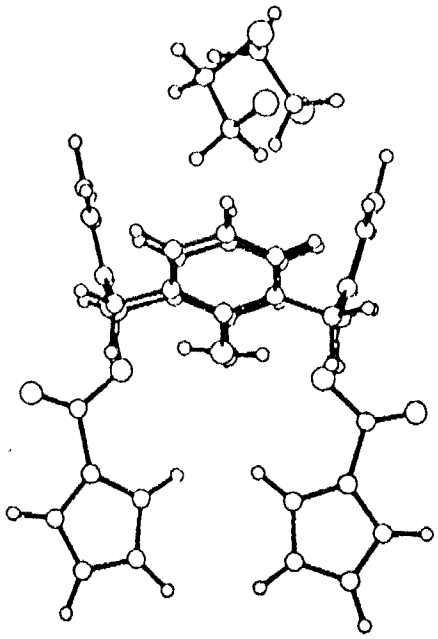

Figure 9 a Energy minimised structure of dichloromethane included in the calix[4]arene (3)

Figure 9 b Energy minimised structure of mustard included in the calixarene (3)

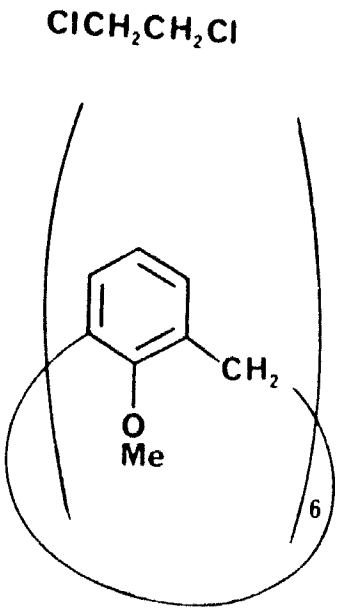


(4)

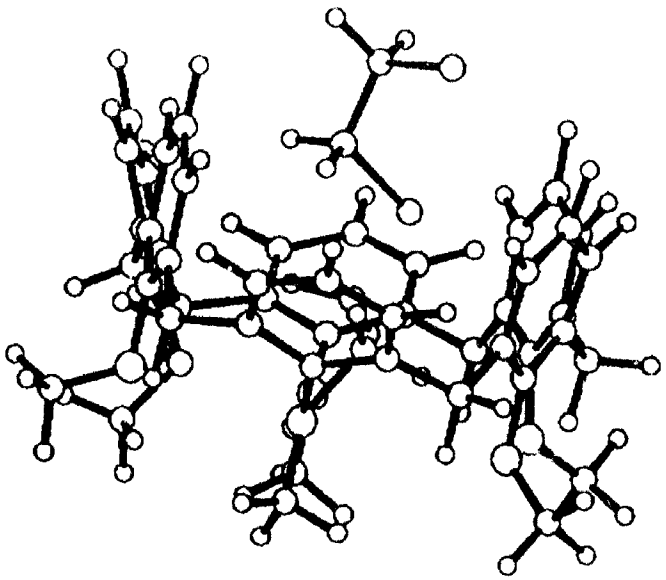

Figure 10 Energy minimised structure of the inclusion of mustard into the hexa methoxy calix[6]arene cavity.

# REACTIONS OF CW AGENTS IN DS2

William T. Beaudry, Linda L. Szafraniec, Dennis K. Rohrbaugh
U.S. Army Chemical Research, Development and Engineering Center
Aberdeen Proving Ground, Maryland 21010-5423, USA

and

D. Ralph Leslie
Materials Research Laboratory,
Defence Science and Technology Organization
Melbourne, Australia

## INTRODUCTION

The standard U.S. Army decontaminating agent DS2 is a clear solution consisting of 70% diethylenetriamine (DETA), 28% ethylene glycol monomethylether (MC) and 2% sodium hydroxide (NaOH) by weight. It is a general purpose decontaminant that will react rapidly with all known chemical warfare agents. When first developed by J. B. Jackson,[1] DS2 was thought to be a simple mixture of a caustic in an alcohol/amine solvent mix. Decontamination was thought to be carried out by the caustic with simple, well understood chemistry. However, a subsequent study[2] showed that DS2 is a unique combination of chemicals with complex chemistry.

Considerable effort has been devoted to the optimization of use factors for DS2. For example, water and carbon dioxide have been shown to have deleterious effects on both storage of DS2 and its use on painted surfaces.[3-5] Preferential evaporation of MC from surfaces treated with DS2 has been suggested as a possible mechanism for reduced decontaminating efficiency on moving vehicles.[6] Efforts to predict the environmental fate of the components of DS2 and the known and assumed products from its reactions with the chemical agents have also been attempted.[7]

Despite a wide variety of models and studies presented in the literature, little investigation and/or detection of the actual products of the reaction has been reported. However, the divinyl sulfide produced from DS2 and HD has been isolated and identified.[8] Sulfur products from the side chain of VX were identified and used to infer the phosphorous products of the VX reaction with DS2. Rate data from the same study indicated that for most of the chemical agents, the rate of destruction would be too fast to be followed by NMR methods (half-lives of $< 2$ s and $< 7$ s for HD and VX, respectively). However, the observed products, product distribution and secondary reactions in the resulting decontaminated solutions are ameniable to NMR investigation. A study of these as a function of starting conditions, additives and time should provide valuable insight into the mechanism of action of DS2 and the factors most important in influencing its efficacy.

BACKGROUND

Each component of the DS2 mixture has been shown to play a role in the effective decontamination of chemical agents. The amine (DETA) has been reported[2] to act as a clathrating agent to sequester the metal cation of the caustic to form an hydroxide "superbase" (i.e. pH > 14). The "superbase" then converts a portion of the MC to an alkoxide ($^-$MCO) which can act as a nucleophile in the non-aqueous system.

$$^-OH + HOCH_2CH_2OCH_3 \rightleftharpoons H_2O + {}^-OCH_2CH_2OCH_3 \qquad (1)$$

MC functions as both a solvent extender and source of the nucleophile. The ratio of MC/DEA has been shown to form an azeotrope important for keeping the NaOH in solution as the mixture evaporates.[2,7]

EXPERIMENTATION

Multinuclear NMR ($^{31}P$ and $^{13}C$) was used to both monitor the reactions and to identify the products formed. A weighed amount of the substrate was added to a 5 mm NMR tube and DS2 added. The tube was capped, sealed with Parafilm, and shaken for complete mixing. The products and course of the reaction were monitored by $^{31}P$ NMR using two minute accumulations until no changes were observed. Starting conditions and additives were varied to assess their influence on the reaction rates, reaction profiles, products and yields obtained. O,S-Diethyl methylphosphonothioate (DEMPS) was used extensively as a simulant for comparison with VX, and 2-chloroethyl methyl sulfide (CEMS) was used for comparison with HD. The reactants, intermediates and products used or identified are listed in Table 1. Representative NMR parameters in the reaction media are given in Appendix A.

In all cases the reaction of neat DS2 with each of the CW agents was complete prior to the NMR experiment (usually < 1 min). Reactions were carried out using neat DS2 and DS2 with added $H_2O$. The DS2 was found to contain a trace of ethylene glycol (EG) as an impurity. Agent reactions with the individual components of the DS2 were used to aid in the assignment of products.

RESULTS

Primary Reactions and Products.

When GB was reacted with DS2, a single product, initially present in > 95% yield, decomposed slowly in the reaction media. The product was identified as 1 (see Table 1) from its $^{31}P$ and $^{13}C$ spectra. Similarly, mixed diesters 2 and 3 were identified as the initial products obtained from the action of DS2 on GD and VX (or DEMPS), respectively. In addition to 3, the formation of a second diester 5 from VX and DEMPS was identified as arising from the trace amount of (EG) in the DS2. The assignment was confirmed by a dramatic increase in 5a when the DS2 was spiked with EG before reaction.

Table 1. Compounds in DS2 Reactions

| REACTANTS[1] | STRUCTURE | REACTANTS[1] | STRUCTURE |
|---|---|---|---|
| GA | $(CH_3)_2NP(O)(OEt)(CN)$ | DEMPS | $CH_3P(O)(OEt)(SEt)$ |
| GB | $CH_3P(O)(OIP)(F)$ | CEMS | $ClCH_2CH_2SCH_3$ |
| GD | $CH_3P(O)(OP)(F)$ | MC | $CH_3OCH_2CH_2OH$ |
| VX | $CH_3P(O)(OEt)(SDAE)$ | DETA | $(H_2NCH_2CH_2)_2NH$ |
| HD | $(ClCH_2CH_2)_2S$ | EG | $(OHCH_2)_2$ |
| PRODUCTS[2] | | PRODUCTS | |
| 1 | $CH_3P(O)(OIP)(OMC)$ | 10 | $CH_3SCH_2CH_2(NR)$ |
| 2 | $CH_3P(O)(OP)(OMC)$ | 11 | $CH_3SCH_2CH_2(NR')$ |
| 3 | $CH_3P(O)(OEt)(OMC)$ | 1a | $CH_3P(O)(OIP)(OH)$ |
| 4 | $CH_3P(O)(OMC)(OMC)$ | 2a | $CH_3P(O)(OP)(OH)$ |
| 5 | $CH_3P(O)(OEG)(OMC)$ | 3a | $CH_3P(O)(OEt)(OH)$ |
| 6 | $CH_3P(O)(OEt)(OEG)$ | 4a | $CH_3P(O)(OMC)(OH)$ |
| 7 | $CH_3P(O)(OEt)(NR)$ | 5a | $CH_3P(O)(OEG)(OH)$ |
| 8 | $(CH_3)_2NP(O)(OEt)(NR)$ | DVS | $(CH_2{=}CH)_2S$ |
| 9 | $(CH_3)_2NP(O)(OEt)(OMC)$ | MVS | $CH_3SCH{=}CH_2$ |

1. $Et{=}CH_2CH_3$, $IP{=}CH(CH_3)_2$, $P{=}CH(CH_3)C(CH_3)_3$, $DAE{=}CH_2CH_2N[CH(CH_3)_2]_2$
2. $NR{=}NHCH_2CH_2NHCH_2CH_2NH_2$, $NR'{=}N(CH_2CH_2NH_2)_2$

Two major products were obtained from the reaction of GA with DS2. One product at a $^{31}P$ chemical shift of 19.5, is suggestive of a phosphorodiamidate, 8. The $^{13}C$ spectrum of the mixture is also consistent with a P-N-C moiety present at 51.6 with a $^{31}P$ coupling constant 5.4 Hz. The same product was also detected in a solution of GA in DETA alone. The second product at 11.8 is consistent with a mixed diester 9 formed by replacement of the CN by OMC. The $^{13}C$ spectrum of the mixture showed $^{31}P$ coupled $OCH_2$ groups consistent for the OMC moiety in 9. However, the spectra have not been completely assigned and product identification is tentative. The two products were observed unchanged in the reaction medium for at least 21 hrs.

Consistent with previous reports,[8] divinyl sulfide (DVS) was obtained as the product from the action of DS2 on HD. The product was identified from $^{13}C$ spectra. Unlike the mixed diesters from the G and V-type agents, DVS appeared to be stable in the reaction media.

Secondary Reactions and Products.

After the primary reactions described above were complete, compounds 1 - 6 produced from GB, GD, VX and DEMPS were observed to further react in the DS2 solutions. The compounds identified in the solutions, 1a - 5a, are shown in Table 1. Reaction rates were estimated from the reaction profiles and are given in Table 2.

Table 2. Rates of Secondary DS2 Reactions Expressed as Half-Lives.

| COMPOUND | CONDITIONS[1] | HALF-LIFE, min |
|---|---|---|
| 1 | GB/DS2, 0.04M | 164 |
| | GB/DS2/5%$H_2O$, 0.03M | 144 |
| 2 | GD/DS2, 0.02M | 550 |
| | GD/DS2/5%$H_2O$, 0.03M | 488 |
| 3 | VX/DS2, 0.06M | 23.2 |
| | DEMPS/DS2, 0.03M | 17.3 |
| | DEMPS/DS2/5%$H_2O$, 0.04M | 21.7 |
| | DEMPS/DS2/50%$H_2O$, 0.04M | 23.1 |

1. Ambient temperature: ~18 °C for all reactions

A typical reaction profile is shown in Figure 1 for compound 1. The disappearance of 1 was directly monitored with the concomitant increase of secondary products 1a and 4a. The half-life for the disappearance of 1 was estimated from the curve and found to be ~164 min at 18 °C. Compounds 1a and 4a accounted for 97 % of the products after 22 hours with a final ratio of 71 to 29 (1a to 4a) after 22 hours.

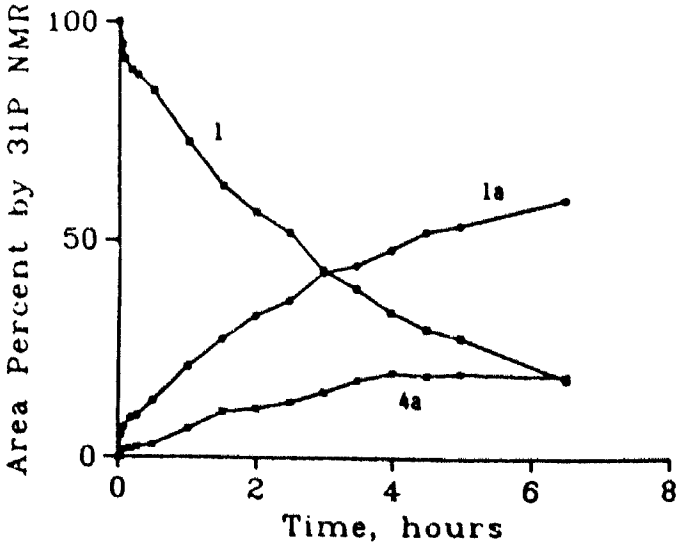


Figure 1. Decomposition of 1 from GB in DS2.

The mixed diester from GD, 2, also produced a reaction profile similar to Figure 1. The products obtained were identified as the phosphonic acids 2a and 4a. However, both the time course of the reaction and the final product ratios were altered. After 22 hours, 18% of 2 was still present and the ratio of 2a to 4a was 96 to 4. The half-life for the disappearance of 2 was estimated to be ~550 min at 18 °C.

The mixed diester 3 from VX or DEMPS appeared to be more reactive than either 1 or 2. The reaction profiles for 3 obtained from VX or from DEMPS were nearly identical and are shown for comparison in Figure 2.

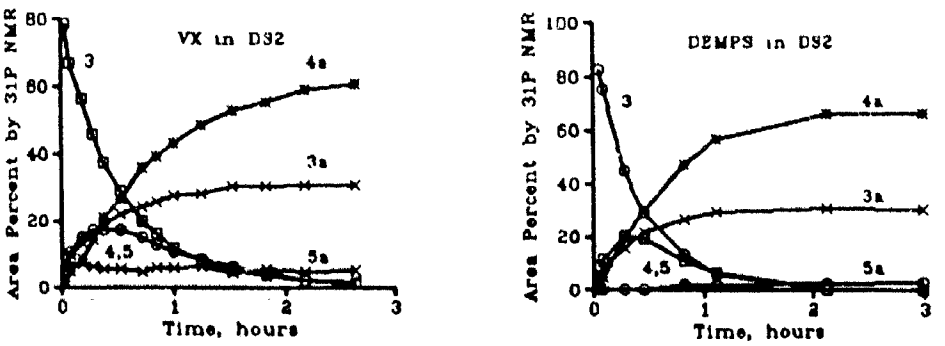


Figure 2. Reaction profile of 3 from VX or DEMPS reactions with DS2.

Unlike Figure 1, with 1 disappearing as products 1a and 4a appear, the reacton profile for either VX or DEMPS clearly shows multiple compounds formed and decomposed in the reaction. The inital yield of diester 3 was ~83% and a second compound, identified as 4, was present at ~9%. In addition, note that the reactions were essentially complete in < 90 minutes and that the final products 3a and 4a were evident after 3 minutes. The measured half-life of 3 appeared to be in the range of 17 to 25 min. Compounds 4a, 3a and 5a were present at 67, 30 and 3 %, respectively, in the final mixture.

Reactions with Water Added

The reactions above were duplicated using DS2 with 5 wt% added $H_2O$. In general, the primary reactions were again complete before the NMR data was obtained. However, the secondary reactions showed changes in the product distribution and/or reaction profile depending on the agent studied. As the water content was increased (up to 50%) both the primary and secondary reactions showed substantial differences, with new products formed and rates slowed.

For GB, the addition of 5% $H_2O$ reduced the initial yield of 1 to 85% and altered the final product distribution in favor of 1a (84%) relative to 4a (16%). Interestingly, the half-life of 1 reduced from ~164 to ~144 min. Similarly, for GD, the initial yield of 2 was reduced to 88%, and the half-life decreased to ~488 min from ~550 min. After 22 hours, 14% of 2 remained and the ratio of 2a to 4a was 85 to 15.

When DEMPS was reacted with the DS2/H2O solutions the primary reaction showed approximately the same amount of 3 as with DS2 alone. However the final product distribution for the secondary reactions showed 60% 3a and 40% 4a in contrast to 31 and 69% with DS2 alone. The addition of 50%

water slowed the primary reaction markedly. DEMPS remained detectable in the solution for at least 55 min. An additional product identified as 7 was produced along with 3 in the solution. 7 decomposed slowly with 17% remaining after 22 hrs.

Chloroethyl methyl sulfide (CEMS) was used as a simulant for HD in a series of reactions with DS2 and water. The reaction was fast in neat DS2 and produced methylvinyl sulfide (MVS). When the water content was varied from 10 to ~50%, approximately 15% of unreacted CEMS remained in the solution, indicating substantial slowing of the primary reaction. At the higher concentrations the samples were initially two phases. As the water content increased, the amount of the MVS decreased (Table 3). Two additional products 10 and 11 were identified based on their $^{13}C$ spectra. At 50% $H_2O$, no MVS was observed.

Table 3. Reaction of CEMS in DS2/$H_2O$ Solutions. Mole % by $^{13}C$ NMR

| %$H_2O$ | ELIMINATION PRODUCT MVS | SUBSTITUTION PRODUCTS 10 | 11 |
|---|---|---|---|
| 0 | 100 | 0 | 0 |
| 10.3[1] | 82.6 | 13.4 | 3.9 |
| 20.3 | 57.8 | 33.9 | 8.3 |
| 30.5[2] | 15.7 | 65.8 | 18.5 |
| 48.6[2] | 0 | 76.9 | 23.1 |

1. ~15% unreacted CEMS remained in solution ~1-2 hrs after mixing
2. Samples were initially 2 phases.

## DISCUSSION

### Reactions of G and V Agents

The reactions of tetracoordinate organophosphorous compounds have been extensively investigated.[10-12] The mechanism proposed involves a controlled facial attack by nucleophiles followed by permutational isomerization of idealized trigonal bipyramidal pentacoordinate intermediates. Products then result from apical departure of a leaving group. (Scheme 1)

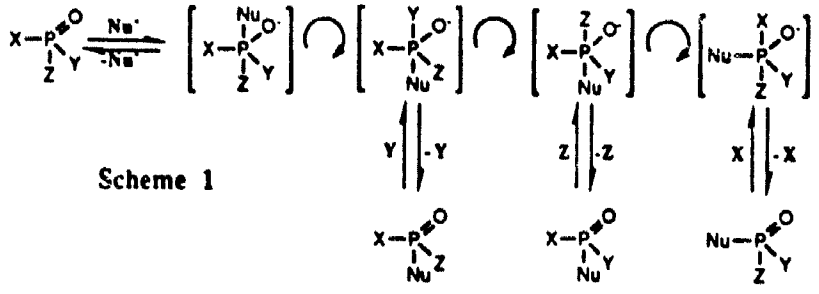

Scheme 1

The susceptibility of a given phosphonate to attack is, in part, governed by the nature of the attacking nucleophile, the transition state and the leaving group. The products are partitioned by the relative ability of the leaving groups (**X**, **Y** or **Z**) to be stablized in the reaction medium.

The primary products in the reactions of DS2 are consistent with a nucleophilic attack by the alkoxide of MC (Nu=⁻OMC) on GB, GD and VX. The primary products observed are diester methylphosphonates **1**, **2** and **3**; not the phosphonic acids **1a**, **2a** and **3a** expected from hydroxide attack. However, the presence of additional products in the GA and VX/DEMPS reactions indicate that competing processes can occur. Since neat DS2 contains the strong nucleophiles ⁻OMC and ⁻OH and the soft base DETA, scheme 1 should contain reaction paths for each nucleophile in the system as shown below:

$$
\begin{aligned}
CH_3P(O)(Y)(Z) + {}^-OMC &\dashrightarrow [\ ] \dashrightarrow CH_3P(O)(Y)(OMC) + {}^-Z \\
+ {}^-OH &\dashrightarrow [\ ] \dashrightarrow CH_3P(O)(Y)(OH) + {}^-Z \\
+ DETA &\dashrightarrow [\ ] \dashrightarrow CH_3P(O)(Y)(NR) + HZ \\
+ {}^-OEG &\dashrightarrow [\ ] \dashrightarrow CH_3P(O)(Y)(OEG) + {}^-Z
\end{aligned}
\qquad (3)
$$

While ⁻OMC is a stronger nucleophile than hydroxide or DETA, its concentration is governed by the equilibrium in eq. 1. Shifting the equilibrium by the addition of small amounts of water should then increase the amount of hydroxide at the expense of alkoxide. As the concentration of the alkoxide decreases, hydroxide and other nucleophiles can then successfully compete for the substrate and account for the additional products observed. The primary product and the product distribution then becomes dependant on the relative strength and concentration of the competing nucleophiles.

Once formed, the diesters also undergo subsequent attack by the nucleophile rich DS2 medium and are eventually converted to their corresponding phosphonic acids. **1**, **2** and **3** differ in only one of the ester groups and have the 2-methoxyethyl moiety in common. The stability of the each diester should thus be governed by the relative ability of ethyl (**3a**), isopropyl (**1a**) or pinacolyl (**2a**) to act as a leaving group. The leaving group should come off more easily the more stable it is as a free entity. This is usually the reverse of its basicity with the best leaving groups being the poorest bases.[9] Literature pKa values for the conjugates of the leaving groups alkylthiol, ethanol, 2-propanol, 2-methyoxyethanol and 1,2-ethandiol are ~12, 15.9, 17.1, 14.8, and 15.1, respectively.[9,13] No literature value was readily available for pinacolyl alcohol, but a comparison of branched versus linear alcohols would indicate a value >17. The leaving groups in increasing basicity (best to worst leaving group) are then predicted to be:

$RS^- < CH_3OCH_2CH_2O^- \leq HOCH_2CH_2O^- < CH_3CH_2O^- < (CH_3)_2CHO^- < (CH_3)_3C(CH_3)CHO^-$

in agreement with the observed rate data (Table 2) where 2 < 1 < 3.

In contrast, the relative leaving ability of the groups are all similar in the VX or DEMPS reaction (ethyl or OMC) and competing processes yield numerous products as shown in scheme 2.

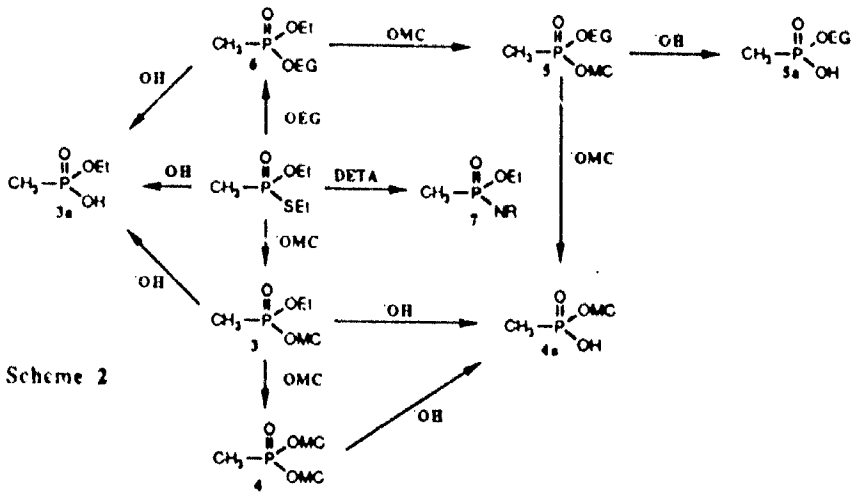


Scheme 2

The relative amount of each of the final products 3a or 4a is governed by changes in the medium which influence the relative amounts and strength of hydroxide and alkoxide. Added water emphasised attack by hydroxide and produced more 3a. The products labeled 5, 5a, and 6, were identified as arising from the ethylene glycol impurity in DS2. Attack by the alkoxide of EG competes with $^-$OMC and produces 6 which subsequently forms both 3a and 5. Further reaction of 5 leads to 5a. Preferential attack by DETA leads to the production of 7 at high water concentrations.

In neat DS2, the observation of 1, 2, 3 and 4 indicates that the dominant nucleophile is overwhelmingly $^-$OMC, but that even in trace amounts, the alkoxide from EG can compete sucessfully to produce 5 and 6 in DEMPS reactions (Scheme 2). Small amounts of water reduce the amount of the strong alkoxide nucleophiles and allow $^-$OH to compete for the substrate. Hence the reduced production of 1, 2,and 3 and increased 1a, 2a and 3a with addition of 5% water. At a higher water content, DETA and hydroxide sucessfully compete with the alkoxide as evidenced by the production of 7 from DEMPS in 50% DS2/$H_2O$ solutions. The rate is considerably slowed as the less nucleophilic hydroxide replaces alkoxide in solution. In contrast, the presence of 8 from the reaction of GA and DS2 suggests that the dimethylamino group may modify the phosphorus center and promote nucleophilic attack by the softer nucleophile DETA. Despite the presence of the strong alkoxide nucleophile, 8 is the major product detected from GA. 8 remains stable in the solution and does not appear to undergo additional reaction.

Reaction of HD and DS2

DVS was obtained as the major product in neat DS2. The reaction, shown below, is similar to known dehydrohalogenation reactions of alkyl halides.[8]

$$(ClCH_2CH_2)S \xrightarrow{^-OMC} (CH_2{=}CH)S + MCOH + CL^- \quad (4)$$

It has been reported that additional products can form (reaction 5) when the DS2 reaction is inhibited by water.[5]

$$(ClCH_2CH_2)S + DETA \rightarrow \begin{cases} ClCH_2CH_2SCH_2CH_2NHCH_2CH_2NHCH_2CH_2NH_2 & (I) \\ \text{or} & (5) \\ S(CH_2CH_2)_2NCH_2CH_2NHCH_2CH_2NH_2 & (II) \end{cases}$$

The data from the CEMS reactions in DS2/$H_2O$ solutions confirm the presence of two products in addition to MVS. The products are consistent with the substitution of DETA for chlorine. The analog of I was identified from its $^{13}C$ spectrum as 10, formed by substitution by the primary amino group of DETA. The second product was identified as 11 from substitution by the secondary amine. No analog for II was expected since CEMS only has a single chlorine and cannot form a ring. Experiments with HD in DS2/$H_2O$ solutions are in progress to attempt to identify II or the analog of 11 as a second substitution product.

Water inhibits the formation of the elimination products and promotes substitution products. The data given in Table 3 indicate that even at low levels of added water, the substitution reaction is significant and at ~20% $H_2O$ the substitution reactions predominate. It is not surprising then that 10 to 20% water is reported to inhibit the decontamination of HD by DS2, since even in more polar solvents like water the hydrolysis of HD is slower (~1-2 min)[14] than the elimination reaction in DS2 (<2 sec).[8]

CONCLUSIONS

The active component in DS2 for decontaminating GB, GD or VX was identified as the alkoxide of methylcellosolve which initially forms a mixed diester via nucleophilic displacement of fluorine (GB, GD) or the S-alkyl moiety (VX). Product diesters were identified by $^{31}P$ and $^{13}C$ NMR. The diesters were found to slowly convert to their corresponding phosphonic acids via further nucleophilic displacement by hydroxide. In contrast, the active nucleophile for GA appears to be DETA forming an alkyl phosphorodiamidate. Competition between the nucleophiles hydroxide, alkoxide and DETA for the phosphonate esters is greatly affected by water. Water reduces the alkoxide concentration and favors substitution by the less nucleophilic hydroxide.

The elimination of HCl from HD to produce divinyl sulfide was confirmed by $^{13}C$ NMR as previously reported via isolation methods Using a simulant (CEMS), water was found to inhibit the action of DS2 by changing the reaction mechanism from eliminatin to substitution. In addition to the elimination product MVS, two products were identified as arising by substitution of either the primary or secondary amino groups in DETA for chlorine. Substitution becomes the dominant mechanism, forming > 50% of the products, at water levels between 20 and 25%.

## REFERENCES

1. Jackson, J. B. Development of Decontaminating Solution DS2. CWLR 2368. April 1960. UNCLASSIFIED REPORT.

2. Richardson, G.A. Development of a Package Decontaminating System. EACR-1310-17. Final Report Contract # DAAA15-71-C-0508. August 1972. UNCLASSIFIED REPORT.

3. Fielding, G.H. Field Decontamination Studies with Chemical Warfare Decontaminating Solution DS2. NRL Report 6191. December 1964.

4. Day, S.E. and Gendason, P. Laboratory Evaluation of the Decontaminating Effectiveness of DS2 and STB Slurry Against Agents on Painted Metal. ED-TR-74057. November 1974. UNCLASSIFIED REPORT.

5. Clark, T.M. and Day, S.E. Degradation Processes of U.S. Army Standard Decontaminant DS2. CRDC-TR-84037. August 1984. UNCLASSIFIED REPORT.

6. Zamejc, E.R.; Doner, J.J. and Frank, G.L. Effects of Airflow on DS-2. DPG/TA-89/010. January 1989. UNCLASSIFIED REPORT.

7. Small, J. M. Compounds Formed From the Decontamination of HD, GB and VX and Their Environmental Fate. AD-A149 515. USAMBRDL-TR-8304. June 1984. UNCLASSIFIED REPORT.

8. Davis, G. T.; Block, F.; Sommer, H.Z. and Epstein J. Studies on the Destruction of Toxic Agents VX and HD by the All-Purpose Decontaminants DS-2 and CD-1. EC-TR-75024. May 1975. UNCLASSIFIED REPORT.

9. March, J. "Advanced Organic Chemistry: Reactions, Mechanisms, and Structure. McGraw-Hill Book Company, 1968. Chapter 10.

10. Westheimer, F. H. *Acc. Chem. Res.* **1968**, 70.

11. Gillespie, P.; Ramirez, F.; Ugi, I .and Marquarding, D. *Angew. Chem. Internat.* **1973**, 12(2), 91-172 and references therein.

12. DeBruin, K.; Tang, C-L.; Johnson D. and Wilde, R. *J. Am. Chem. Soc.* **1989**, 111, 5871-5879.

13. "The Chemistry of the Hydroxyl Group" (ed) S. Patai. Interscience (1971). Chapter 20.

14. Yang, Y.-C.; Ward, J. R.; Luteran, T. *J. Am. Chem.* **1986**, 51, 2756-2759.

Appendix A. Representative NMR Parameters in DS2

| COMPOUND | $\delta^{31}P$, ppm | $\delta^{13}C$, ppm ($J_{C-P}$, Hz) |
|---|---|---|
| 1 | 30.9 | |
| 2 | 31.4 | |
| 3 | 31.8 | $\underline{C}H_3P$, 10.9(142.7); $O\underline{C}H_2CH3$, 61.6(6.0); $OCH_2\underline{C}H3$, 16.6 (6.2); $O\underline{C}H_2CH_2$, 64.7(6.3); $\underline{C}H_2O$, 72.0(5.8); $O\underline{C}H_3$, 58.7 |
| 4 | 32.4 | |
| 5 | 32.4 | |
| 6 | 31.8 | |
| 7 | 39.2 | |
| 8 | 19.5 | |
| 9 | 11.8 | |
| 10 | - | $\underline{C}H_3S$, 15.4; $S\underline{C}H_2$, 34.5; $N\underline{C}H_2$'s, 49.0, 49.6, 49.8; $H_2N\underline{C}H_2$, 53.1; $H_2NCH_2\underline{C}H_2$, 42.1 |
| 11 | - | $\underline{C}H_3S$, 15.7; $S\underline{C}H_2$, 32.4; $SCH_2\underline{C}H_2N$, 54.4; $\underline{C}H_2NH_2$, 40.4; $H_2N(CH_2\underline{C}H_2)_2$, 58.1 42.1 |
| 1a | 20.6 | $\underline{C}H_3$, 12.2(142.9); $\underline{C}H$, 69.6(6.1); $(\underline{C}H_3)_2$, 25.5(4.4) |
| 2a | 20.8 | $\underline{C}H_3P$, 14.2(137); $\underline{C}H$, 77.2(6.4); $CH\underline{C}H_3$, 17.5; $\underline{C}$, 35.1 (5.9); $(\underline{C}H_3)_2$, 26.0 |
| 3a | 21.5 | $\underline{C}H_3P$, 12.8(134.7); $O\underline{C}H_2$, 59.1(5.0); $\underline{C}H_3$, 17.0(6.4) |
| 4a | 22.0 | $\underline{C}H_3P$, 12.7(134.7); $PO\underline{C}H_2$, 62.7(5.0); $O\underline{C}H_2$, 72.9(6.7); $\underline{C}H_3$, not observed. |
| 5a | 23.1 | |
| DEMPS | 30.0 | $\underline{C}H_3P$, 19.8(109.5); $O\underline{C}H_2$,61.4(6.7); $S\underline{C}H_2$, 25.1(3.3); $OCH_2\underline{C}H_3$, 16.4(6.6); $SCH_2\underline{C}H_3$, 16.9(4.7) |
| DVS | - | $\underline{C}H_2$, 114.7; $\underline{C}H$, 130.4 |
| MVS | - | $\underline{C}H_3$, 13.6; $\underline{C}H_2$, 108.4; $\underline{C}H$, 133.7 |

# $^{27}Al$ AND $^{11}B$ NQR OF CERAMIC MATERIALS

Chuck Connor
Defence Research Establishment Pacific
CFB Esquimalt, FMO Victoria, B.C. V0S 1B0

and

Jih-Wen Chang and Alex Pines
Materials and Chemical Sciences Division,
Lawrence Berkeley Laboratory
and
Department of Chemistry, University of California,
Berkeley, CA 94720

## INTRODUCTION

The study of advanced materials is an area of critical importance in defence research. Among the many techniques available to study these materials, NMR spectroscopy has proven very useful, especially in work on non-crystalline materials. In particular, solid state NMR is widely used to study the molecular structure and dynamics of organic solids such as polymers.[1] This widespread usage is largely due to the extremely successful cross polarization-magic angle spinning (CP-MAS) experiment, applied to $^{13}C$ nuclei.[2] This technique effectively solves the problems of low sensitivity, long relaxation times, and broad lines due to reduced molecular motion in the solid state.

However, several problems hinder a correspondingly widespread application to inorganic solids, such as ceramics. One of the most serious problems is that many nuclear species found in inorganic solids possess a quadrupole moment. Nuclei with quadrupole moments, which include $^{27}Al$, $^{11}B$, $^{10}B$, $^{14}N$, and $^{17}O$, may experience a quadrupolar coupling, due to the interaction between the nuclear spin and the electric field gradient at the nuclear site.[3] This quadrupolar coupling broadens the resonance lines observed in high field NMR. In almost all cases the broadening, even with MAS, is so severe that

resonance lines from nuclei with different chemical shifts cannot be resolved. Thus quadrupolar coupling seriously hinders the ability of high field NMR spectroscopy to obtain meaningful chemical and structural information about inorganic solids.

Several approaches are being used to reduce the effect of quadrupolar broadening in high field NMR spectra. One approach is simply to perform the MAS experiment in a larger magnetic field. This has the dual benefits that line broadening is reduced while the chemical shift interaction disperses the resonance lines over a wider frequency range. Although fairly effective, this technique is limited by the technology available for producing high field NMR magnets. Another approach involves developing new techniques which can more effectively average the residual quadrupolar interaction. This approach has produced the double order rotation (DOR) and double angle spinning (DAS) experiments, which are expected to find wide use in a variety of applications.[4]

The approach described in this paper is arrived at by noting that the quadrupolar broadening, in powder samples, is a direct result of the distribution of crystallite orientations with respect to the magnetic field. As has long been recognized, by working in zero field one may obtain a pure nuclear quadrupole resonance (NQR) spectrum in which the line positions are determined solely by the quadrupolar interaction.[3] Relatively narrow, well dispersed lines are usually observed with the zero-field experiments. However, conventional NMR spectrometers usually lack the sensitivity required for pure NQR of nuclei with quadrupolar splittings less than a few megahertz. This is because almost all NMR spectrometers use Faraday detectors, for which the sensitivity decreases rapidly at lower resonance frequencies.[5] Thus pure NQR studies of only a few nuclear species can be readily performed with conventional equipment.

There is no fundamental reason why a Faraday detection scheme must be employed in NMR spectrometers. The work described in this paper was carried out on a spectrometer based on a Superconducting QUantum Interference Device (SQUID) detector.[6] The SQUID system has excellent low frequency sensitivity, but is less useful at frequencies above a few hundred kilohertz. Thus the magnetic resonance technique used with this SQUID-based

spectrometer differs considerably from the standard pulsed NMR technique.

**EXPERIMENTAL TECHNIQUE**

The technique used with the SQUID spectrometer,[7] called longitudinal magnetic resonance, is best understood by examining the energy level diagram of a spin-3/2 nucleus in a small magnetic field (Figure 1). The shift in the energy levels caused

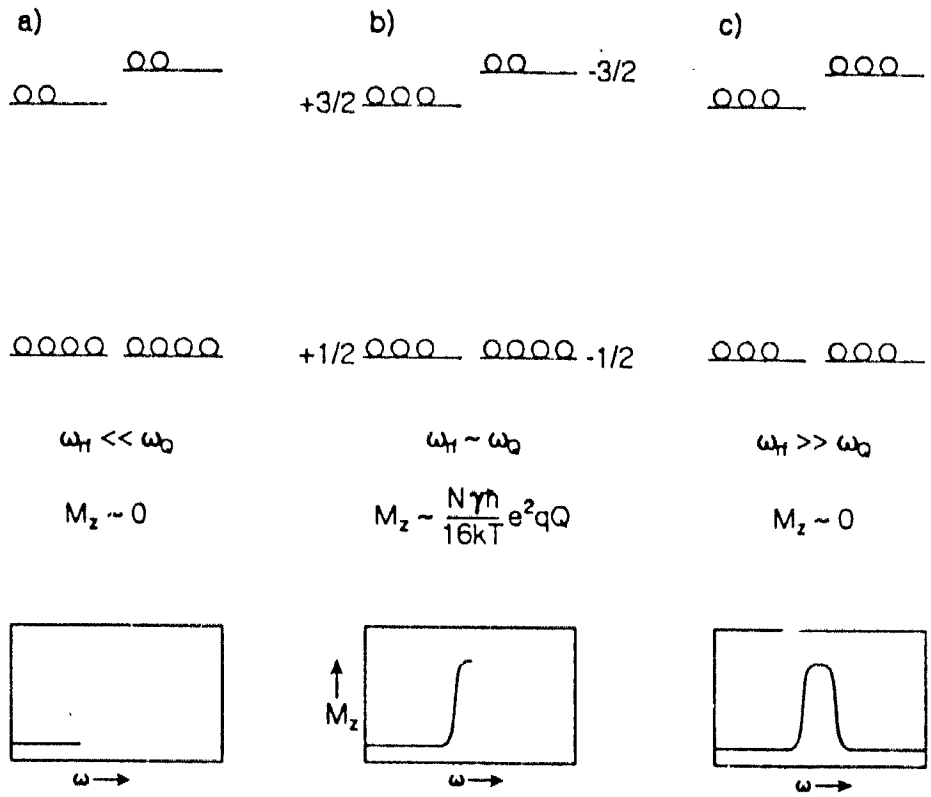


Figure 1: This figure demonstrates the principle behind longitudinal NQR. The energy level diagrams schematically show the relative populations of the energy levels when a) the rf frequency is much below resonance, b) the rf field is at resonance, and c) the rf frequency in far above resonance. A plot of the longitudinal magnetization, $M_z$, as a function of the rf frequency, $\omega_{rf}$, shows a peak at the quadrupolar splitting frequency.

by the magnetic field is small compared to the splitting due to the quadrupolar interaction. At thermal equilibrium (Figure 1a), a population imbalance exists between the ±1/2 and the ±3/2 states. However, the spin system does not exhibit a significant magnetization because the contributions due to the +m and to the -m pairs cancel each other. A small rf field, swept from low to high frequency, destroys this balance by initially saturating the (+1/2,+3/2) component of the transition (Figure 1b). The spin system now exhibits a longitudinal magnetization, $M_z$, proportional to the quadrupolar splitting. As the sweep is continued, the populations of the -1/2 and -3/2 states are equalized, returning the sample magnetization to a negligibly low value (Figure 1c). A plot of $M_z$ as a function of the rf frequency shows a peak at the quadrupolar splitting frequency.

The change in $M_z$ is monitored by a dc SQUID (Biomagnetic Technologies, Inc., San Diego, CA). A schematic of the coil arrangement is shown in Figure 2.[8] The sample, rf coil, and pickup coil are immersed in a dc field generated by magnetic flux trapped in a superconducting cylinder. Samples consist of about 0.20 $cm^3$ of material, held at 4.2 K during data acquisition. The spectra shown in the following section required about an hour each to collect.

**RESULTS AND DISCUSSION**

The SQUID spectrometer was initially applied to $^{27}Al$ nuclei in a single crystal of corundum ($\alpha$-$Al_2O_3$). This well studied material[9] served as a standard to test many of the principles of longitudinal NQR, both in our work and in the original application of the technique by Jach.[10] In particular, because the signal strength depends on the crystal orientation, it was not clear that a powder sample would give a measurable signal.[7] However, as can be seen from the the experimental spectra shown in Figure 3, the powder sample provides a signal-to-noise ratio comparable to that from the single crystal sample. The quadrupolar splitting can be easily determined from either spectrum. The linewidth of the single crystal spectrum is determined by dipolar coupling between the $^{27}Al$ nuclei,[9b),9c)] demonstrating that this sample is highly crystalline as expected.

$^{11}B$ in boron nitride (BN) was also studied. This

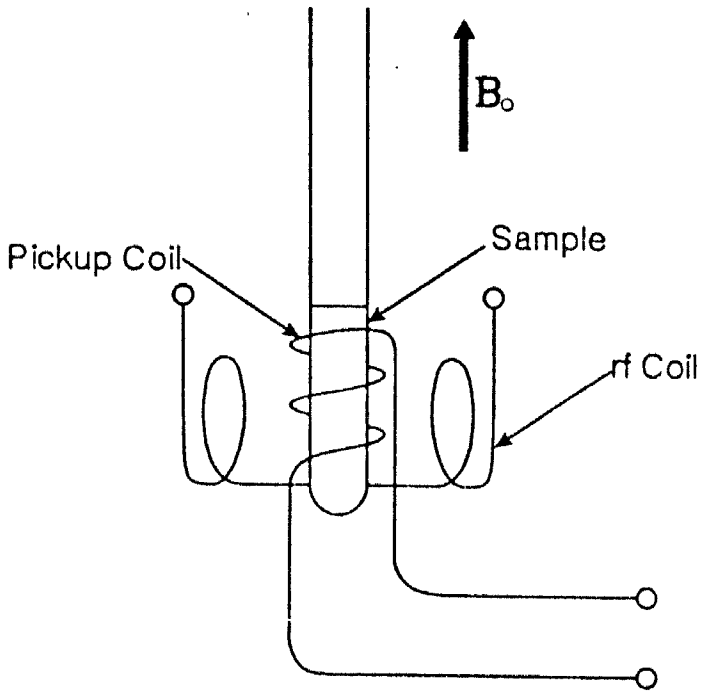


Figure 2: The coil arrangement for longitudinal NQR consists of an rf coil and a pickup coil. The rf coil generates an rf field orthogonal to the dc magnetic field, while the pickup coil, coupled to the SQUID, detects the component of sample magnetization parallel to the dc field.

material, which is isoelectronic with carbon, has two phases analogous to graphite and to diamond. The cubic phase, in which boron and nitrogen nuceli are tetrahedrally bound, has properties similar to diamond. This arrangement of nuclei generally produces a very small quadrupolar splitting, suggesting this material is amenable to study by MAS techniques. Thus the hexagonal form, which is similar in structure to graphite, was examined. The boron and nitrogen nuclei are trigonally bound in layered planes of six-membered rings, but unlike graphite the nuclei in one

plane lie directly above the nuclei in the plane below.[11]

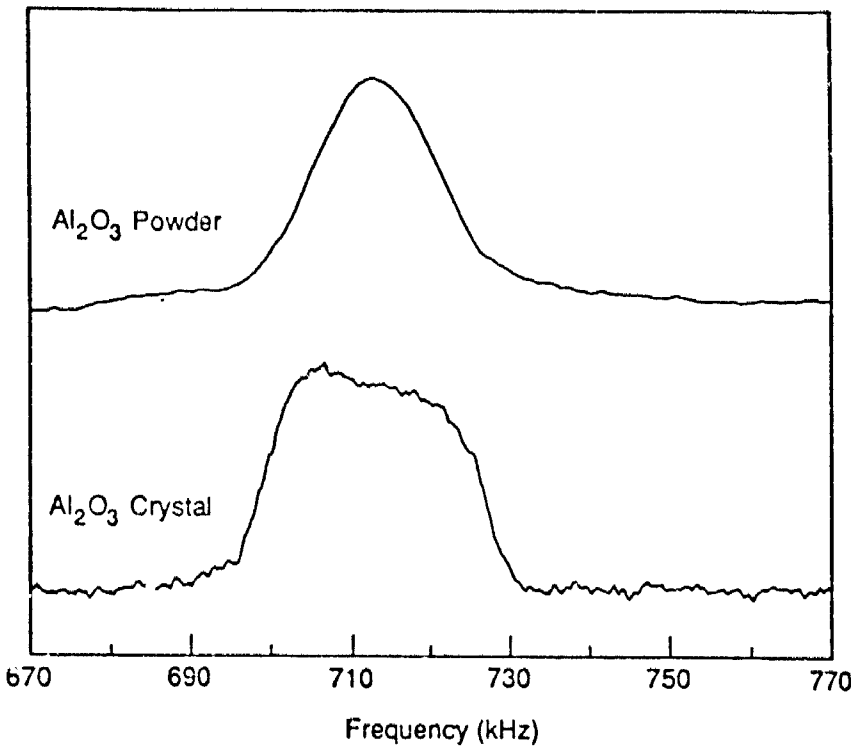


Figure 3: Longitudinal NQR spectra of the (±3/2,±5/2) $^{27}Al$ transition in single crystal and polycrystalline powder samples of corundum are shown. A comparison of these spectra shows that the quadrupolar splitting, 717 kHz, can readily be determined from a powder sample, which is not often the case in high field NMR.

A longitudinal NQR spectrum of the powdered material is presented in Figure 4. A hot-pressed rod of the material was also examined. According to the supplier (ESFI International, Agoura, CA), the plate-like crystals of the material become partially ordered during pressing, so there is a preferred orientation of the planes. To get an estimate of the extent of this ordering, we prepared three samples: one was cut so its cylindrical axis was parallel to that of the rod, one had its cylindrical axis perpendicular to that of the rod, and a third

was a 50 mesh (300 $\mu$m) powder from the same supplier. Preferred

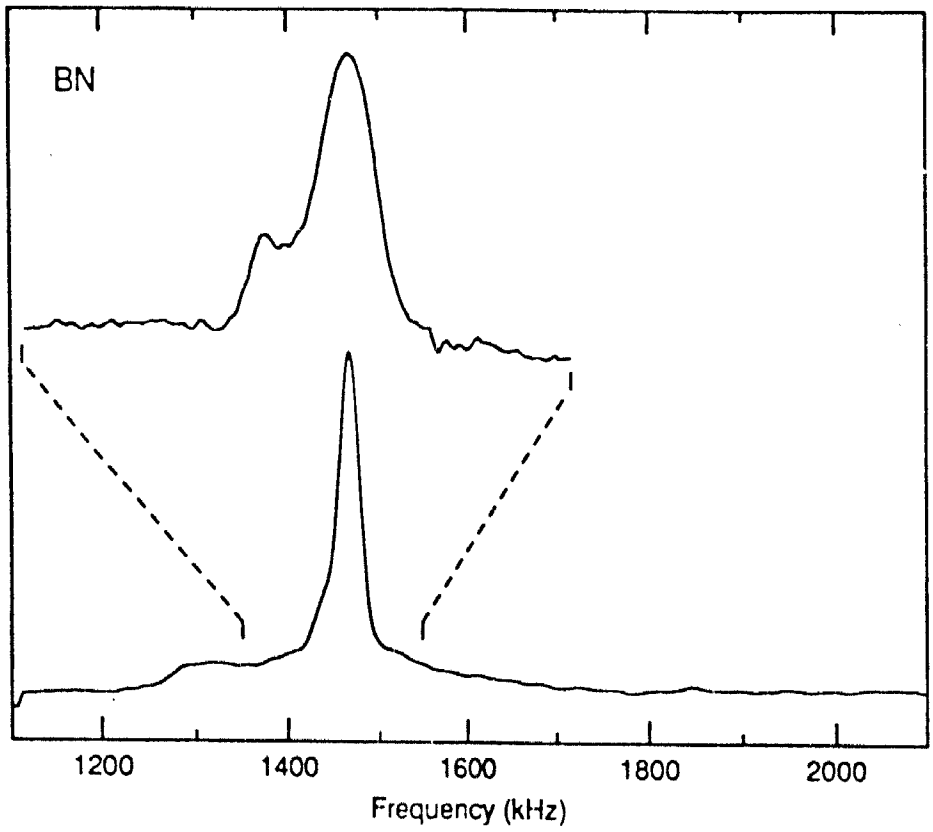


Figure 4: The broad resonance at 1350 kHz in these longitudinal $^{11}B$ spectra of polycrystalline boron nitride is due to $B_2O_3 \cdot xH_2O$ impurities. The origin of the low frequency shoulder, more clearly visible in the upper trace, has yet to be satisfactorily explained.

orientation within either hot-pressed sample will affect the intensity of the spectrum from that material. We found that both hot-pressed samples gave signals of comparable magnitude, while the powder sample gave a signal about half as intense. This factor of two is expected purely from the reduced filling factor of the powder sample. These data indicate that the degree of ordering of the platelets is quite low. Further longitudinal NQR work is required to accurately measure the degree of ordering.

Several features are readily apparent in the spectrum of boron nitride. The broad peak near 1350 kHz is due to $B_2O_3 \cdot xH_2O$ impurities in the boron nitride. The borates are known to be degradation products of the breakdown of boron nitride by steam, so it seems reasonable that exposure of the boron nitride powder to moist air will produce $B_2O_3 \cdot xH_2O$. This 1350 kHz peak was not observed in samples cut from the hot-pressed rod, for which a far smaller surface area is presented to the atmosphere. The assignment is confirmed by longitudinal NQR spectra of the borates with x = 3, 1, and 0, which displayed resonances at 1282, 1333, and 1308 kHz respectively. Another feature to note in the spectrum is the shoulder on the low frequency side of the main peak, more clearly seen in the upper trace. The upper trace was recorded using conditions that maximize the resolution, at the expense of some signal intensity. While it is possible that two boron sites are present, the relatively simple structure of boron nitride suggests that all boron nuclei should be found in one type of site, producing a single resonance line. Other obvious explanations for the shoulder, such as other impurities in the sample, appear unlikely. However, the shoulder did not appear in spectra obtained from boron nitride supplied by Alfa Products (Ward Hill, MA). Thus the origin of this shoulder has yet to be confirmed. It should be noted that high field NMR techniques could be used to measure the quadrupolar splitting of boron nitride powder, but it seems quite unlikely that the shoulder, or the 1350 kHz resonance, could be resolved.[12]

$B_2O_3$ glass, which is a representative disordered material, was also studied by longitudinal NQR. This compound, in common with the other borates, is made up of tetrahedral $BO_4$ units and trigonal $BO_3$ units.[12] The tetrahedral sites do not experience a significant quadrupolar splitting, so are generally not observed with the longitudinal NQR technique. The quadrupolar splitting of the $BO_3$ unit usually falls in the range from 1200 to 1600 kHz. Longitudinal NQR can be used to answer several questions about disordered materials, such as glasses, that can not be easily addressed by conventional techniques. Often one would like to know if a material is completely glassy, or whether small crystalline domains are present. It is also of interest to characterize the degree of variation between the

nuclear sites within the material. For example, one wants to know if the $^{11}B$ nuclei are located in similar sites within the sample, or whether a very wide variation of sites exists. The absence of a sharp peak in the NQR spectrum of $B_2O_3$ glass, shown in Figure 5, confirms that this sample does not contain a

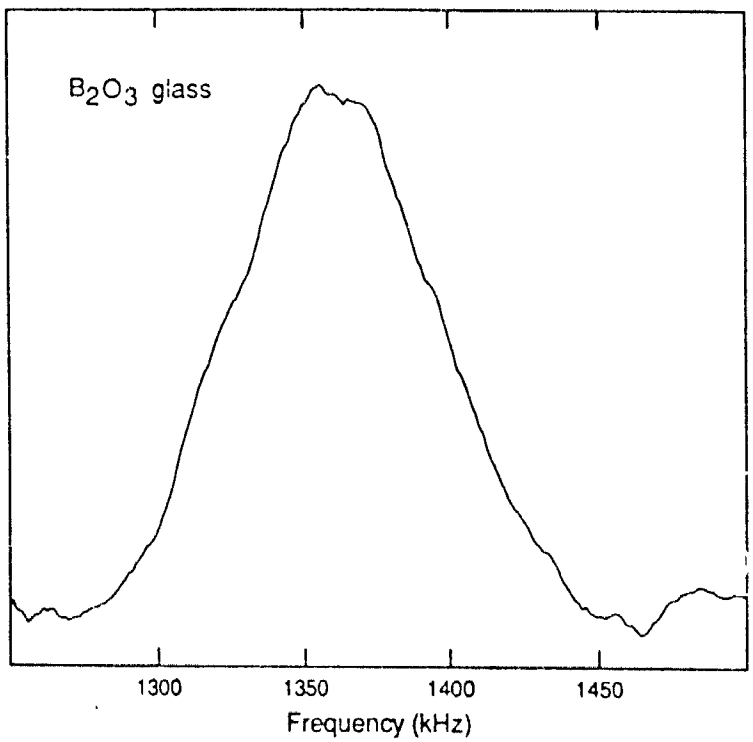


Figure 5: The resonance line in this longitudinal NQR spectrum of $B_2O_3$ glass is about twice as broad as the corresponding line in polycrystalline $B_2O_3$. The linewidth provides a measure of the variation in the trigonal $BO_3$ site within the glass.

significant crystalline fraction. Note that the linewidth, about 60 kHz, is significantly larger than that for the polycrystalline material, which is about 30 kHz. This additional broadening is attributed to the variation of the local environment of the $^{11}B$ nuclei throughout the sample. Large distortions of the $^{11}B$ site would produce correspondingly large shifts in the quadrupolar splitting, yielding a much broader line. Thus this spectrum shows that the variation in $^{11}B$ sites is not great. A more

quantitative result would be obtained by numerical simulations of the experimental spectrum.

## CONCLUSIONS

The longitudinal NQR technique can be applied to ceramic materials to probe their internal structure. Initial application of the technique to $\alpha$-$Al_2O_3$ demonstrated that the quadrupolar splitting can be determined as readily in polycrystalline materials as in single crystals. Work on boron nitride powder shows that the powder contains $B_2O_3 \cdot xH_2O$ impurities, and hints of a more complex structure than is generally accepted. The technique is also able to provide data that is helpful in determining the degree of structural disorder in glasses and amorphous materials.

## ACKNOWLEDGEMENT

This work was supported by the Director, Office of Energy Research, Office of Basic Energy Sciences, Materials Sciences Division of the U.S. Department of Energy, and by the Director's Program Development Fund of Lawrence Berkeley Laboratory, under Contract No. DE-AC03-76SF00098.

## REFERENCES

1. a) C.A. Fyfe, Solid State NMR for Chemists, (CFC Press, Guelph, 1983)
   b) V.D. Fedotov and H. Schneider, NMR-Basic Principles and Progress, edited by P. Diehl, E. Fluck, H. Günther, R. Kosfeld, and J. Seelig, Vol. 21 (Springer-Verlag, Berlin, 1989).

2. C.S. Yannoni, Acc. Chem. Res. **15**, 201 (1982).

3. T.P. Das and E.L. Hahn, Solid State Physics, edited by F. Seitz and D. Turnbull, Suppl. 1, (Academic Press, New York, 1958).

4. B.F. Chmelka, K.T. Mueller, A. Pines, J. Stebbins, Y. Wu, and J.W. Zwanziger, Nature (London), **339**, 42 (1989).

5. D.I. Hoult and R.E. Richards, J. Magn. Reson. **24**, 71 (1976).

6. a) J. Clarke, in Superconductor Applications: SQUIDs and Machines, edited by B.B. Schwartz and S. Foner (Plenum, New York, 1977).
   b) R.L. Fagaly, Sci. Prog. (Oxford) **71**, 181 (1986).

7. C. Connor, J. Chang, and A. Pines, J. Chem. Phys., accepted for publication.

8. C. Connor, J. Chang, and A. Pines, Rev. Sci. Instrum. **61**, 1059 (1990).

9. a) R.V. Pound, Phys. Rev. **79**, 685 (1950).
   b) A.H. Silver, T. Kushida, and J. Lambe, Phys. Rev. **125**, 1147 (1962).
   c) C.M. Verber, H.P. Mahon, and W.H. Tanttila, Phys. Rev. **125**, 1149 (1962).

10. T. Jach, Appl. Phys. Lett. **28**, 49 (1976).

11. R.S. Pease, Acta Cryst. **5**, 356 (1952).

12. P.J. Bray, AIP Conf. Proc. **140**, 142 (1986).

# SOLID STATE CARBON-13 NMR STUDIES OF RUBBER BLENDS

David E. Axelson and Aruna Sharma
NMR Technologies Inc, #132, 9650-20 Ave. Edmonton, Alberta T6N 1G1

John Collyer
Department of National Defence, Defence Research Establishment Ottawa, Chemical Protection Section, Polymer Research Group, 3701 Carling Ave, Ottawa, Ontario K1A 0Z4

## INTRODUCTION

Although there have been numerous papers concerning the NMR analysis of rubbers, few have specifically considered the use of carbon-13 (13C) cross polarization / magic angle spinning (CPMAS) to obtain correlations with physical and mechanical properties. This situation arises, in part, from the fact that rubbery materials, by their very nature, do not lend themselves to efficient cross polarization; high resolution solid state spectra are readily obtainable from simple Bloch decay experiments with minimal broadband proton decoupling. However, the CPMAS experiment may be able to shed some light on the nature of the interactions that give rise to significant differences in physical and mechanical properties of rubber blends as a function of composition, degree of degradation, aging, temperature, etc.

This objective may be pursued through the measurement of cross polarization relaxation times ($T_{CH}$) and proton rotating frame spin-lattice relaxation times ($T_{1\rho}{}^{H}$), which have been shown to be relatively consistent indicators of changes in polymer solid state properties. The present paper therefore summarizes our preliminary efforts towards obtaining an understanding of the basic relaxation parameters that characterize a variety of rubber blends. It is most important to remember that the degree of molecular motion in polymer chains in the solid state can affect numerous chemical and mechanical properties of the system including: diffusivity of gases, solubility of gases, kinetics of degradation and photooxidation, kinetics of swelling and impact resistance to name but a few properties of general interest.

The advantages of using any form of solid state NMR for the characterization of rubber blends are many-fold. All rubber blends under investigation contained additives, such as carbon black, that normally severely complicate the analysis of filled, vulcanized, elastomeric materials. Infrared spectroscopy usually requires pretreatment of the sample by ODCB (orthodichlorobenzene) solubilization or pyrolysis to yield a soluble polymeric component free of carbon black. (The present situation is further exacerbated by the fact that the 'exposed' samples may not be soluble under any circumstances.) It cannot be assumed that the soluble fraction is representative of the original composition of the blend. Some part of the polymers present may be selectively adsorbed on the surface of the filler and the remaining (solubilized) polymer may not be representative of the whole sample. Furthermore, it is necessary to calibrate the IR procedure by using standard polymers or blends of known composition. One then must assume that any unknown samples contain only the standards which have been created or which are otherwise available. Unfortunately, no one standard rubber sample exists that can be used to represent all variations in structure.

The goals of the present study included: determining the basic solid state NMR relaxation properties of a series of blends and their corresponding starting materials; determining the precision of the measurements; using this information to derive the necessary conditions for quantitative analysis; determining the problem areas associated with these measurements, as well as the advantages; determining the degree of spectral resolution

attainable in the solid state; illustrating where solid state measurements must be made due to such factors as the insolubility of oxidized or degraded samples; and attempting to correlate NMR-derived solid state information with the corresponding physical and mechanical properties of the blends. Only a few of these topics will be discussed in this paper due to space limitations.

The results shown in this paper can be divided into two separate, but related, discussions. In part 1 we dicuss a series of six pairs of rubber blends and related starting materials were studied by solid state $^{13}C$ NMR. The samples consisted of 'control' and 'exposed' samples where the term 'exposed' refers to treatment of the rubber with ozone. Other than this treatment step, the samples were studied without any further preparation whatsoever. In part 2 we investigate the effect of sample preparation and subsequent ambient temperature aging on one particular formulation.

## EXPERIMENTAL

All experiments were performed on a Bruker AC-F 200 NMR spectrometer operating at 50.306 MHz for $^{13}C$ observation. Unless otherwise noted, data acquisition parameters were as follows: spectral width 15151 Hz, filter width 19000 Hz, quadrature detection, quadrature phase cycling, 4.95 $\mu$s 90° pulse, contact time 0.3$\mu$s - 20 ms, recycle delay 3s - 5s, 2K data points , 1K time domain data points (ie, 1 zero fill), ambient temperature (20°C), 0.033s acquisition time spectrometer frequency 50.323 MHz, 300 scans/spectrum, 33 $\mu$s dwell delay, 43.80 $\mu$s pre-scan delay, 12 bit digitizer resolution, 25-100 Hz line broadening due to exponential multiplication of free induction decay.

The initial slope of the curve at short contact times was used to determine the value of $T_{CH}$, while the long contact time region is used to calculate the value of $T_{1\rho}{}^{H}$. Data were also acquired with the 'one-pulse', or Bloch decay, experiment. In this instance we applied a 90° pulse and acquired the free induction decay with high power proton decoupling.

Six pairs of rubber bromobutyl rubber blends, denoted by the terms 'control' and 'exposed', were studied along with various individual rubber components of these blends. The 'exposed' samples were treated with ozone under the following conditions: time: 121 hours (457F) and 144 hours (all other samples), temperature 40°C, ozone concentration: 50 pphm.

The Banbury mixing temperature was kept in the temperature range of 250°F- 266°F at all times. Total mixing time was 8 minutes; the rubber was added at time 0, at 2 minutes 1/3 of the filler, the colours, stearic acid and antidegradants were added, at 4 minutes 1/3 of the filler and the clay were added, at 6 minutes 1/3 of the filler and the processing aids were added, at 7 minutes the top of the Banbury was cleaned and the sample was dumped at 8 minutes. Curatives were added on mill and then rubber was sheeted out for slabs.

## RESULTS AND DISCUSSION

### PART 1 Effect of Ozone Treatment on Bromobutyl Rubbers of Varying Composition

Relaxation times were measured for the three major resonances of the bromobutyl rubber component in all blends (a methyl group, a quaternary carbon and a methylene carbon). Figure 1 summarizes the cross polarization ($T_{CH}$) relaxation and proton rotating frame spin-lattice relaxation ($T_{1\rho}{}^{H}$) data obtained for the $CH_2$ and $CH_3$ carbons for all samples as a function of sample treatment (control vs exposed). The $T_{CH}$ values for the control samples for the $CH_2$, C and $CH_3$ carbons were in the range 125-263 $\mu$s, 427-1136 $\mu$s, and 144-567 $\mu$s, respectively. The corresponding $T_{CH}$ values for the $CH_2$, C, and $CH_3$ carbons in the exposed / ozone-treated samples were 254-284 $\mu$s, 594-858 $\mu$s, and 113-543 $\mu$s, respectively.

There are several trends shown in Figure 1. For the $CH_2$ carbon $T_{CH}$ values the exposed samples tend to have very similar relaxation times, whereas the control samples exhibit much wider variations. This may reflect the more dynamically homogeneous composition of the treated samples, ie, in terms of the molecular motions involved, treatment with ozone has tended to make them much more similar. The starting materials vary more in this respect since there may have been variations in composition and sample preparation to which the NMR measurements are sensitive. In general, the $CH_2$ $T_{CH}$ values become longer with sample treatment. The $CH_3$ $T_{CH}$ values, however, are virtually independent of sample treatment even for samples with widely varying compositions. This arises from the fact that the relatively high degree of molecular mobility associated with rapidly rotating methyl groups masks any changes in main-chain molecular motions brought about by chain scission or cross linking. This effect illustrates that if one wishes to make NMR - physical property correlations one must be careful to choose a carbon resonance that is not affected by motions or interactions irrelevant to the chemical or physical treatment imposed on the sample.

The $CH_2$ $T_{1\rho}{}^H$ relaxation times show different trends. The exposed values tend to be equal to or shorter than the control values (except for FP460). This observation is qualitatively consistent with the fact that $T_{1\rho}{}^H$ measurements are sensitive to different frequencies of molecular motions than the cross polarization times. This will be discussed later. Furthermore, the chemical/physical changes induced in the polymer by ozone treatment will vary according to the nature and amounts of the additives present. In the current suite of samples, very specific changes in addditive type and content were made so that differences in degree of crosslinking, for instance, would be expected. Finally, the methyl carbon proton $T_{1\rho}{}^H$ values in Figure 1 are relatively insensitive to sample treatment. Thus, this resonance is not diagnostic of chemical changes in the samples regradless of the frequency regimes sampled. It should be noted that major compositional changes may be reflected in the methyl carbon relaxation behaviour; this is evidenced by the effect of incorporating EPDM/NR into the BIIR matrix, the methyl carbons relaxation times are extremely different. This is also reflected in the $T_{CH}$ values, which are much shorter for the $CH_3$ carbons in this sample.

Let us now consider more specific details. FP460 is a compound which contains 62.5% bromobutyl rubber, 1.3% carbon black and silica (17.5wt%). The difference between FP460 and FP460A is that the latter contains 1.2% of di-ß-naphthyl-p-phenylenediamine as an antidegradant. The $T_{CH}$ value of the control is less than that of the exposed sample (125 $\mu$s vs 193 $\mu$s), suggesting a decrease in the solid-like character of the interactions after ozone treatment (ie, possible chain scission reactions dominate). It is known that in silica filled BIIR the addition of p-phenylenediamine has a tendency to slightly retard the cure.

FP457A is a bromobutyl rubber with 61.6% BIIR and 24.5 % carbon black. There are three different grades of carbon black in this sample: N-231,N-234 and N-550. This compound also contains 1.3% of a zinc soap of mixed high molecular weight fatty acids. The difference between FP457A and FP457F is that the latter contains 1.3% of di-ß-naphthyl-p-phenylenediamine. The latter sample exhibits a reduced $T_{CH}$ compared with the control (150 $\mu$s vs 204 $\mu$s). It is known that in carbon black filled bromobutyl rubbers the addition of p-phenylenediamine to the mix accelerates the cure, leading to increased crosslinking and less mobile rubber chains. FP463 is a silica filled (17.5%) blend of bromobutyl rubber(50%), ethylene-propylene-diene terpolymer(EPDM, 6.5%) and natural rubber (SMR-SL, 6.5%). Carbon black N-330 is added (1.25%) for colour.

Although not shown, we should note that there were no significant differences in the chemical shifts observed in any of the spectra acquired for these treated samples. Whatever compositional changes are occurring, they were below the detection limits for the experimental conditions used in this investigation.

We therefore conclude that NMR experiments that give information on the relative amount of molecular motion within the various rubber components and individual carbons are most likely to show differences in comparing 'control' and 'exposed' samples. Significant changes in polymer physical properties can be induced by chemical (crosslinking) reactions that involve so few polymer chains or reaction sites that chemical shift changes

are below the limits of detection. One crosslink per number average molecular weight, for instance, while capable of inducing gel formation, might involve only one C-C bond formation per several thousand carbons. In complex polymer spectra these changes are indistinguishable from existing resonances. 'Control' samples were consistently different from the 'exposed' samples in this respect, the $T_{CH}$ values increased for the exposed samples compared with the controls. The $T_{1\rho}^{H}$ values decreased for the exposed samples compared with the controls; the magnitude of the changes depended on the exact type of carbon under consideration. Some types of carbons are more reliable indicators of physical / mechanical differences /changes; specifically, methylene ($CH_2$) carbons are more diagnostic than quaternary or methyl carbons due to difficulties in ensuring that quantitative / equilibrium conditions exist in the CPMAS experiment.

The cross polarization (CP) experiment, while necessary for characterizing the molecular dynamics of these polymers, is relatively ineffective for obtaining high quality chemical shift information in many rubbers due to the high degree of molecular mobility inherent in these polymer molecules, even in carbon black filled blends. Therefore, the Bloch decay (or so-called 'one-pulse' experiment) should be used for obtaining simple quantitative chemical shift information on these blends. Since the CP experiment does give rise to NMR spectra, it shows that there is still substantial amounts of low frequency/ static/ solid-like motions in the blends. This may be due to the presence of carbon black filler - polymer interactions in the blends as well as the effects of chain entanglement for polymers whose molecular weights are above the critical molecular weight for chain entanglement (both of which cause restricted molecular motions for at least part of the polymer chains present). Due to the complex, and time dependent, nature of the degradation processes that can occur in rubber blends that have undergone treatment with ozone (a combination of crosslinking and chain scission), it is not unexpected that there is a wide variation in measured NMR parameters.

Of more practical interest, we also measured some physical properties of these samples before and after treatment with ozone, including hours to first crack, tensile strength and modulus. There were correlations between the NMR relaxation times and these variables, further indicating the utility of solid state NMR measurements in complex blends.

**PART 2 Ambient Temperature Aging of Bromobutyl Rubbers**

The purpose of this investigation was to follow the natural aging (at ambient temperature) of a series of eight carbon black filled bromobutyl rubber composites made under similar, highly controlled, conditions at approximately the same time. During the course of the study both solid state $^{13}C$ NMR spectroscopy measurements and various physical tests were performed (tensile strength, modulus, elongation and tear). Bloch decay NMR measurements were made of the chemical shifts using long term data averaging to obtain very high signal-to-noise ratio spectra. This was intended to define the limits of detection of any products of the chemical degradation of the samples. Measurements were also made of various NMR relaxation time parameters: $T_{CH}$ and $T_{1\rho}^{H}$. These techniques allow one to investigate processes that occur upon aging that do not result in significant changes in the chemical composition of the composites. As previously noted, substantial changes in polymer properties may occur with little or no alteration of the chemical composition. Solid state NMR measurements constitute one of the very few characterization methods that allows one to investigate both degradation routes.

This study involved the following applications of solid state NMR: (1) defining the nature and extent of the individual variations in blend properties / measurements taken immediately after they were made and (2) monitoring the changes in the samples that occur upon aging / degradation due to exposure to light, heat and oxygen under ambient conditions. The specific objectives of the study were to systematically determine the rate of aging, ascertain the parameters most sensitive to aging and to what degree, determine whether (unavoidable) differences in the initial blending procedures could give rise to differential aging effects and use C-13 NMR to determine whether such changes, if they occurred, were readily characterized from specific investigation of the

fundamental structure of the bromobutyl rubber component. All relevant additives were also included in the blends so that degradation would be occurring under conditions approximating the actual use of these materials.

There are several levels of interpretation that can be applied to the data. First, we are investigating the individual variations in the physical properties and the corresponding NMR relaxation and chemical shift parameters of the eight blends in the study. This approach therefore dwells on the nuances of the blending procedures, the heterogeneity of the initial starting materials, and the concomitant chemical and physical changes that occur upon aging. Previous studies of this type have not been reported in the literature and the mechanism(s) of degradation of these materials is sufficiently complex that they too have not been unambiguously defined to date.

Second, we can consider the sample suite as a whole and determine suitable statistical measures of location and dispersion (ie, means and standard deviations, etc). Due to the small sample size we have applied so-called 'robust' statistical methods as a first step in the analysis of the data obtained. After a sufficiently large amount of data have been compiled we will be applying multivariate statistical analysis methods (eg, factor analysis) to the results.

*Blend Study*

This section specifically considers the physical test data and the NMR results for the first round of testing conducted shortly after the samples were prepared. As previously noted, we were interested in determining the nature and extent of the variability of the samples at an early stage of aging to minimize (or eliminate) degradation effects.

Figure 2 summarizes some of the initial test data for modulus, tensile strength, and $CH_2$ carbon $T_{CH}$ and $T_{1\rho}H$. These plots allow one to visually observe the variations among the samples and indicate real differences in the physical / mechanical properties of the samples. We also observed variations in some minor resonances in the chemical shift data obtained.

*Aging Study*

Figure 3 summarizes some of the relaxation time data for four of the eight samples as a function of aging time. The purpose of this plot is to illustrate that any given sample undergoes ambient temperature, aging-induced changes that are not monotonic with time and that each sample exhibits behaviour that can be quite distinct from that of another sample prepared at almost the same time. Figures 4 and 5 summarize the average behaviour of each set of samples as a function of time. Again, the average increases and decreases with time, the trends also being different for the two relaxation times measured.

Solids can be characterized by a distribution of frequencies representing all of the molecular motions occurring in the sample. In liquids these frequency components are very high (eg, > 50 MHz), whereas in solids they may be quite low (near 0 Hz). Distributions occur for a variety of reasons. First, each molecule may comprise a wide number of functional groups and chain lengths. Second, many different interactions among the components are possible. Third, many different phases are possible when we are discussing semicrystalline and glassy polymer composites and finally, chemical and physical aging processes combine to further modify the frequency distribution of the molecular interactions as a function of time, temperature, etc. It is the exact nature of this frequency distribution that reflects the current state of the sample in terms of its physical and mechanical properties.

Let us consider just one relevant possibility. Degradation processes may actually comprise both crosslinking reactions and / or chain scission reactions. In the former case, we can envision that the molecular

motion of the crosslinked polymer chains is significantly decreased or hindered as the crosslink density increases. In the latter instance, the formation of low molecular weight chain fragments should also give rise to increased average molecular mobility. A continuum of possibilities therefore exists. From the practical viewpoint we know that both crosslinking and chain scission lead to dramatic differences in the physical and mechanical properties of polymers. We can now begin to see the connection with the NMR relaxation time experiments. First, they are sensitive to changes in molecular motion. Second, since we can measure relaxation times for individually resolved chemical shifts / carbons in a complex material, we obtain information on very specific parts of these molecules. This enables us to ascertain which parts of the molecules are most affected by the processes in question and to what extent. To some degree the relative differences in relaxation times are more important than the actual values.

Finally, it is important to note that one must, ideally, choose an NMR relaxation time measurement / parameter that is most sensitive to the changes in the spectral density / frequency distribution that one expects to encounter in a given problem. For instance, it is usually of no value whatsoever to choose a relaxation parameter that is sensitive to very high frequency motions (>50 MHz) when one is studying solids. Regardless of what happens to the sample during aging, or whatever form of treatment, these relaxation times usually exhibit no change. Conversely, for solids or rubbery-type materials or mixtures thereof, one should choose relaxation time parameters that are sensitive to lower frequencies of molecular motion. $T_{CH}$ is most sensitive to motions near 0 Hz (ie, near static frequencies), while $T_{1\rho}{}^{H}$ is most sensitive to frequencies of motion in the mid-kilohertz range, ie, 10 - 100 kHz. Since the two relaxation times are actually derived from the same experiment, there is no penalty for determining them simultaneously.

We note at this time that we have also attempted to correlate the physical test data with the NMR results. Several good correlations have been found. Detailed discussion of these findings will be the subject of a more extensive paper to be submitted in the open literature. The NMR parameter that yields the most consistently good correlations is the cross polarization relaxation time, $T_{CH}$. As noted, this variable is most sensitive to low or near zero frequency motions. This finding indicates that the major differences occurring in the samples as a result of the preparation procedures relates to low frequency differences in molecular mobility. In Figure 6 we summarize our preliminary correlations in the form of observed versus predicted values for the physical properties using both the $T_{CH}$ and $T_{1\rho}{}^{H}$ values measured.

In terms of their averaged behaviour, the samples are exhibiting substantial aging effects over a relatively short period of time. 'Substantial' in used in the sense that unambiguous differences in sample properties are manifested in this short time period. The long term aging effects have yet to be elucidated, although the study is in progress and is anticipated to last approximately two years in total.

## CONCLUSIONS

C-13 solid state NMR measurements provide unambiguous qualitative and quantitative measures of the aging / oxidation of the bromobutyl rubber component in composites studied under ambient conditions over very short periods of time after initial sample preparation. Some general observations and conclusions made from this study to date are as follows.

* NMR chemical shift analysis provides direct observation of the nature and extent of vulcanization and ambient temperature oxidation in the solid samples studied, (Figure 7)

* olefinic carbon concentrations in the range of 0.5% and greater were readily observed as were changes in the relative concentrations of these species; there was chemical shift evidence for a variety of functional groups associated with the possible presence of acids, hydroperoxides, peroxides or alcohols,

• structural (ie, chemical shift) differences were observed immediately after the samples were prepared,

• additional changes in chemical composition have been observed throughout the duration of the study,

• measured NMR relaxation times exhibited wide variability both within the suite of eight samples and for a given sample as a function of time, consistent with the chemical differences noted above,

• the data are consistent with the proposed mechanism(s) of oxidation of hydrocarbon polymers; the key to the process is the initial formation of free radicals; in the present case they arise from the (1) the mechanical shearing during processing, (2) localized heating at any time in the thermal history of the raw polymer, and (3) the non-localized heating the composite undergoes during sample preparation; free radicals formed then react with oxygen to form peroxide derivatives which can undergo further (low temperature) reactions with the polymer / hydrocarbon chains to form hydroperoxides, peroxides, alkenes, acids and alcohols, among other products, both reactive and inert in nature,

• correlations among the $^{13}C$ NMR relaxation times ($T_{CH}$ and $T_{1\rho}{}^{H}$) and the mechanical properties measured (tensile strength, elongation, modulus, tear) were also demonstrated, both for the individual sample data and the averaged data for each test period,

• the rate of change appeared to be relatively slow for the first two months of aging and apparently accelerated during the next two month period; changes are not monotonic with time,

• variations in the rate of aging of the blends can be attributed to several factors: (1) differences in the initial degree of vulcanization (variations in time, temperature, viscosity, shear rate, localized heating effects, effective degree of mixing of components), (2) differences in the number and type of free radicals formed during processing which are then transformed to various reactive peroxide species that initiate ambient temperature oxidation, (3) differences in chemical composition as a consequence of the subsequent ambient temperature aging of these species, and (4) differences in the molecular mobility of the polymer chains in the samples at all stages due to both chemical and physical aging processes,

• further studies of these samples might be used to determine the relationship between the initial processing conditions and the physical properties of the samples after much longer storage times; predictive correlations may then be derived that minimizes the overall testing procedures for these particular materials.

Figure 1 Relaxation Time Data For CH2 and CH3 Carbons of 'Control' and Ozone -'Exposed' Rubbers

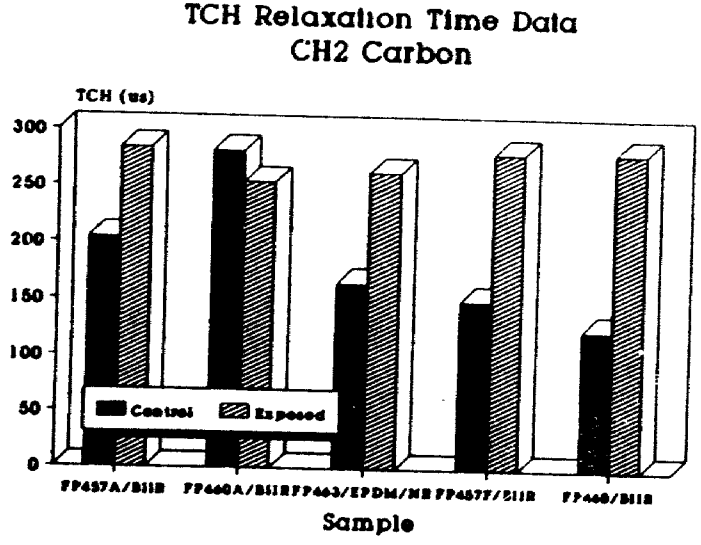


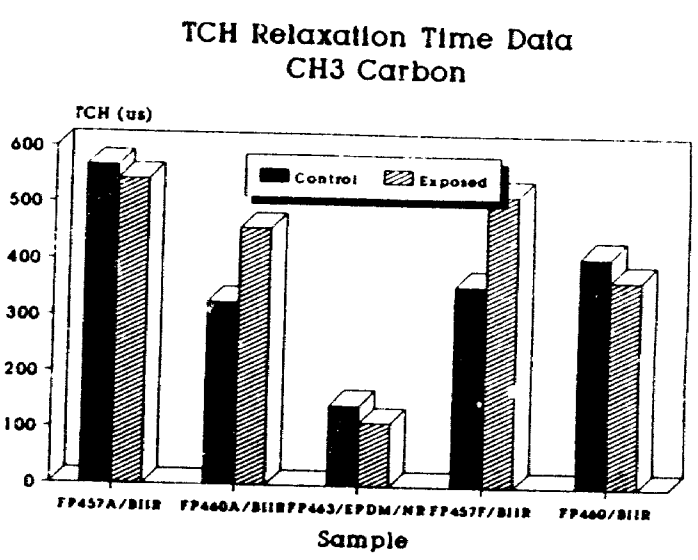


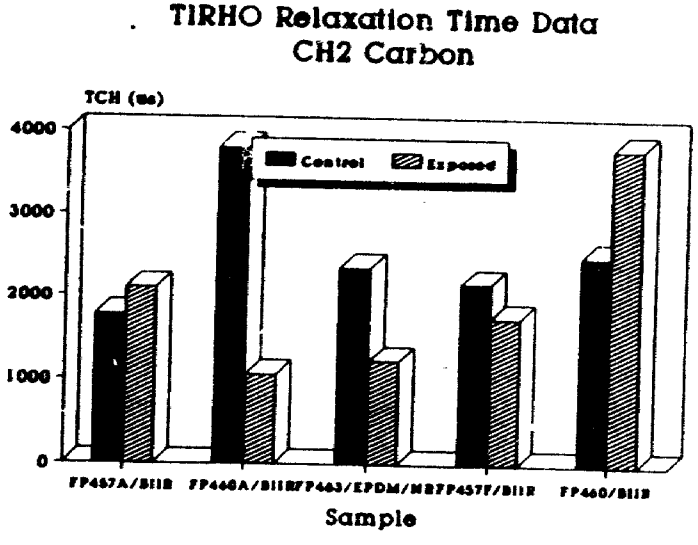


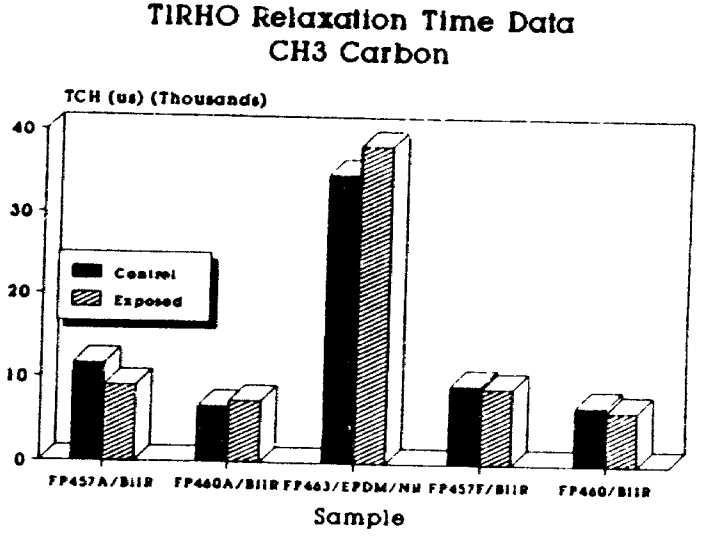

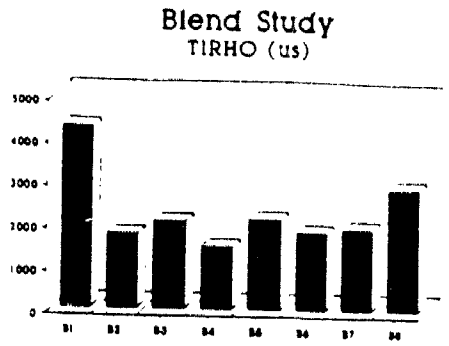


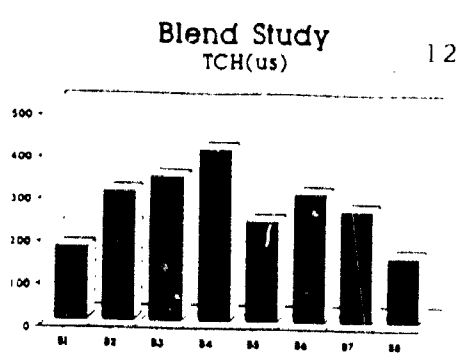


Figure 2

NMR and Physical Property Data Obtained Immediately After Sample Preparation

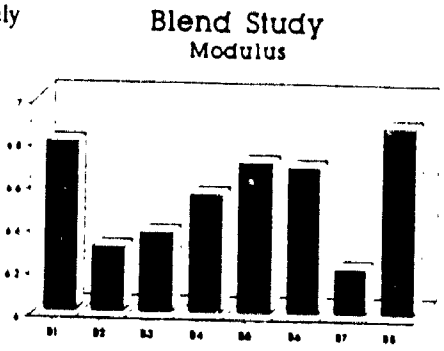


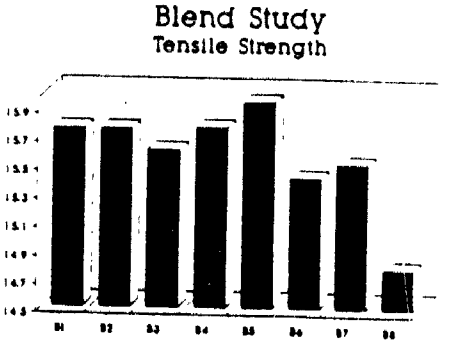


Figure 3

Relaxation Time Data For Rubbers As A Function of Time

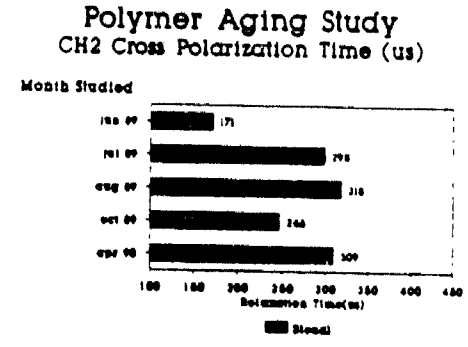


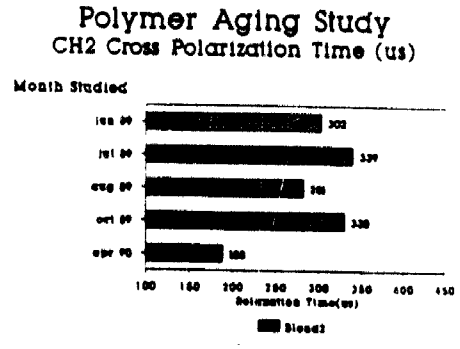


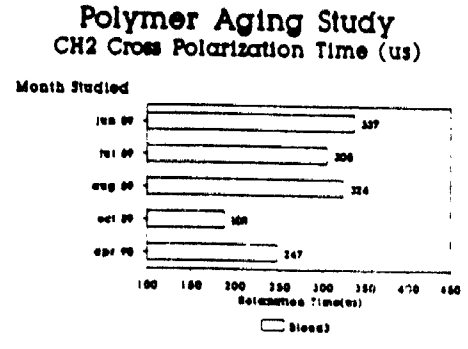


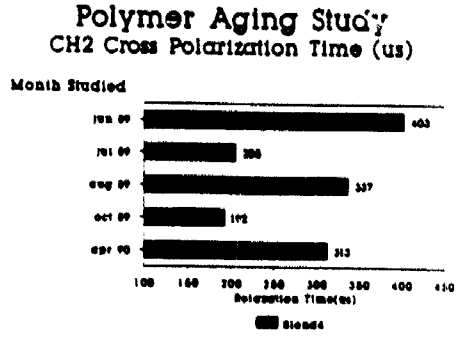

Figure 4

Statistical Summary For TCH Relaxation Time of Methylene Carbon.

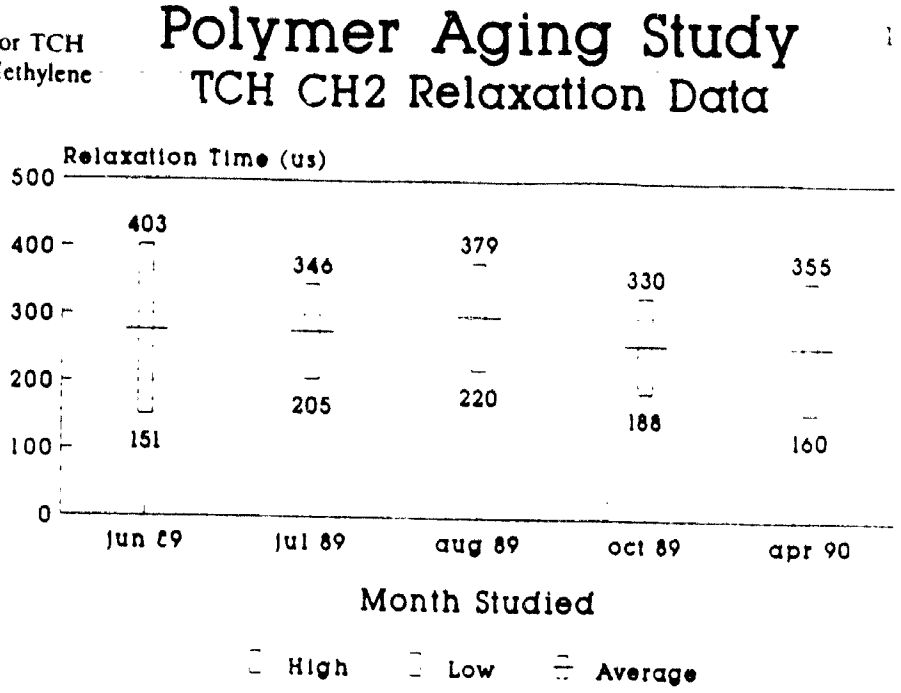


NMR Technologies Inc.

Figure 5

Statistical Summary for T1ρH Relaxation Time of Methylene Carbon.

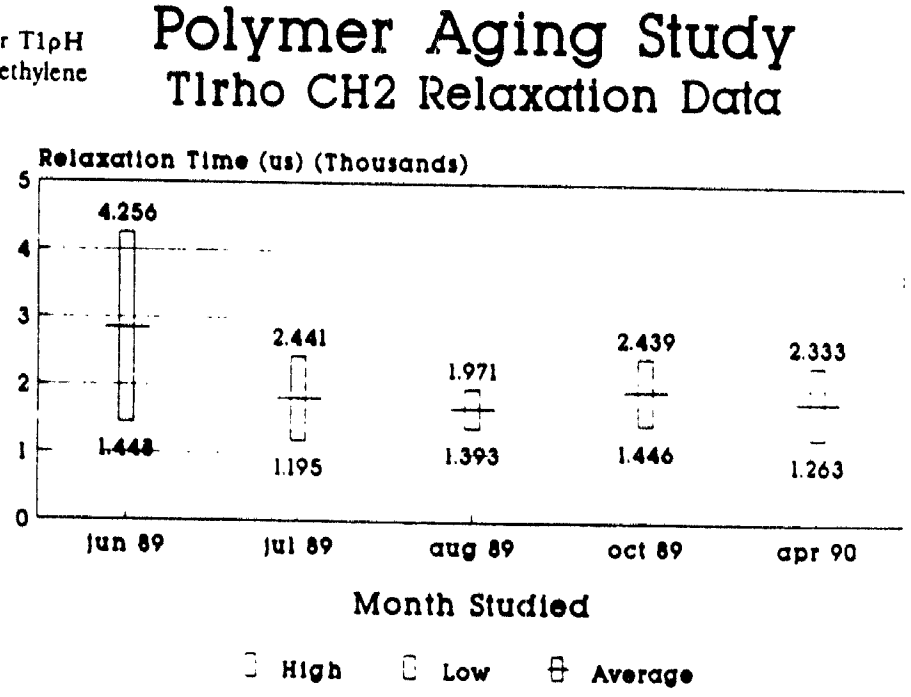


NMR Technologies Inc.

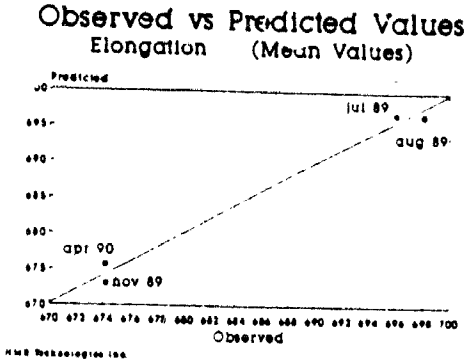


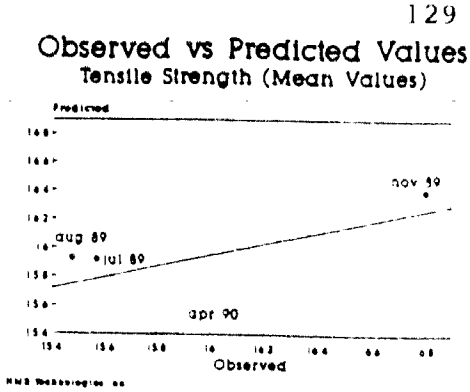


Figure 6

Observed versus Predicted Physical Properties Derived From NMR Relaxation Time Values.

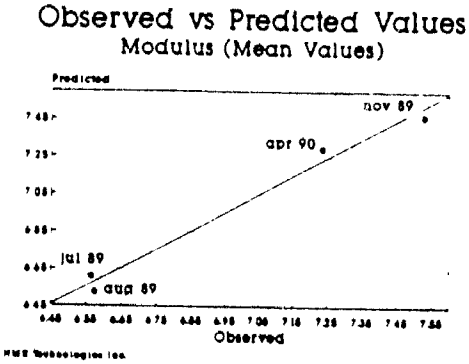


Notes:

least squares fit was made using cross polarization and proton rotating frame spin-lattice relaxation times as independent variables

Figure 7

13C MAS NMR Spectrum of Typical Bromobutyl Rubber. Broad hump is carbon black filler, while other resonances are as marked.

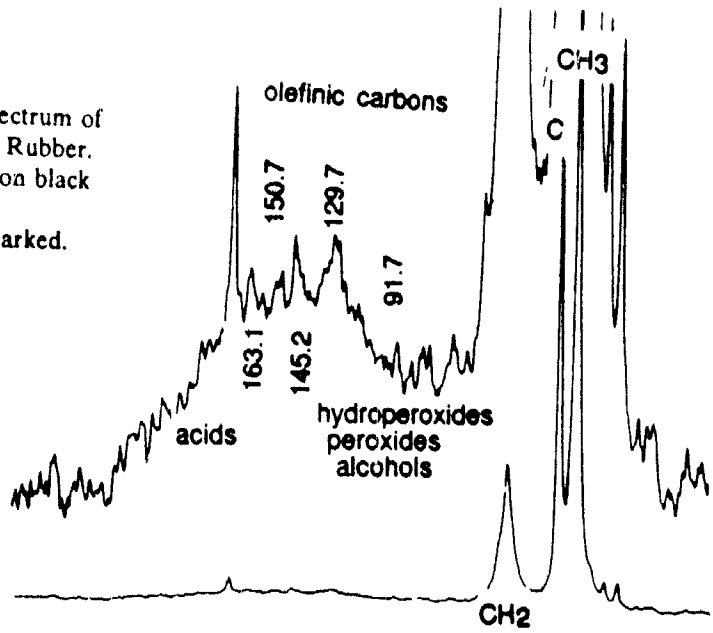

# DOCUMENT CONTROL DATA

(Security classification of title, body of abstract and indexing annotation must be entered when the overall document is classified)

1. ORIGINATOR (the name and address of the organization preparing the document. Organizations for whom the document was prepared, e.g. Establishment sponsoring a contractor's report, or tasking agency, are entered in section 8.)

Defence Research Establishment Suffield
Box 4000
Medicine Hat, AB T1A 8K6

2. SECURITY CLASSIFICATION (overall security classification of the document including special warning terms if applicable)

Unclassified

3. TITLE (the complete document title as indicated on the title page. Its classification should be indicated by the appropriate abbreviation (S,C,R or U) in parentheses after the title.)

Proceedings of NMR in Defence Sciences 1990

4. AUTHORS (Last name, first name, middle initial. If military, show rank, e.g. Doe, Maj. John E.)

Boulet, Camille A.

5. DATE OF PUBLICATION (month and year of publication of document)

May 1991

6a. NO. OF PAGES (total containing information. Include Annexes, Appendices, etc.)

136

6b. NO. OF REFS (total cited in document)

6. DESCRIPTIVE NOTES (the category of the document, e.g. technical report, technical note or memorandum. If appropriate, enter the type of report, e.g. interim, progress, summary, annual or final. Give the inclusive dates when a specific reporting period is covered.)

Symposium Proceedings

8. SPONSORING ACTIVITY (the name of the department project office or laboratory sponsoring the research and development. Include the address.)

Defence Research Establishment Suffield

9a. PROJECT OR GRANT NO. (if appropriate, the applicable research and development project or grant number under which the document was written. Please specify whether project or grant)

9b. CONTRACT NO. (if appropriate, the applicable number under which the document was written)

10a. ORIGINATOR'S DOCUMENT NUMBER (the official document number by which the document is identified by the originating activity. This number must be unique to this document.)

SSO 142

10b. OTHER DOCUMENT NOS. (Any other numbers which may be assigned this document either by the originator or by the sponsor)

11. DOCUMENT AVAILABILITY (any limitations on further dissemination of the document, other than those imposed by security classification)

( X ) Unlimited distribution
( ) Distribution limited to defence departments and defence contractors; further distribution only as approved
( ) Distribution limited to defence departments and Canadian defence contractors; further distribution only as approved
( ) Distribution limited to government departments and agencies; further distribution only as approved
( ) Distribution limited to defence departments; further distribution only as approved
( ) Other (please specify):

12. DOCUMENT ANNOUNCEMENT (any limitation to the bibliographic announcement of this document. This will normally correspond to the Document Availability (11). However, where further distribution (beyond the audience specified in 11) is possible, a wider announcement audience may be selected.)

13. ABSTRACT ( a brief and factual summary of the document. It may also appear elsewhere in the body of the document itself. It is highly desirable that the abstract of classified documents be unclassified. Each paragraph of the abstract shall begin with an indication of the security classification of the information in the paragraph (unless the document itself is unclassified) represented as (S), (C), (R), or (U). It is not necessary to include here abstracts in both offical languages unless the text is bilingual).

14 KEYWORDS, DESCRIPTORS or IDENTIFIERS (technically meaningful terms or short phrases that characterize a document and could be helpful in cataloguing the document. They should be selected so that no security classification is required. Identifiers, such as equipment model designation, trade name, military project code name, geographic location may also be included. If possible keywords should be selected from a published thesaurus. e.g. Thesaurus of Engineering and Scientific Terms (TEST) and that thesaurus-identified. If it is not possible to select indexing terms which are Unclassified, the classification of each should be indicated as with the title.)

Nuclear Magnetic Resonance
NMR
Decontamination
Two-dimensional (2D) NMR